



# International Nuclear Energy Research Initiative

Fiscal Year 2013 Annual Report

## Disclaimer

This document was prepared as an account of work sponsored by an agency of the United States Government. Neither the United States Government nor any of its employees makes any warranty, expressed or implied, or assumes any legal liability or responsibility for the accuracy, completeness, or usefulness of any information, apparatus, product, or process disclosed, or represents that its use would not infringe upon privately owned rights. Reference herein to any specific commercial product, process, or service by trade name, trademark, manufacturer, or otherwise does not necessarily constitute or imply its endorsement, recommendations, or favoring by the United States Government. The views and opinions expressed by the authors herein do not necessarily state or reflect those of the United States Government, and shall not be used for advertising or product endorsement purposes.

## Cover

South Texas Project Electric Generating Station. Photo courtesy of Public Domain

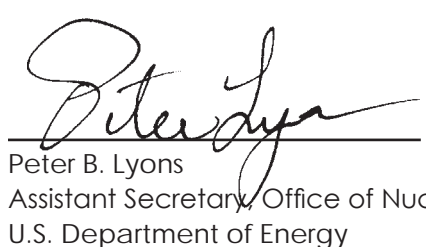
# Foreword

Nuclear energy represents the single largest carbon-free baseload source of energy in the United States, accounting for nearly 20 percent of the electricity generated and over 60 percent of our low-carbon energy production. Thirty-one states have operating commercial nuclear reactor, generating over 789 billion kilowatt-hours of reliable, clean energy; and over 430 commercial nuclear reactors safely operating in 31 countries, with over 370,000 MWe of total capacity. Worldwide, nuclear power generates over 12 percent of global electricity. This will increase as the 72 new commercial nuclear reactors currently under construction are completed and connected to the electric grid. Continually increasing demand for clean energy both domestically and globally, combined with research designed to make nuclear power ever-safer and more cost-effective, will enable nuclear energy to continue being part of the energy mix for the foreseeable future.

U.S. researchers are collaborating with nuclear scientists and engineers around the world to develop new technologies that will lower costs, maximize safety, minimize proliferation risk, and handle used fuel and radioactive waste. These are international concerns that the international nuclear community must address together. Just as all nations stand to benefit from nuclear energy, the risk of nuclear proliferation or the consequences of an accident know no national borders. Bilateral and multilateral collaborations build international consensus, capitalize on limited resources, and promote innovation far more effectively than any one nation can do alone.

The International Nuclear Energy Research Initiative, or I-NERI, is perhaps even more relevant today than at its establishment. Designed to foster bilateral international partnerships, I-NERI crosses both geographical and institutional boundaries, forging teams from universities, industry, and government organizations including federal laboratories. I-NERI agreements have resulted in collaborative research and development that investigates next-generation nuclear systems and fuel cycles, helping to determine tomorrow's solutions to today's challenges. I-NERI research teams have made substantial contributions to the knowledge base that directs critical decisions about nuclear energy.

This annual report provides information on how these efforts are collectively helping to establish a solid foundation for advanced nuclear technologies. One project at a time, the global nuclear community is building tomorrow's nuclear energy systems and technologies.



Peter B. Lyons  
Assistant Secretary, Office of Nuclear Energy  
U.S. Department of Energy



# Table of Contents



Shin Kori Nuclear Power Plant Unit 2

Photo courtesy of National Research Foundation of Korea

## 1 About This Document

### 3 1 The I-NERI Program

- 1.1 Purpose
- 1.2 International Agreements
- 1.3 Funding
- 1.4 Program Participants

### 11 2 Research Work Scope

- 2.1 Reactor Concepts Research, Development and Demonstration
- 2.2 Fuel Cycle Research and Development

### 15 3 Summary of FY 2013 Projects

- 3.1 Research Activities
- 3.2 Program Activities

### 17 4 Project Summaries and Abstracts

- 4.1 United States–Euratom Collaboration
- 4.2 United States–Republic of Korea Collaboration

### 106 Appendix I: Acronyms



Photo courtesy of National Research Foundation of Korea

# About This Document

The International Nuclear Energy Research Initiative (I-NERI) supports the advancement of nuclear science and technology through bilateral collaborative research between the United States and international partners. I-NERI is one of several mechanisms the U.S. Department of Energy's Office of Nuclear Energy (DOE-NE) utilizes to promote scientific and engineering research and development (R&D) with other nations. Innovative research performed under the I-NERI umbrella addresses key issues affecting the future use of nuclear energy and its global deployment. By teaming with international partners, U.S. researchers gain broader perspectives on issues of global importance and can potentially achieve faster results at reduced cost.

The I-NERI 2013 Annual Report provides an update of I-NERI accomplishments achieved during Fiscal Year (FY) 2013, including activities and findings of completed projects and comprehensive progress summaries of ongoing projects.

- Section 1 provides an overview of the I-NERI program, including updates on funding and program participants.
- Section 2 describes the scope of work supported by I-NERI collaborations.
- Section 3 provides a summary of FY 2013 projects.
- Section 4 presents the R&D work scope for current I-NERI collaborative projects between the United States and the two currently active partners: the European Union and the Republic of Korea. For these partnerships, the report provides summary information for individual projects that were initiated, ongoing, or completed in FY 2013.
- Appendix I defines the acronyms used throughout the report.



Nuclear High Flux Reactor (HFR)  
Photo courtesy of Euratom

# 1 The I-NERI Program

## 1.1 Purpose

The United States is confronting two powerful imperatives that are driving today's resurgence of nuclear power: the escalation of energy demands and the increasing urgency to establish a clean energy portfolio to meet these demands. Nuclear power plants presently provide more than 60 percent of our clean energy supply. However, expanded use of nuclear energy as a baseload power source faces four major challenges that require further R&D for resolution. These are:

- To develop technologies and other solutions that can improve the reliability, sustain the safety, and extend the life of current reactors.
- To develop improvements in the affordability of new reactors to enable nuclear energy to help meet the Administration's energy security and climate change goals.
- To develop sustainable nuclear fuel cycles.
- To understand and minimize risks of nuclear proliferation and terrorism.

Fortunately, the United States stands with a global nuclear community that shares our desire to resolve these challenges. Scientists worldwide are exploring ways to improve today's processes and to discover and implement next-generation methods that will ultimately promote safer and more cost-efficient use of nuclear energy. The nature of these partnerships, whether bilateral or multilateral, takes on two different but complementary roles: the United States advances the state of scientific knowledge and benefits from existing research by collaborating with countries that have mature nuclear energy programs, while providing useful assistance to those countries with developing technology and advancing global nuclear safety standards and non-proliferation frameworks.

In 2010, former Secretary Chu established the Blue Ribbon Commission on America's Nuclear Future to conduct a comprehensive review and develop recommendations for the backend of the fuel cycle. In January 2013, DOE issued the Strategy for the Management and Disposal of Used Nuclear Fuel and High-Level Radioactive Waste. In addition to responding to recommendations of the Blue Ribbon Commission on America's Nuclear Future, that Strategy establishes the Administration's policy regarding the importance of addressing the disposition of used fuel and high-level waste.

In an increasingly global society, the importance of international cooperation has escalated beyond the advantages of information sharing. Bilateral and multilateral R&D collaborations develop a common global understanding, and an integrated development approach incorporating nonproliferation, safeguards, and security technologies into the most basic elements of nuclear systems and fuel, thereby strengthening nonproliferation frameworks and protocols.

The I-NERI Program was established by DOE-NE in fiscal year (FY) 2001 to conduct R&D with international partners in advanced nuclear energy systems development in response to the clear need for global cooperation in the nuclear arena. The I-NERI program, one of several international partnerships managed by the Office of International Nuclear Energy Policy and Cooperation (NE-6), promotes bilateral research to expand the contribution of nuclear power towards meeting U.S. energy goals. Bilateral agreements established by NE provide frameworks for innovative scientific and engineering R&D undertaken in cooperation with partnering international countries, foster closer collaboration among international researchers, improve communications, and promote sharing of nuclear research information.

Cooperative research projects funded through the I-NERI program are aligned with major NE R&D programs. Projects conducted under the I-NERI umbrella aim to:

- Develop advanced concepts and scientific breakthroughs in nuclear energy and reactor technology in order to address and overcome the principal technical and scientific obstacles to expanding the global use of nuclear energy.
- Promote bilateral and multilateral collaboration with international agencies and research organizations to improve the development of nuclear energy.
- Promote a nuclear science and engineering infrastructure to meet future technical challenges.

Through the I-NERI program, DOE-NE has coordinated wide-ranging scientific discussions among governments, industry, academia, and the worldwide research community regarding the development of advanced reactor concepts and advanced fuel cycles. Figure 1 illustrates key features of the I-NERI program.

## 1.2 International Agreements

In order to initiate an international collaboration, a government-to-government agreement must first be in place. I-NERI bilateral agreements serve as vehicles to conduct joint R&D under various DOE-NE programs, enabling U.S. researchers to establish collaborative projects with their international colleagues that support the development of next-generation nuclear energy systems and fuel cycle technologies and the continued safe operation and sustainability of the existing commercial nuclear power reactors, both domestically and worldwide.

To date, DOE-NE has implemented agreements with six countries and two international organizations, signed by DOE and the international partners noted in Table 1. However, collaboration under I-NERI is presently being performed with the Republic of Korea and the European Union. The table also presents the number of projects undertaken to date with each partner.

## VISION

Promote innovative scientific  
and engineering R&D through  
international cooperation

## GOALS/OBJECTIVES

Address potential technical and scientific obstacles  
Foster international collaboration to develop nuclear technology  
Promote and maintain a nuclear infrastructure

## SCOPE OF PROGRAM

Advanced nuclear energy systems

Advanced nuclear fuels/fuel cycles

## R&D PRIORITIES

Advanced reactors, systems, and components

Advanced fuels

Alternative energy conversion cycles

Transmutation science and engineering

LWR Sustainability

Fuel cycle systems analysis

Advanced structural materials

Advanced Modeling and Simulation tools

Used nuclear fuel separations, waste forms, and fuel resources technologies

## IMPLEMENTATION STRATEGY

Collaborative research efforts

Continuous national laboratory oversight

Program management support

Annual reviews and bilateral meetings

## RESULTS

Worldwide partnerships

Innovative technologies

Nuclear infrastructure development

Advances in nuclear engineering

Global nuclear awareness

Leverage of DOE funding

Table 1. I-NERI historical international partners and number of projects awarded. (December 2013)

COLLABORATOR	ORGANIZATION	TOTAL
ACTIVE PROJECTS		
European Union	European Atomic Energy Community (Euratom)	25
Republic of Korea	Ministry of Science Information & Communication, Technology and Future Planning (MSIP) <sup>2</sup>	49
INACTIVE PROJECTS		
Brazil	Ministério da Ciência e Tecnologia (MST)	2
Canada	Department of Natural Resources Canada (NRCan) and Atomic Energy of Canada Limited (AECL)	12
France	Commissariat à l'énergie atomique (CEA)	21
Japan	Agency of Natural Resources and Energy (ANRE) and the Ministry of Education, Culture, Sports, Science, and Technology (MEXT)	2
Organisation for Economic Co-operation and Development (OCED)	The Nuclear Energy Agency (NEA) of OECD	1

The I-NERI program is a spoke in a much larger wheel of U.S. participation in the international nuclear energy community. Outside the I-NERI program, the United States has negotiated bilateral action plans with China, India, Japan, France, and Russia. There is also extensive multilateral collaboration with the international community via the Generation IV International Forum (GIF); the International Atomic Energy Agency (IAEA); the International Framework for Nuclear Energy Cooperation (IFNEC); the International Nuclear Cooperation (INC) framework, a cooperative effort with Eastern European countries; and the Nuclear Energy Agency (NEA). NE-6 coordinates U.S. involvement in each of these programs. Please visit their websites for more information.

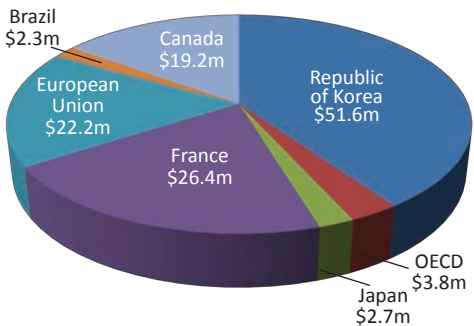
### 1.3 Funding

I-NERI is an important vehicle for enabling international R&D in nuclear technology on a leveraged, cost-shared basis. Each country in an I-NERI collaboration provides funding for its respective project participants; funding provided by the United States may be spent only by U.S. organizations. The United States funds I-NERI projects through its national laboratories, with the annual contribution based upon current-year budgets for DOE-NE R&D programs. I-NERI projects typically last three years, although budgeting protocols require the U.S. portion to be funded annually. While actual cost-share amounts are determined jointly for each selected project, the program's goal is to achieve matching

<sup>2</sup> Signatory agency was the Ministry of Science and Technology (MOST), superseded by MEST in March 2008. Nuclear R&D responsibilities were transferred from MEST to MSIP in 2013..

contributions from each partnering country. This section provides approximate domestic and international funding numbers for FY 2013 and the I-NERI program.

To date, I-NERI sponsors have committed a total R&D investment of \$270.8 million: \$144.2 million contributed by the United States and \$126.6 million by international collaborators (see Figure 2).



#### 1.4 Program Participants

I-NERI encourages global sharing of resources. The program crosses both institutional and geographical boundaries, soliciting projects from international proposal teams that comprise participants from universities,

Figure 2. Breakdown of \$126.6 million in foreign funding since I-NERI's inception, by international collaborator (numbers are approximate).

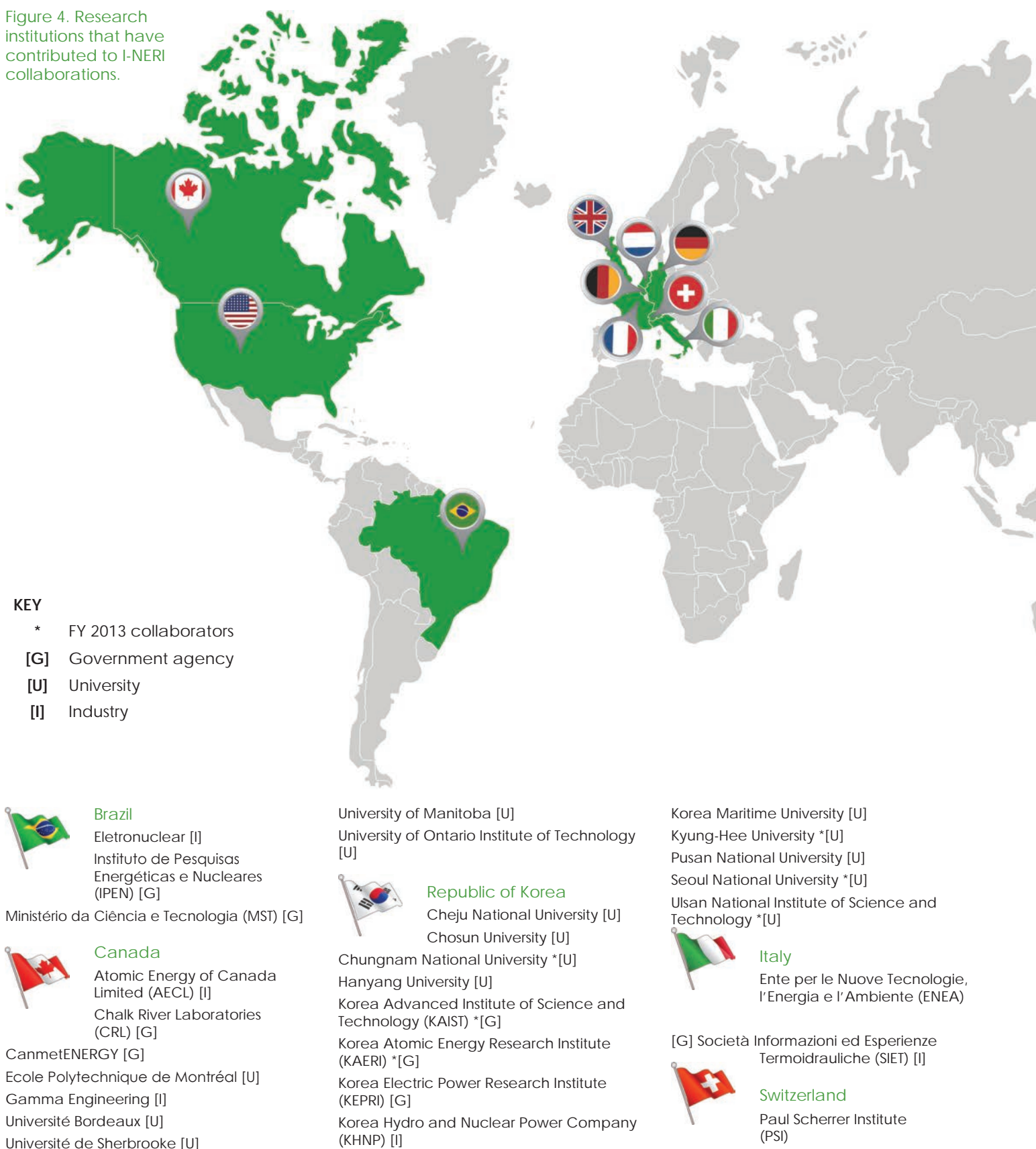
industry, and government organizations, including federal laboratories.

Collaborative efforts between the public and private sectors in both the United States and partnering international entities have resulted in significant scientific and technological enhancements in the global nuclear power arena. I-NERI collaborative projects produce findings that would take the United States alone far more time and money to accomplish. The international infrastructure also brings multiple perspectives and priorities together to address shared obstacles. Figure 4 (pages 8 and 9) shows the broad spectrum of participants in the I-NERI program since its inception; asterisks indicate participants in ongoing projects.

#### Academia Participation

One benefit of the I-NERI program is development of nuclear-related educational research opportunities. Encouraging young academics to participate in nuclear R&D promotes the nuclear science and engineering infrastructure, both in the United States and abroad. Support from the I-NERI program helps educational institutions remain at the forefront of science education and research, advance the important work of existing nuclear R&D programs, and create training for the next generation of nuclear scientists and engineers—those who will resolve future technical challenges. In FY 2013, eleven U.S. and six foreign academic institutions participated in I-NERI research projects.

Figure 4. Research institutions that have contributed to I-NERI collaborations.





#### National Laboratories

Argonne National Laboratory (ANL) \*  
Brookhaven National Laboratory (BNL)  
Idaho National Laboratory (INL) \*  
Lawrence Livermore National Laboratory (LLNL) \*  
Los Alamos National Laboratory (LANL) \*  
National Institute of Standards and Technology (NIST)  
Oak Ridge National Laboratory (ORNL) \*  
Pacific Northwest National Laboratory (PNNL) \*  
Sandia National Laboratories (SNL) \*

#### Industry

Gas Technology Institute  
General Atomics  
Ultra Safe Nuclear Corporation, Inc. \*  
Westinghouse Electric

#### Universities

Colorado School of Mines \*  
Idaho State University  
Iowa State University  
Massachusetts Institute of Technology \*  
Ohio University  
The Ohio State University  
Pennsylvania State University  
Purdue University  
Rensselaer Polytechnic Institute  
Texas A&M University \*  
University of California-Berkeley \*  
University of California-Santa Barbara  
University of Central Florida \*  
University of Florida \*  
University of Idaho  
University of Illinois-Chicago  
University of Maryland  
University of Michigan \*  
University of Nevada-Las Vegas  
University of Notre Dame  
University of North Texas \*  
University of Tennessee \*



University of Wisconsin \*  
Utah State University  
  
**Belgium**  
Ghent University \*[U]  
Joint Research Centre-Institute for Energy (JRC-IE) \*[G]

Joint Research Centre-Institute for Reference Materials and Measurements (JRC-IRMM) \*[G]

Joint Research Centre-Institute for Transuranium Elements (JRC-IUT) \*[G]

SCK•CEN (Belgian Nuclear Research Centre) \*[G]



**UK**  
University of Manchester [U]



#### France

Commissariat à l'énergie atomique (CEA) \*[G]  
Electricité de France (EDF) [G]  
Framatome ANP [I]  
Laboratoire des Composites Thermostructuraux (LCTS) [G]  
Organisation for Economic Co-operation and Development-Nuclear Energy Agency (OECD/NEA) [G]



#### Germany

Karlsruhe Institute of Technology \*[U]



#### Japan

Hitachi, LTD [I]  
Hitachi Works [I]  
Japan Atomic Energy Agency (JAEA) [G]  
Japan Atomic Energy Research Institute (JAERI) [G]  
Tohoku University [U]  
Toshiba Corporation [I]  
University of Tokyo [U]



#### Netherlands

Nuclear Research and Consulting Group \*[I]

\* 2013 I-NERI Collaborators



Photo courtesy of National Research Foundation of Korea

# 2 Research Work Scope

I-NERI project work scopes are jointly developed by the United States and the collaborating country based on terms of the bilateral agreement and current common R&D needs. Potential topics for collaboration in the coming year are selected at each annual joint planning and project review meeting. For the United States, the work scope of I-NERI projects must be directly linked to the scientific and engineering needs of the principal NE research programs: Reactor Concepts Research, Development and Demonstration (Reactor Concepts RD&D) and Fuel Cycle Research and Development (FCR&D).

Past I-NERI project teams have contributed to the extensive and growing knowledge base in both of these R&D programs. In support of reactor concepts, I-NERI projects have investigated such topics as next-generation materials (e.g., nano-composited and oxide dispersion-strengthened steels, silicon carbide composites, and zirconium alloys); improved energy conversion through the Brayton cycle; advanced sensors, instrumentation, and controls; hydrogen production through thermochemical reactions and high-temperature electrolysis; production viability and efficiency; safety issues and proliferation risk reduction; and analysis of distribution and storage methods. In addition, the program has contributed to our knowledge of modeling and simulation; some of the first I-NERI project teams utilized these tools, and roughly half the current projects explicitly call for the use, qualification, and/or improvement of numerical techniques within their objectives. Sample new nuclear fuels being investigated include advanced transmutation fuels and inert matrix fuels. Fuel cycle research includes accident-tolerant fuels, waste forms, separation of fission products from nuclear waste, and advanced head-end processes that condition used fuel.

This section provides an overview of the current work scopes for these NE R&D programs.

## 2.1 Reactor Concepts Research, Development and Demonstration

The mission of the Reactor Concepts RD&D program is to develop new and advanced reactor designs and technologies with broader applicability and improved affordability and competitiveness. RD&D activities address technical, cost, safety, proliferation, and reliability challenges associated with the program elements described below.

### Advanced Reactor Technologies (ART)

The Office of Advanced Reactor Technologies Program focuses on the development of advanced reactor concepts with increased efficiency, significantly reduced carbon emissions, state of the art safety systems, and improved fuel utilization. This reflects a consolidation of the

Advanced Reactor Concepts, Advanced Small Modular Reactor and Next-Generation Nuclear Plant Programs. The ART program is currently focused in five areas:

- **Fast Reactor Technologies**
  - For actinide management and electricity production
  - Current focus on sodium coolant
- **High Temperature Reactor Technologies**
  - For electricity and process heat production
  - Current focus on gas- and liquid salt-cooled systems
- **Advanced Reactor Generic Technologies**
  - Common design needs for advanced materials, energy conversion, decay heat removal systems and modeling methods
- **Advanced Reactor Regulatory Framework**
  - Development of licensing requirements for advanced reactors
- **Advanced Reactor System Studies**
  - Analyses of capital, operations and fuel costs for advanced reactor types

### **Small Modular Reactor (SMR) Advanced Concepts R&D**

SMRs provide simplicity of design, enhanced safety features, the economics and quality afforded by factory production, and more flexibility (financing, siting, sizing, and end-use applications) than larger nuclear power plants. SMRs can provide power for applications where sites lack the infrastructure to support a large unit, such as smaller electrical markets, isolated areas, smaller grids, sites with limited water and acreage, or unique industrial applications. Thus this concept is of benefit not only to countries with highly developed economies and mature nuclear programs but also to those with limited resources. The program supports RD&D activities that advance the understanding and demonstration of these innovative reactor technologies and concepts.

### **Light Water Reactor Sustainability**

Over the next three decades, most currently operating nuclear power plants will reach the ends of their operating licenses. To help meet the nation's expanding electricity requirements, however, existing reactors must continue operating beyond 60 years. This program supports acquiring the scientific understanding needed to develop and demonstrate technologies that support safe and economical long-term operation of existing reactors, as well as new technologies that enhance performance. Extending the life of the current fleet requires fundamental science to predict and measure changes in materials, systems, structures, and components as they age in environments found within operating reactors.

## Advanced Modeling and Simulation

Two major initiatives are developing the advanced modeling and simulation that will provide the validated tools necessary to enable fundamental change in how the United States designs and manages both existing and future nuclear facilities. The Consortium for Advanced Simulation of Light Water Reactors (CASL) is a DOE-sponsored energy innovation hub that brings together industry, universities, and the national laboratories to create a virtual model with advanced predictive and simulation capabilities for the current generation of reactors. The Nuclear Energy Advanced Modeling and Simulation (NEAMS) program is a longer-term initiative that is developing a suite of integrated codes and cross-cutting numerical tools to support the entire range of NE's nuclear energy R&D.

## 2.2 Fuel Cycle Research and Development

One of the four NE R&D objectives is achievement of sustainable fuel cycle options, defined as those that improve uranium resource utilization, maximize energy generation, minimize waste generation, improve safety, and limit proliferation risk. Through a long-term science-based approach, the FCR&D program is developing a suite of technology options that will enable informed decisions about the management of nuclear waste and used reactor fuel.

Today's commercial nuclear power plants run on a once-through fuel cycle, which utilizes only about five percent of the fuel's energy potential before the used fuel is placed in storage for future disposal. Advanced and innovative fuel cycles recycling technologies are being developed to process this fuel for re-use in reactors. This may allow substantially more energy to be drawn from the same amount of nuclear material, while reducing the quantity of long-lived radioactive elements in the used nuclear fuel. Fuels R&D aims to increase the efficient use of uranium resources, reduce the amount of used fuel requiring disposal, and evaluate the inclusion of non-uranium materials to reduce the long-lived radioactive elements in used fuel. In a full recycle system, only waste products will require disposal, not used fuel. The mission of the FCR&D program is: (1) to develop used nuclear fuel management strategies and technologies to support meeting federal government responsibility to manage and dispose of the nation's commercial used nuclear fuel and high-level waste; and (2) develop sustainable fuel cycle technologies and options that improve resource utilization and energy generation, reduce waste generation, enhance safety, and limit proliferation risk. The program is applying a methodical systems engineering analysis approach to identify suitable technologies.

FCR&D has five campaigns addressing different program elements that support the overall objectives of sustainable fuel cycle options.

### Fuel Cycle Options

This campaign is developing methods and tools to evaluate, screen and identify fuel cycles options in order to guide the selection of one or more sustainable options and strengthen and support nuclear fuel cycle R&D needs. Researchers perform integrated fuel cycle analyses and technical assessments and provide information that can be used to inform NE's fuel cycle R&D activities and strategies. The campaign is studying options for once-through, modified recycle and full recycle systems, looking at all stages from mining to disposal.

### Advanced Fuels

NE is supporting R&D for various fuel forms, including cladding, that are needed to implement those fuel cycle options. For any given fuel type, fuel qualification requires engineering-scale

demonstration of the fabrication processes and irradiation of lead-test assemblies to demonstrate in-reactor performance. NE is working toward developing a state-of-the art R&D infrastructure to support a goal-oriented science-based approach. The campaign is investigating both transmutation fuels, which have potential for enhanced resource utilization and proliferation resistance, and next-generation light water reactor (LWR) accident-tolerant fuels that exhibit enhanced performance and safety and reduced waste generation.

### Separations, Waste Forms, and Fuel Resources

Features of a sustainable fuel cycle include reduced processing waste generation and proliferation risk. NE is working towards advanced and innovative fuel cycle separation and waste management technologies that enable these improvements. Research scope includes developing advanced waste forms and developing and demonstrating technologies that separate transuranic elements and fission products from used nuclear fuel, as well as investigating cutting-edge alternatives that could widen fuel cycle options.

### Used Fuel Disposition

This program aims to provide a sound technical basis for a new national policy to manage the back end of the nuclear fuel cycle, including identification and evaluation of safe and secure options for storage, transportation, and permanent disposal of radioactive wastes resulting from existing and future fuel cycles. Objectives range from identifying and addressing gaps in existing data and methodologies to using advanced modeling tools for studies of potential disposal system concepts and environments; research scope ranges from interim storage to final disposal. International activities are a cornerstone of these efforts and include participation in international working groups addressing relevant challenges, support for bilateral interactions between the United States and the Republic of Korea and the United States and Japan, and planning for U.S. involvement in disposal R&D in European underground research laboratories (URLs).

### Material Protection, Accounting, and Control Technologies

As nuclear systems grow more complex and their use becomes more widespread, NE aims to enhance safety and security while minimizing proliferation risk. This program supports efforts to develop innovative technologies and analysis tools to enable next-generation nuclear materials management for future U.S. nuclear fuel cycles, significantly advancing the state-of-the art in accounting and control. NE is also supporting the necessary research to integrate safeguards and security into the earliest stages of the design cycle.

# 3 Summary of FY 2013 Projects

## 3.1 Research Activities

Since the program's inception, 112 projects have been awarded. There are currently 19 active projects, 7 collaborations with Euratom and 12 with the Republic of Korea. Of these 19 projects, seven were successfully completed in FY 2013. Both the number of awards and the consistency of project achievement demonstrate I-NERI's success in fostering international collaboration. A summary of findings and accomplishments for completed, on-going, and new projects can be found in Section 4 of this annual report.

## 3.2 Program Activities

I-NERI programmatic accomplishments include successful completion of three U.S.-Euratom collaborative research projects:

- 2010-002-E Spherical Particle Technology Research for Advanced Nuclear Fuel/ Target Applications
- 2010-003-E Irradiation and Testing of Advanced Oxide Dispersion-Strengthened Ferritic Martensitic Steels
- 2010-005-E Interoperability of Material Databases).

Two U.S.-Euratom projects received approval to continue:

- 2010-006-E State-of-the-Art Post-Irradiation Examination of Advanced Nuclear Fuels
- 2012-001-E High-Fidelity Thermal Hydraulic Fuel Assembly Simulations for Nuclear Reactors

Two new projects were initiated with the Euratom:

- 2013-001-E Novel Technology for Synthesis of Nuclear Fuels
- 2013-002-E Phase Equilibria and Thermochemistry of Fission Products in Uranium Fuel

Four U.S.- Republic of Korea (ROK) collaborative research projects were successfully completed in 2013:

- 2010-001-K Investigation of Electrochemical Recovery of Zirconium from Spent Nuclear Fuel
- 2010-002-K Science-Based Approach to Ni-Alloys Aging and Its Effects on Cracking in PWRs
- 2010-003-K Low Loss Advanced Metallic Fuel Casting Development
- 2010-004-K Development and Characterization of Nano-particles Strengthened Dual Phase Alloys for High-Temperature Nuclear Reactor Applications

Five U.S.-ROK projects received approval to continue:

- 2011-001-K Atomic Ordering in Alloy 690 and Its Effect on Long-Term Structural Stability and Stress Corrosion Cracking Susceptibility
- 2011-002-K Development of Microcharacterization Techniques for Nuclear Materials
- 2011-003-K Verification and Validation of High-Fidelity Multi-Physics Simulation Codes for Advanced Nuclear Reactors
- 2011-004-K Development of Diagnostics and Prognostics Methods for Sustainability of Nuclear Power Plant Safety Critical Functions
- 2011-005-K Fully Ceramic Microencapsulated Replacement Fuel for Light Water Reactor Sustainability

In 2013, three new projects were initiated with the Republic of Korea:

- 2013-001-K Generation of Physics Validation Database and Analysis of Fast Reactor Depletion Capability and Core Characteristics Calculations Using MC2-3/DIF3D/REBUS-3
- 2013-002-K Development of Oxidation Protective Coating Technology on Graphite for VHTR Core Support Structure
- 2013-003-K Development of Advanced Long Life Small Modular Fast Reactors)

Key management of each I-NERI agreement takes place during an annual project performance review and bilateral program planning meeting (BINERIC). These annual meetings facilitate information exchange and provide opportunities for the parties to review ongoing projects, investigate new opportunities for collaboration, and update research scopes to support current R&D priorities.

The BINERIC meetings serve as a forum to discuss areas of mutual interest for future research. At each meeting, participants from the two collaborating countries establish general topics for joint research for the coming year, along with a schedule for requesting and evaluating proposals. Each respective I-NERI country coordinator sends out a request for proposals following the agreed guidance, and the submitted proposals are jointly evaluated for funding.

In FY 2013, DOE held a combined Annual Review/BINERIC meeting with their Euratom colleagues at the Idaho National Laboratory, located in Idaho Falls, Idaho, and another with the Republic of Korea at DOE Headquarters in the Washington, D.C. All ongoing projects were approved for continued funding at the most recent BINERIC meetings, as the research efforts are proceeding well and continue to meet NE objectives. For the upcoming FY 2014 I-NERI solicitations for proposed joint research projects, both bilateral partnerships agreed to retain existing joint research topic areas, as summarized in the introductions to Sections 4.1 and 4.2.

In FY 2014, both Euratom and the Republic of Korea will host the I-NERI Annual Review Meeting/BINERIC. The proposed locations are Brussels, Belgium; and Seoul, Korea, respectively.

As appropriate, DOE will continue to pursue new cooperative agreements with prospective partner countries.

# 4 Project Summaries and Abstracts

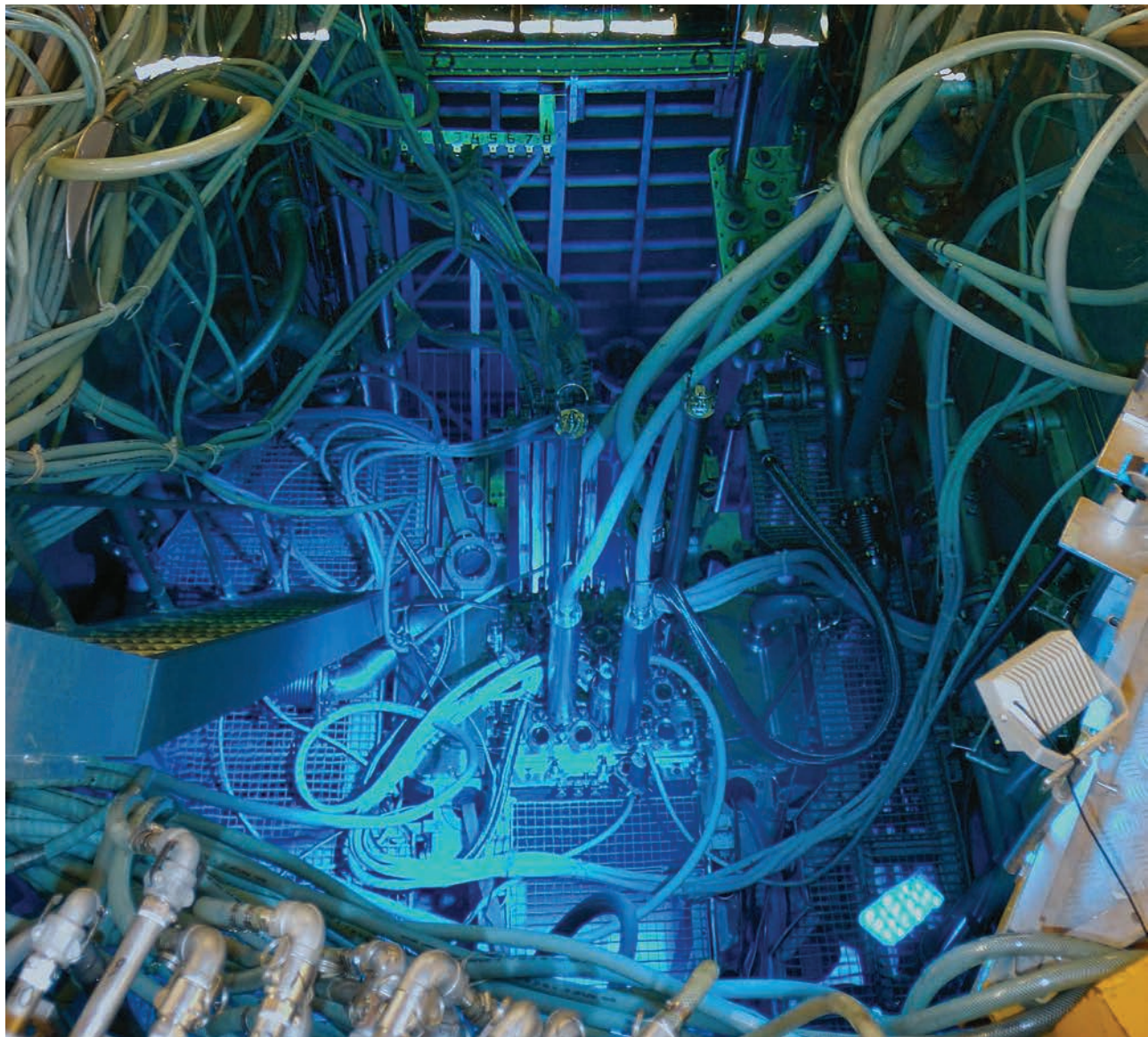


Photo courtesy of Euratom

## 4.1 United States–Euratom Collaborative Projects

DOE and the European Commission (EC) signed a bilateral agreement on March 6, 2003. Secretary of Energy Spencer Abraham signed the agreement for DOE, and Commissioner for Research Phillippe Busquin signed on behalf of the EC. Euratom serves as the implementing agent for the EC for I-NERI collaboration.

Research areas of interest to both the United States and Euratom include advanced reactor concepts and associated fundamental nuclear science; existing plant life extension, integrity of components, and performance optimization; waste transmutation and management; reactor safety; severe accident management; advanced fuels; uranium programs; and modeling and simulation.

In 2013, three projects came to a successful completion and efforts continued on two ongoing projects. Two new projects were selected for award and started in 2013.

Below in Table 1 is an overview listing of completed, on-going, and new I-NERI U.S.-Euratom projects, followed by summaries of their FY 2013 accomplishments and overviews.

Project Number**	Project Title	Completion Year
2010-002-E	Spherical Particle Technology Research for Advanced Nuclear Fuel/Target Applications	2013
2010-003-E	Irradiation and Testing of Advanced Oxide Dispersion-Strengthened and Ferritic-Martensitic Steels	2013
2010-005-E	Interoperability of Material Databases	2013
2010-006-E*	State-of-the-Art Post-Irradiation Examination of Advanced Nuclear Fuels	2014
2012-001-E	High-Fidelity Thermal Hydraulic Fuel Assembly Simulations for Nuclear Reactors	2015
2013-001-E	Novel Technology for Synthesis of Nuclear Fuels	2016
2013-002-E	Phase Equilibria and Thermochemistry of Fission Products in Uranium Fuel	2016

\* Project received a 1-year extension to original 3-year award.

\*\* The 2010, for example, indicates project initiation date and "E" represents Euratom

# Spherical Particle Technology Research for Advanced Nuclear Fuel/Target Applications

Project Number: 2010-002-E

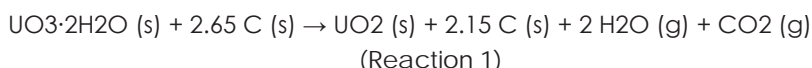
## Research Objectives

The goal of this work is to advance the state of understanding of particle fuel technology by addressing technical questions related to fuel/target fabrication and performance. A key objective is the evaluation of spherical particles for use as (1) a potential near-dustless feed for ceramic fuel fabrication, and (2) a host matrix for the infiltration of a second actinide phase. The actinide-bearing kernels may be dispersed in a ceramic or metal forming a ceramic-ceramic or ceramic-metallic composite. In 2013, the process for synthesizing nitride microspheres was studied. The goal was to accomplish complete nitride conversion from oxide starting material, achieve near fully dense microspheres, and maintain particle microstructural integrity.

## Research Progress

Carbon-incorporated uranium oxide microspheres ( $\text{UO}_2 + \text{C}$ ) are heat treated in nitrogen environments to synthesize UN. The internal gelation process was used to produce hydrated uranium trioxide ( $\text{UO}_3 \cdot 2\text{H}_2\text{O}$ ) microspheres with carbon black dispersed throughout the gel spheres [1].  $\text{UO}_3 \cdot 2\text{H}_2\text{O}$  microspheres were calcined then the  $\text{UO}_2 + \text{C}$  reactants were converted into dense intermediates of uranium carbide (UC) plus  $\text{UO}_2$  followed by transformation of the carbide and remaining oxide into the nitride. A thermogravimetric analyzer (TGA) was used to measure mass changes of carbon-bearing uranium microspheres as a function of time, temperature, and defined atmosphere.

In the calcinations step, microspheres of  $\text{UO}_3 \cdot 2\text{H}_2\text{O} + 2.65$  carbon were calcined to  $\text{UO}_2 + 2.15$  carbon as shown in Reaction 1. The microspheres were heated to 873 K at a rate of 200 K/h and then held at 873 K for 2 h.



Simultaneous thermogravimetry, temperature profile, and mass spectrometry for this process were obtained and are shown in Fig. 1. The  $\text{H}_2\text{O}$  trace displays two peaks representing removal of

**PI (U.S.):** Stewart Voit, Oak Ridge National Laboratory

**PI (Euratom):** Joseph Somers, Joint Research Center–Institute for Transuranium Elements

**Collaborators:** Los Alamos National Laboratory

**Program Area:** Fuel Cycle R&D

**Project Start Date:** February 2010

**Project End Date:** January 2013

adsorbed and chemically bound water. The oxygen trace (not shown for clarity) was analyzed for behavior that may indicate partial decomposition of UO<sub>3</sub> to a lower oxide such as U<sub>3</sub>O<sub>8</sub>. Four distinct peaks are associated with oxygen species and all correspond to indicated H<sub>2</sub>O and CO<sub>2</sub> peaks. Decomposition of UO<sub>3</sub> to lower oxides, carbonate decomposition, and residual organic decomposition, if present, overlap with other TG and MS traces. Two distinct CO<sub>2</sub> peaks are revealed with onset temperatures of 442 K and 792 K respectively. The TG and CO<sub>2</sub> traces are consistent with Reaction 2.

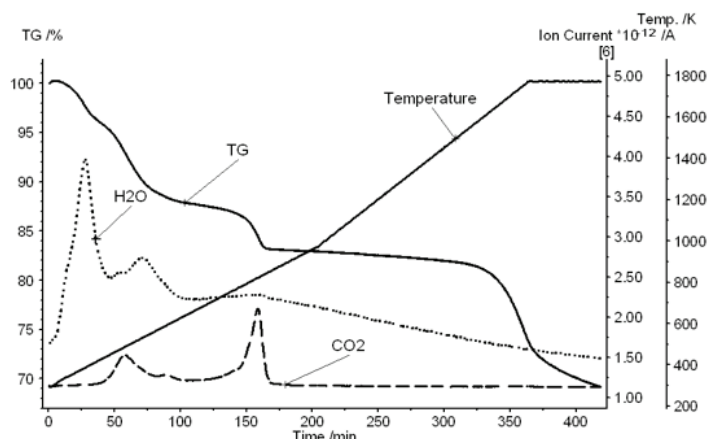
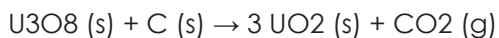


**Fig. 1 Characteristics of calcination of air-dried  $\text{UO}_3 \cdot 2.65\text{C}$  in argon from Figure 1. Characteristics of calcination of air-dried  $\text{UO}_3 \cdot 2.65\text{C}$  in argon from thermogravimetry and mass spectrometry.**

Conversion and sintering was performed following two different approaches: a conventional two-step method in which the conversion and sintering takes place in separate steps, and a single conversion/sintering method. All of the experiments using the conventional two-step method resulted in low density kernels with, in many cases, excessive cracking and incomplete conversion. Successful conversion was achieved by following a single-step process adopted from Ledergerber et al. [2]. Table 1 lists the single-stage conversion/sintering experimental conditions similar to the Ledergerber approach.

Table 1. Experimental conditions for single-stage conversion/sintering.

		Conversion / Sintering			
C:U	Target Diameter ( $\mu\text{m}$ )	Ramp Rate (K/min)	Temperature (K)	Atmosphere	Hold Time (hours)
2.65	850	3	973	Ar-H <sub>2</sub>	0.5
		5	1923	Ar-H <sub>2</sub>	0.5
		5	2073	N <sub>2</sub>	20

Oxide to nitride conversion proceeds via the general reaction 3. UC/UO<sub>2</sub> ratio in excess of 2 would lead to UC<sub>1-x</sub>N<sub>x</sub> and possibly free carbon.



Synthesis of high-density UN or UC<sub>1-x</sub>N<sub>x</sub> with low carbon content, especially at large-scale fabrication is a challenging task. Batch conversion in which the process gas flows across the top of a static bed of particles typically yields a distribution of conversion across the particle bed. Conversion is most effective in the top center of a static bed where the reaction gas CO

can easily be swept away. Conversion for particles near the bottom or side-wall of the crucible is suppressed due to poor CO removal. Sampling particles from the top of the particle bed was performed to determine if complete conversion could be achieved under ideal conditions and the results are presented below.

X-ray diffraction of powdered kernels indicated approximately 0.7 molar ratio of C in UC<sub>x</sub>N<sub>1-x</sub> based on lattice parameter comparison with Vegard's law between pure UC and pure UN. There was no indication of UO<sub>2</sub> present. SEM images of UCN kernels that had the highest density are displayed in Figure 2 and reveal the kernel exterior and interior surfaces in the left and right images respectively. The average density of UCN kernels from a population of 34 was 90% of theoretical. Although initial results from batch processing produced inhomogeneous conversion, characterization of select samples indicate that the single-stage conversion/sintering process can indeed yield dense UCN microspheres. Excess carbon in the product microspheres suggests that additional process optimization is needed. The amount of carbon added during sol-gel processing can be reduced and/or hydrogen gas can be introduced during conversion and sintering to remove excess carbon as HCN.

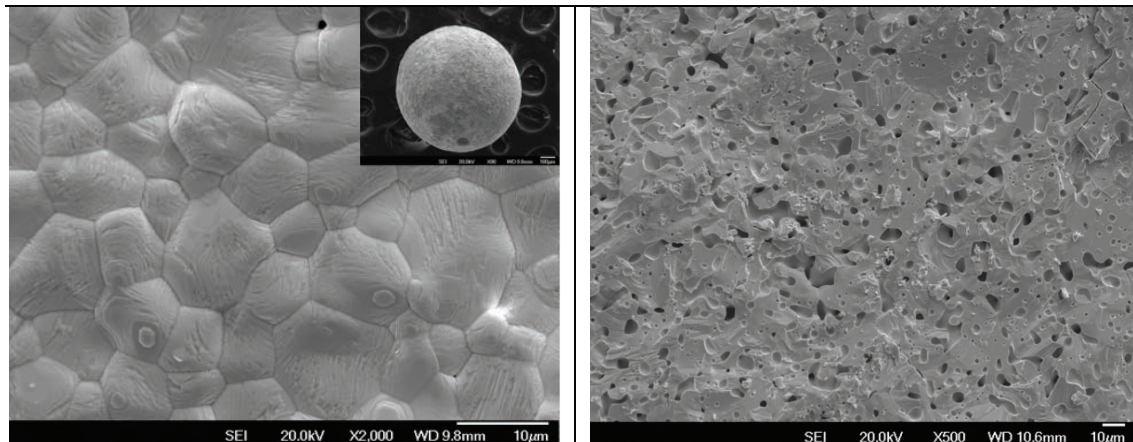


Fig. 2. Scanning electron microscopy of UCN kernels showing kernel surface (left image) and kernel interior (right image).

### Planned Activities

Programmatic activities will continue in CY2014 and including an assessment of the effect of a furnace crucible modification to allow process gas to flow up through the static bed of particles. This improvement should allow more effective reaction gases removal and reduce the partial pressure of CO thereby increasing conversion efficiency.

[1] R.D. Hunt, T.B. Lindemer, M.Z. Hu, G.D. Del Cul, J.L. Collins, Radiochim. Acta 95 (2007) 225–232

[2] G. Ledergerber, Z. Kopajtic, F. Ingold, R.W. Stratton, Preparation of uranium nitride in the form of microspheres, J. Nucl. Mater. 188 (1992) 28–35.

# Irradiation and Testing of Advanced Oxide Dispersion-Strengthened and Ferritic–Martensitic Steels

Project Number: 2010-003-E

## Research Objectives

This collaboration is investigating irradiation and corrosion effects in materials used for innovative reactor systems, including fast reactors cooled with sodium, heavy liquid metal (HLM), and gas. The project team is developing and characterizing advanced oxide dispersion-strengthened (ODS) and ferritic–martensitic (F/M) steels, investigating corrosion effects of these steels in sodium, and examining the ODS steels' irradiation behavior. They are utilizing several irradiation programs, such as those conducted at MEGAPIE and the Fast Flux Test Facility (FFTF), to prepare materials for post-irradiation analysis and gather data for modeling.

Sharing collaborative research results among scientists at U.S. national laboratories, the U.S. Department of Energy, and Euratom's GETMAT (Generation IV and Transmutation Materials) will improve understanding of these innovative systems' potential viability and competitiveness, support development of improved safety features, and provide information about transmutation systems using HLM coolant and a fast-spectrum spallation neutron flux.

## Research Progress

### Development of Advanced ODS Steels (including welds)

The U.S. team produced a 50-kilogram heat of the mechanically alloyed (MA) ODS ferritic alloy 14YWT, performed 40-hour milling on this heat of material at Zoz GmbH in Germany and have consolidated materials for mechanical testing. A summary of the stress/strain curves measured at temperatures up to 800°C is shown in Fig. 1. The U.S. team shared these data with GETMAT research scientists, making similar progress on development of 12Cr and 9Cr ODS alloys.

PI (U.S.): Stuart Maloy, Los Alamos National Laboratory

PI (Germany): Concetta Fazio, Karlsruhe Institut für Technologie (formerly Forschungszentrum Karlsruhe)

Collaborators: Idaho National Laboratory, Lawrence Livermore National Laboratory, Oak Ridge National Laboratory, Pacific Northwest National Laboratory, Paul Scherrer Institute, SCK•CEN (Belgian Nuclear Research Center)

Program Area: Fuel Cycle R&D

Project Start Date: December 2009

Project End Date: December 2013

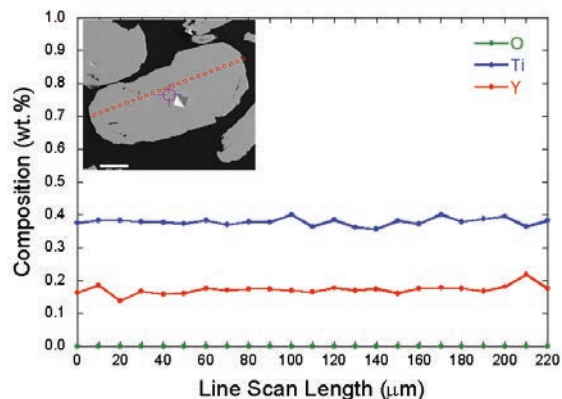


Figure 1. Graph showing stress/strain curves measured on new heat of 14YWT, FCND-NFA1, tested from room temperature up to 800°C.

## **Advanced Materials Coolant Compatibility**

Los Alamos National Laboratory (LANL) restarted the DELTA loop and successfully ran a corrosion test for over 1500 hours at 488°C. This corrosion test centered on testing materials at high flow rates and flow rates up to 3.5 m/s were achieved. Simultaneously, GETMAT researchers are conducting long-term (up to 10,000 hours) corrosion testing on ODS alloys in lead and lead–bismuth.

## **Irradiation Behavior of Advanced ODS Steels**

U.S. researchers completed testing of STIP IV irradiated materials. This irradiation included ODS alloys such as 14YWT and 12YWT. Significant hardening was observed in 12YWT and ductility was reduced but still greater than 5% after irradiation to 21 dpa. Euratom researchers will obtain high-dose irradiation data from materials irradiated in the MATRIX program, which reproduces the fast spectrum conditions for core components. However, this activity is presently delayed because of hot cell repairs.

## **Information Sharing**

Significant data sharing progress has been made through collaborative meetings. In particular, the U.S. principal investigator (PI) and an ORNL collaborator presented highlights of the post irradiation testing and 14YWT development at the final GETMAT technical meeting in Berlin, Germany, September 2013.

## **Multiscale Modeling**

U.S. researchers are developing creep models of F/M iron–chromium alloys and validating those models through experimental results. Although this activity was initially sponsored through the NEAMS program, it will no longer be pursued under the scope of I-NERI, as funding is discontinued in FY 2013.

## **Planned Activities**

This was a final meeting for the GETMAT collaboration and this I-NERI is completed now. A final joint report is in progress.

# Interoperability of Material Databases

## Research Objectives

This project is investigating the viability of using standards-compliant schemas and ontologies to address interoperability of materials databases, facilitating data exchange between research partners. As numerous components in Gen IV systems are exposed to high temperatures, neutron fluences, and corrosive environments, safe and economic system operations necessitate extended materials qualification testing. However, existing materials test databases currently present compatibility challenges: they differ in format and associated semantics; they are stored in both heterogeneous and distributed database repositories; these repositories have a variety of working environments and software tools to access the data; and these environments and tools are in a constant state of change.

The main goal of the project is the implementation of web-service software for data import and export using an agreed standardized schema at Oak Ridge National Laboratory (ORNL) and the Joint Research Centre (JRC). Database interoperability will reduce costs associated with redundant materials testing programs, promote long-term data preservation, enable improved auditing traceability, and support the reuse of data.

The work is undertaken within the broader scope of international efforts to develop technologies that enable interoperability of materials databases. The present project builds on the results of a recently completed European Committee for Standardization (CEN) workshop on the viability of standards-compliant data formats, starting with a tensile test schema derived from documentary technology standards and a guide for using and developing data formats for engineering materials test data.<sup>1</sup> The introduction and adoption of standards-compliant data formats (schemas and ontologies that are a faithful representation of procedural standards for mechanical testing) will allow researchers to leverage established and emerging web-based technologies for data storage and retrieval.

Project Number: 2010-005-E

**PI (U.S.):** Lianshan Lin and Weiju Ren,  
Oak Ridge National Laboratory

**PI (Euratom):** Timothy Austin, Peter Hähner, Hans-Helmut Over, Joint Research Centre–Institute for Energy and Transport

**Collaborators:** None

**Program Area:** Reactor Concepts  
RD&D

**Project Start Date:** January 2011

**Project End Date:** December 2013

<sup>1</sup> CWA 16200:2010 (2010), "A Guide to the Development and Use of Standards-Compliant Data Formats for Engineering Materials Test Data," retrieved February 27, 2012, from [ftp://ftp.cen.eu/CEN/Sectors>List/ICT/CWAs/CWA16200\\_2010\\_ELSI.pdf](ftp://ftp.cen.eu/CEN/Sectors>List/ICT/CWAs/CWA16200_2010_ELSI.pdf).<sup>2</sup> Ibid.

Progress has been on hold since the end of FY 2013 due to some changes in the Gen IV Materials Handbook Project at ORNL. The major impact factors include:

- 1) A significant increase of workload in the Gen IV Materials Handbook project as its development was phasing into a digitized-data-intensive effort from an electronic-document-intensive effort to meet the growing needs and requirements in the international collaboration under agreement of the Gen IV International Forum (GIF).
- 2) A funding cut for the Gen IV Materials Handbook project in FY 2014.

Before progress was put on hold, the project had achieved its major objectives for establishing the capability of massive data exchange between the MatDB at JRC and the Gen IV Materials Handbook at ORNL.

The MatDB and the Gen IV Materials Handbook have different database structures. The MatDB structure has a mainly hierarchical configuration (see Figure 1), while the Gen IV Materials Handbook has a mainly network configuration (see Figure 2).

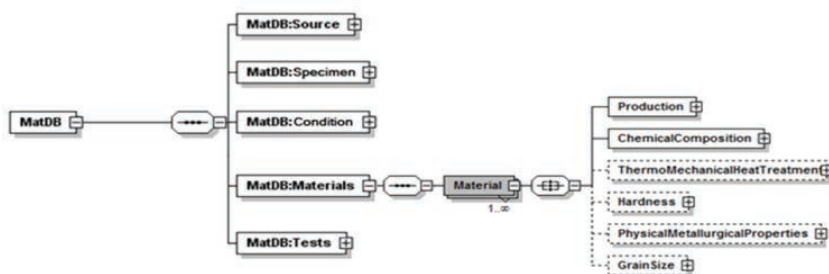


Figure 1. Hierarchical structure of the MatDB.

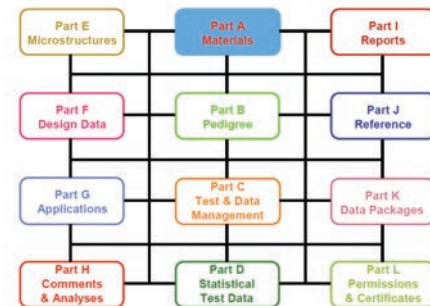


Figure 2. Network structure of the Gen IV Materials Handbook.

Both systems have the capability of massive digital data import and export through the XML mechanism (see Figure 3 and Figure 4).

Despite the massive digital data transfer capability that had already been established in both systems, detail analyses indicated that for same mechanical testing types different

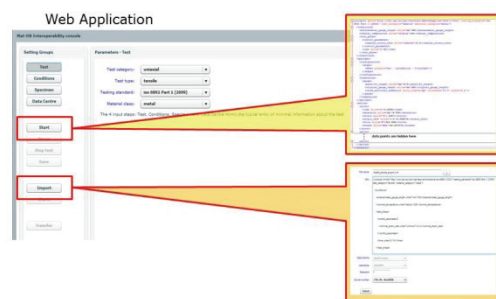


Figure 3. MatDB's massive digital data transfer capability.

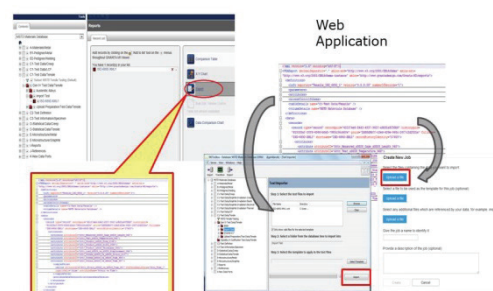


Figure 4. Gen IV Materials Handbook's massive digital data transfer capability.

names were often found for same attributes in the two systems. In addition, the two systems obviously had a mismatch in the database structure. The differences of the two systems resulted in a technical barrier that XML exports generated from one system would not accurately communicate with those from the other (see Figure 5).

To overcome the technical barrier, an XML interpreter is needed to translate corresponding data elements from one XML file into the other, and the EXtensible Stylesheet Language Transformations (XSLT) was chosen to develop a solution. EXtensible Stylesheet Language (XSL) is a style sheet language for XML documents, which describes how the XML document should be displayed. However, XSL is more than a Style Sheet Language. The World Wide Web Consortium (W3C) started to develop XSL because there was a need for an XML-based Stylesheet. It was eventually developed into three parts: XSLT (for transforming XML documents), XPath (for navigating in XML documents) and XSL-FO (for formatting XML documents). The XSLT was chosen for the present project as it would best fit the task requirements (see Figure 6).

The solution developed using the XSLT was a success. The developed mechanism for massive digital data exchange.

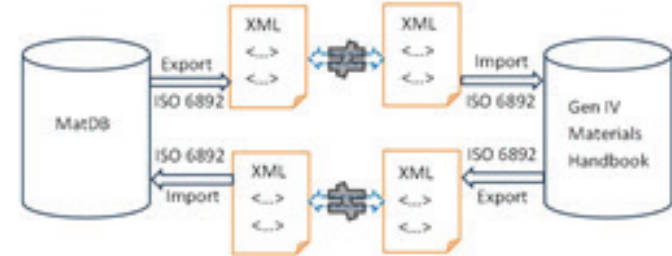


Figure 5. Technical barrier between two systems in data exchange.

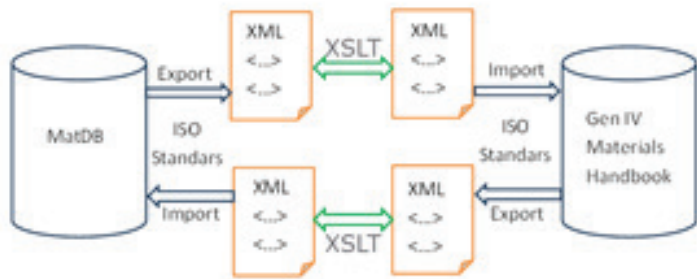


Figure 6. Achieving interoperability for massive digital data exchange.

A small module was established in MatDB for testing the developed mechanism for massive digital data exchange. Some tensile test datasets were successfully transferred from the Gen IV Materials Handbook to the MatDB across continents.

## Planned Activities

Currently, two publications on the accomplishment of the project are under preparation. To resume the progress, the following two action items should first be completed:

- 1) Identify recent changes in both systems and update the interoperability mechanisms.
- 2) Identify data for exchange and negotiate exchange conditions if the identified data are not covered by existing GIF agreements.

Once the two actions above are completed, the ORNL and JRC teams can resume the progress and cooperate to exchange data records between MatDB and the Handbook systems. The data exchange will entail a two-way communication process, with an intermediate step of exporting data into XML files before importing to the other database, and vice versa. The initial exchange will be data from the "Generation IV International Forum Very High-Temperature Reactor System Materials Project Plan." Further exchanges will be based on the result of action 2 above.

Techniques developed through this project can be further extended to enable interoperability between database and computational simulation software, which will open a door of great opportunities for Integrated Computational Materials Engineering (ICME) and Materials Genome Initiative (MGI) that are expected to bring forth revolutionary advancements in materials research and development.

# State-of-the-Art Post-Irradiation Examination of Advanced Nuclear Fuels

## Research Objectives

New concepts for nuclear energy development are considered in both the USA and Europe within the framework of the Generation-IV International Forum (GIF) as well as in various US-DOE programs (e.g. the Fuel Cycle Research and Development - FC RD) and as part of the European Sustainable Nuclear Energy Technology Platform (SNE-TP).

Since most new fuel cycle concepts envisage the adoption of a closed nuclear fuel cycle employing fast reactors, the fuel behavior characteristics of the various proposed advanced fuel forms must be effectively investigated using state of the art experimental techniques before implementation. More rapid progress can be achieved if effective synergy with advanced (multi-scale) modeling efforts can be achieved. The fuel systems to be considered include minor actinide (MA) transmutation fuel types such as advanced MOX, advanced metal alloy, inert matrix fuel (IMF), and other ceramic fuels like nitrides, carbides, etc., for fast neutronic spectrum conditions. Most of the advanced fuel compounds have already been the object of past examination programs, which included irradiations in research reactors. The knowledge derived from previous experience constitutes a significant, albeit incomplete body of data. New or upgraded experimental tools are available today that can extend the scientific and technological knowledge towards achieving the objectives associated with the new generation of nuclear reactors and fuels.

The objectives of this project will be three-fold: (1) to extend the available knowledge on properties and irradiation behavior of high burnup and minor actinide bearing advanced fuel systems; (2) to establish a synergy with multi-scale and code development efforts in which experimental data and expertise on the irradiation behavior of nuclear fuels is properly conveyed for the upgrade/development of advanced modeling tools; (3) to promote the effective use of international resources to the characterization of irradiated fuel through exchange of expertise and information among leading experimental facilities. The priorities in this project will be set according to the down selection procedure of U.S. and European development programs.

Project Number: 2010-006-E

**PI (U.S.):** J. R. Kennedy, Idaho National Laboratory

**PI (Euratom):** V. V. Rondinella, Joint Research Centre–Institute for Transuranium Elements

**Collaborators:** Colorado School of Mines, University of Central Florida, Massachusetts Institute of Technology, Los Alamos National Laboratory

**Program Area:** Fuel Cycle R&D

**Start Date:** January 2011

**End Date:** December 2014

## Research Progress

Experimental work in the US related to this collaboration during the 2013 timeframe was primarily directed towards development of high spatial resolution instrumentation for thermal conductivity and mechanical properties determination for eventual coupling with computational modeling and simulation efforts, atom probe tomography (APT) studies on fresh fuel samples from samples prepared with use of the focused ion beam (FIB), and higher spatial resolution microstructure studies of as-cast fuels from transmission electron microscope (TEM) studies for input into computational modeling and simulation efforts.

### Atom Probe Tomography (APT) and Transmission Electron Microscopy (TEM) Studies

Advanced characterization techniques such as TEM and APT have been widely utilized for non-radiological materials; however, the extreme difficulty of working with radioactive samples has inhibited their application in nuclear energy. These advanced techniques provide the ability to obtain critical experimental data on the evolution of microstructure, dislocation density, grain size and orientation, and composition in irradiated materials from the atomic to the mesoscale. Atom probe tomography (APT) allows high resolution, "atom-by-atom" identification of element distribution in a sample. Dr. Melissa Teague at INL has used a focused ion beam (FIB) to produce site specific samples for the first ever APT studies of AFC transmutation fuels, performed at the Center for Advanced Energy Studies (CAES) facility at INL. Samples for APT were prepared using the hot FIB at the Materials and Fuels Complex and then transferred to CAES for analysis using the cutting edge LEAP 4000x HR atom probe. The first alloy studied was U-55Pu-20Zr in the annealed state. Due to instrumentation issues, an oxide layer formed on the outside of the samples.

Figure 1 shows a reconstruction of an oxidized U-55Pu-20Zr sample. An interesting feature is the different oxidation behavior of the elemental components. The extent and depth of oxidation were element dependent with Zr having the thickest oxidation layer followed by U and then Pu. The presence of oxidized zirconium within metallic U/Pu is an interesting observation and further analysis is planned. A Pu/U rich and Zr depleted region was seen at the edge of the tip, which is hypothesized to be along a former grain boundary (Figure 2). Though preliminary in scope, the application of APT to transmutation fuels is an exciting advance and has great potential for helping to understand the complex behavior observed in both irradiated and unirradiated fuels. Further quantification of these type studies will be employed in conjunction with computational efforts (e.g. the MARMOT code at INL) to fully simulate the microstructure evolution in fuels under irradiation.

In order to better understand the nature of the transmutation fuels and to better integrate experiment with computation and modeling, Dr. Dawn Janney initiated transmission electron microscopy (TEM) studies on

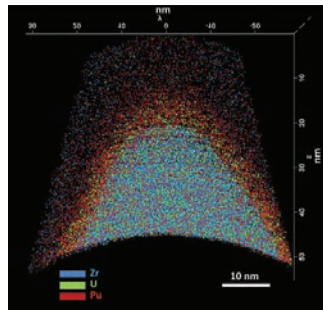


Figure 1. APT reconstruction of oxidized U-55Pu-20Zr sample showing the different oxidation depths of the components. Only the metallic ions of Zr, U, and Pu are displayed to highlight different oxidation behavior.

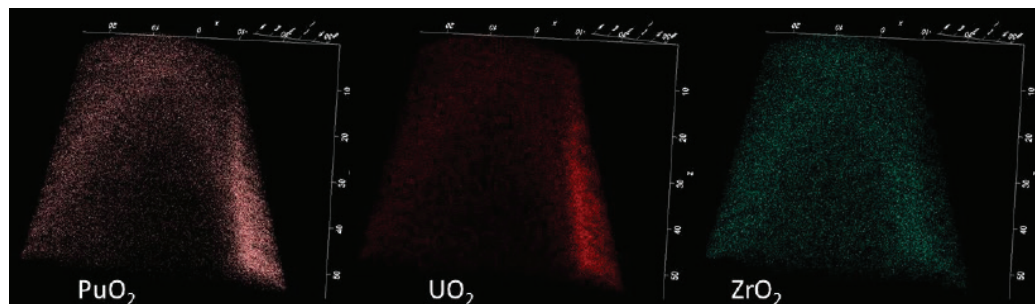


Figure 2. Reconstruction of U-55Pu-20Zr samples showing the Pu/U rich and Zr depleted region at the edge of the samples that is hypothesized to be a former grain boundary region.

various fuel types. These high spatial resolution microstructure studies are investigating a base U-Pu-Zr alloy in collaboration with Lawrence Livermore National Laboratory, a 52U-20Pu-3Am-2Np-8.0Ln-15Zr fuel composition that includes both minor actinides (MA) and lanthanides (Ln), and diffusion couples between U-Pu-Zr alloys and iron (Fe, representing cladding). These studies are the first of their kind with regard to use of the focused ion beam (FIB) for sample preparation of metallic transmutation fuels (TRU bearing fuel type materials) and the use of the TEM and its associated techniques (electron diffraction for single phase crystallite structure determination, energy dispersive spectroscopy for microchemical analysis) to investigate specific microstructural features of the fuel materials. Data from the U-Pu-Zr work and diffusion couple studies are still forthcoming but some very interesting and important results from the 52U-20Pu-3Am-2Np-8.0Ln-15Zr study given below.

Many Scanning Electron Microscopy (SEM) studies that do not allow the high spatial resolution possible with TEM have observed the as cast U-Pu-Zr fuels microstructure to appear as an undefined mixture of light and dark contrast phases but including also various shading of gray contrast material. It was speculated that this interesting feature could represent a nanosized grain structure composed of  $\zeta$ -(U,Pu,Zr) and  $\square$ -(U,Pu)Zr<sub>2</sub> phases. Figure 3 shows a micrograph of a gray shaded area and reveals that indeed the as-cast microstructure is composed of nano-sized grains on the order of only a few tens of nanometers across. Electron diffraction analysis strongly suggests that one of the phases is in fact  $\zeta$ -(U,Pu,Zr).

The ubiquitous Zr inclusions observed in virtually all U-TRU-Zr fuels have generally been interpreted to form due to impurities such as oxygen, nitrogen, silicon, etc. introduced as part of the feedstock material or from the casting process and should exist in the  $\square$ -Zr structure. Single-crystal electron diffraction analyses (Figure 4) on these inclusions show this isn't necessarily true and, in fact, the high-Zr inclusions have a face-centered cubic (fcc) structure that haven't been reported previously in the literature. This study was recently published (D. E. Janney, J. R. Kennedy, J.W. Madden, T.P. O'Holleran "Crystal structure of high-Zr inclusions in an alloy containing U, Pu, Np, Am, Zr and rare-earth elements", J. Nucl. Mater. 448 (2014) 109–112)

Additional interesting findings show that, as previously reported in SEM data, there are two kinds of RE inclusions: high-Nd ("dark") and high-Am ("light"). Although all of the RE inclusions are high in Nd, proportions of other elements differ. High Nd content inclusions can have significant concentrations of oxygen and low concentrations of actinides. High Ce content inclusions are also high in Am and have significant concentrations of Pu. Interestingly, all of the observed high Zr inclusions are adjacent to high Ce inclusions, but not all high Ce inclusions are adjacent to high-Zr inclusions (Figure 5). The implications of these observations are still under consideration.

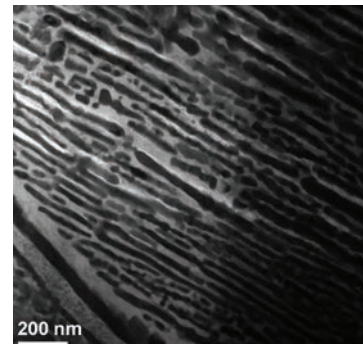


Figure 3. TEM micrograph obtained from an as-cast 52U-20Pu-3Am-2Np-8.0Ln-15Zr sample showing nano-sized light and dark contrast grain structure.



Figure 4. Electron diffraction pattern from a Zr rich inclusion along the [110] axis revealing it to be in the, to date, unreported face-centered-cubic structure.

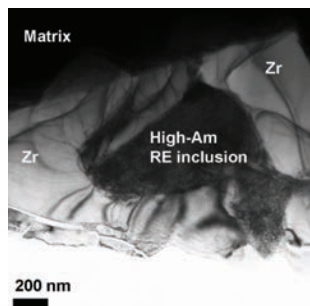
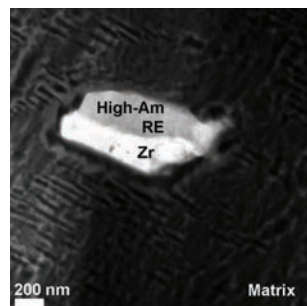


Figure 5. Left: high Am content RE inclusion surrounded by high Zr content inclusion.

Right: combined high Zr content and high Am content inclusion.



## Thermal Conductivity Studies and Modeling Developments

Thermal conductivity studies in ITU have continued during the reporting period. The cause for thermal conductivity decrease associated with increasing fractions of Pu in MOX fuel has been investigated. The results of this study are published in [Staicu and Barker, Thermal conductivity of heterogeneous LWR MOX fuels, J. Nucl. Mater. 442 (2013) 46-52].

Thermal conductivity degradation of LWR MOX fuel compared to that of pure UO<sub>2</sub> is usually attributed to the substitution of U atoms by Pu. However, Duriez and Philipponneau indicate that the thermal conductivity of MOX is independent of the Pu content in the ranges 3 - 30 wt. % PuO<sub>2</sub>. In fact, heterogeneity in the plutonium distribution in the fuel causes a variation in the local O/M ratio. This feature has a strong impact on the thermal conductivity. A model quantifying this effect was defined and validated using a new set of Laserflash measurements on homogeneous and heterogeneous MOX fuels. The stoichiometry perturbations are sufficient to explain the lower thermal conductivity of heterogeneous MOX fuel when compared to UO<sub>2</sub>. The effect due to the presence of Pu in heterogeneous MOX is thus overestimated in the correlations available in literature.

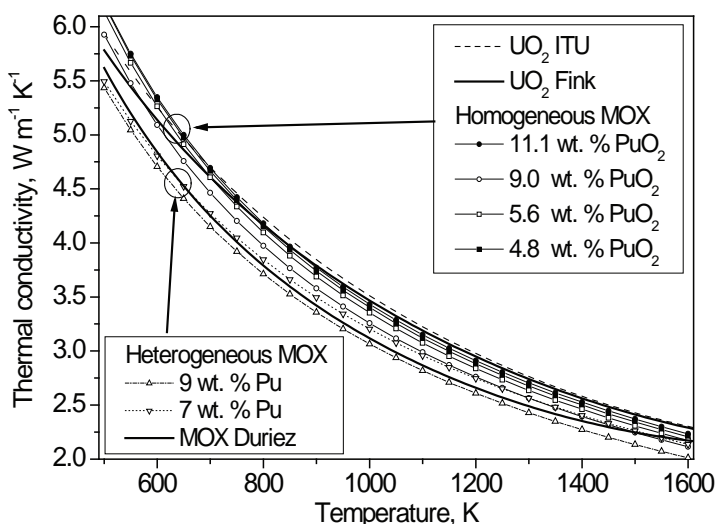


Figure 6. Experimental thermal conductivity of homogeneous and heterogeneous MOX compared to UO<sub>2</sub> (95 %TD) [from Staicu & Barker, 2013].

The oxygen local distribution effect can be expected to disappear in irradiated fuel, as the concentration of irradiation-induced defects, including oxygen defects, is much higher than the oxygen defects due to non-stoichiometry. In irradiated fuel both fission and the temperature gradient in the pellet cause oxygen redistribution, as shown by Lassmann [Lassmann, K., J. Nucl. Mater., 1987. 150: p. 10-16.] and Sari [Sari, C. and G. Schumacher, J. Nucl. Mater., 1976. 61: p. 192-202]. Therefore, under irradiation a rapid thermal conductivity convergence between heterogeneous MOX and UO<sub>2</sub> can be predicted, due to the overall oxygen sub-lattice evolution with burn-up. This interpretation is consistent with previous out-of-pile thermal diffusivity measurements at ITU [see e.g. Cozzo, C., et al., *Thermal diffusivity of homogeneous SBR MOX fuel with a burn-up of 35 MWd/kgHM*. J. Nucl. Mater., 2010. 400: p. 213-217. 6. Staicu, D., et al., *Thermal conductivity of homogeneous and heterogeneous MOX fuel with up to 44 MWd/kgHM burn-up*. J. Nucl. Mater., 2011. 412: p. 129-137].

Positive developments of the collaboration between INL and ITU have occurred in the domain of modeling and code applications. Such effort has resulted in a paper with joint INL, ITU and University Politecnico di Milano authorships: G. Pastore, L.P. Swiler, J.D. Hales, S.R. Novascone, D.M. Perez, B.W. Spencer, L. Luzzi, P. Van Uffelen, R.L. Williamson, "Uncertainty and sensitivity analysis of fission gas behavior calculations in engineering-scale fuel modelling", J. Nucl. Mater., submitted.

The paper reports about a sensitivity analysis on parameters related to a physics-based model coupling fission gas release and swelling performed using the BISON fuel performance code.

## Advanced Instrumentation

Two key areas of instrument development at INL in the advancement of laser-based techniques are to determine mechanical and thermal properties of nuclear fuel and these are the Mechanical Properties Microscope and the Thermal Conductivity Microscope. These developments come out of the group of Dr. David Hurley.

The Mechanical Properties Microscope (MPM), shown in the left pane of Figure 7, is being designed to operate in a radiation hot cell environment via remote control manipulation. The MPM provides micron-level mechanical property information that is commensurate with microstructure heterogeneity. The development of the MPM connects closely with INL's larger PIE effort to provide new validation metrics for fundamental computational material science models. Currently in stage I mockup, the MPM is being used to provide important data on surrogate fuel samples. One example includes measuring the elastic anisotropy resulting from deformation texture in UMo fuel surrogates. Another example involves measuring the elastic constants of the UZr system as a function of composition (data presented in units of GPa in the left-middle pane of Fig. 7).

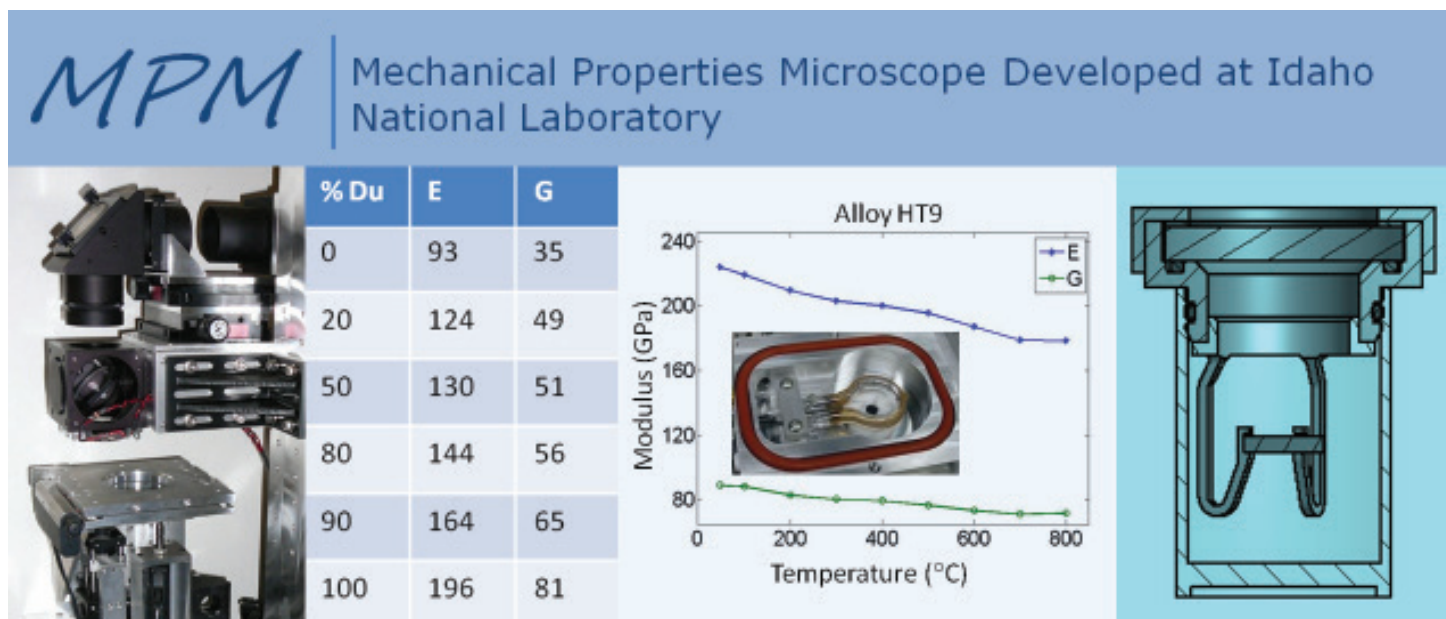


Figure 7. Left: Photograph of MPM, Left-middle: Elastic constants of UZr system vs. composition (values reported in GPa), Right-middle: Elastic constants of HT9 vs. temperature (inset: heating furnace), Right: Sample loading capsule.

A high temperature furnace was designed and constructed that can heat samples to 1000 °C. The furnace, which utilizes radiative heating, is shown in the inset of the middle-right pane of Figure 7. To minimize heat transfer to the environment, the sample chamber is evacuated, which increases the maximum sample temperature and reduces optical lensing issues. As shown in right-middle pane of Figure 7, the functionality of the furnace has been demonstrated by measuring the elastic constants of a Ferritic-Martensitic alloy (HT-9) up to 800 °C.

The MPM requires optical access to both the top and bottom surfaces of a sample. Irradiated samples also require preparation and loading in a remote environment. To meet these requirements, a sample capsule along with a sample loading technique have been developed (right pane of Fig. 7). The sample is held in place by four thin "J" shaped legs. A notch on the short side of each leg supports the sample. The legs deflect to allow the sample to be loaded into position. With the sample held captive in the sample holder, the holder is sealed under vacuum to a quartz tube with a quartz window in the bottom. This sealed capsule containing the sample can then be transported to the MPM for high temperature measurements. The long thin legs minimize thermal conduction away from the sample and allow maximum exposure of the sample to the IR radiation from the heating element.

A similar laser-based instrument, used to measure thermal conductivity, is also being developed. The optical access requirements for the Thermal Conductivity Microscope are similar to the MPM. As a consequence, some system components have dual-platform utility. For instance, a similar heating furnace as described above is being developed for the TCM. Minor changes to the existing furnace will include moving the sample closer to the front window to enable strong focusing with a microscope objective and removal of the backside window. Moving the sample closer to the front window will raise issues concerning uniform heating and uniform sample temperature. These issues are currently being addressed.

## **Additional activities**

The exchange of information and sharing of knowledge between INL and ITU continues as, for example, with the exchange of know-how on EPMA nuclearization and operation. In addition to regular email communication and meetings at conferences, dedicated visits were organized. The exchange of information covers all EPMA related topics such as adaptation of devices to the nuclear environment (e.g. application of coating and decontamination procedures for sample preparation, hot cell – EPMA lab transport containers and shielded connections for sample introduction in the device), EPMA related software, reference materials, sample preparation and analytical methodology. Karen Wright (INL) will visit ITU (P. Poeml, S. Brémier) for 2 weeks in April 2014. Karen will observe how EPMA of irradiated fuels is performed at ITU. The objective is also to share tips and compare the daily practices of the 2 laboratories. The specific case of EPMA on metallic fuel alloys is a topic of interest for ITU whereas INL benefits from the general experience of handling irradiated materials developed in ITU. INL participates in the informal group of shielded microprobe users that ITU launched some years ago. INL and ITU participate in the forum of users of the "Probe for EPMA" software that both laboratories use.

INL and ITU will co-organise a nuclear related symposium at the next Microscopy and Microanalysis conference in Hartford, US in 08/2014.

The exchanges on the EPMA are considered as a fruitful example by the researchers involved. This type of collaboration will be extended to the FIB. In this case, INL is already operating a FIB on irradiated fuel whereas ITU is still at an installation stage. Another area where technical exchanges and synergies are envisaged is the thermal transport characterization of irradiated fuel using techniques that cover different scale ranges (from micron to millimetre).

## **Planned Activities**

Continue to find resolution to the issues associated with sample sharing transport of higher level radioactive materials, including fuels. The identification of a viable transport solution to exchange samples between INL and ITU is essential for the deployment of the full scope of the present collaboration program. Until a solution is found, the scope of the joint work will remain forcibly limited.

Continue interactions related to post irradiation examinations with emphasis on operation of EPMA as well as advanced technique development such as micro X-ray diffraction, focused ion beam (FIB), thermal conductivity measurements, and mechanical property measurements.

# Development of a 2E-2V Instrument for Fission Fragment Research

## Research Objectives

The objective of the project is to produce accurate data files of fission measurements and evaluations for several key isotopes over the incident neutron energy range relevant to present and future nuclear applications. Design, optimization, and safety assessment of future fast reactor systems require improved fission fragment nuclear data for major and minor actinides. The project will contribute to the ENDF/B-VII and JEFF 3.1 nuclear data libraries.

The research team is developing instrumentation for high-resolution measurements of fission product velocity, energy, and nuclear charge. The resulting data provides fission product mass and the corresponding yield curves. This work supports ongoing developments at two spectrometer facilities: the VERDI (VElocity foR Direct particle Identification) spectrometer at the Institute for Reference Materials and Measurements, and a similar dual-arm spectrometer at Los Alamos National Laboratory (LANL). The current VERDI spectrometer measures energy and velocity from only one of the two fission products emitted in binary fission (hence, 1E-1V), while the advanced instruments will simultaneously measure both fission fragments (2E-2V). In addition, the LANL dual-arm instrument will also use Bragg curve spectroscopy to measure nuclear charge.

The collaboration consists of exchange of expertise and technologies, joint experimental efforts, sharing of detector designs, and communication of technical and scientific information. The two instruments are being developed in parallel, and the teams share technologies that benefit the joint program. Experimental activities are also being carried out with other facilities at both laboratories, including the Geel Linear Accelerator (GELINA), the 7-MV Van de Graaff neutron source (MONNET), and the Los Alamos Neutron Science Center (LANSCE). Key project tasks are as follows:

- Complete the design study.
- Prepare prototype design/technical report.
- Conduct initial measurements.

Project Number: 2011-001-E

**PI (U.S.):** Fredrik Tovesson, Los Alamos National Laboratory

**PI (Euratom):** Stephan Oberstedt, Joint Research Center–Institute for Reference Materials and Measurements

**Collaborators:** Idaho National Laboratory

**Program Area:** Reactor Concepts RD&D

**Start Date:** October 2011

**End Date:** September 2014

## Research Progress

Work during the first year focused on testing the individual parts of the detector array to develop a design for the full system. In order to build a 2E-2V instrument with high resolution, it is necessary to design detectors that measure time of flight with high timing resolution (100–200 picoseconds [ps]) and an instrument that provides high-resolution (<1%) energy measurements of fission fragments.

Researchers completed testing of a time-of-flight instrument based on thin conversion foils, electrostatic mirrors and ultra-fast micro channel plates. The system's timing resolution was tested with fission fragments from a Cf-252 spontaneous fission source and with alpha particles from a Th-229 calibration source. As shown in Figure 1, the measurement using the Th-229 source indicates five peaks in the time-of-flight histogram—one for each of the five main alpha-particle energies. The time resolution extracted from this measurement is 190 ps, corresponding to 135 ps per detector, which meets the design requirement. Based on these results, the project team decided to use this basic design for the time-of-flight section of the full instrument.

Detection efficiency of the time-of-flight detectors is important to ensure high counting statistics in fission yield measurements. Using a calibration source, the research team evaluated efficiency by registering coincidences between the timing detector and a silicon detector. The number of coincidences was measured for different accelerating potentials on the timing detector's electrostatic mirror, and the result is shown in Figure 2. The efficiency for alpha-particles was shown to be about 70% and fairly insensitive to the acceleration potential. The next step will be to check the efficiency for fission fragments, which is expected to be significantly higher because of their higher specific ionization in the conversion foil.

The project team also designed a first ionization chamber prototype for fission fragment energy measurements, shown in Figure 3a. In this case, a tri-isotope alpha-source was used to investigate the resolution, which was determined to be 1.1% (see Figure 3b). This still needs to be improved slightly, and there is work in progress to build a second prototype that will be run with different counting gases, at lower pressures, and with more sophisticated signal processing to further improve the resolution.

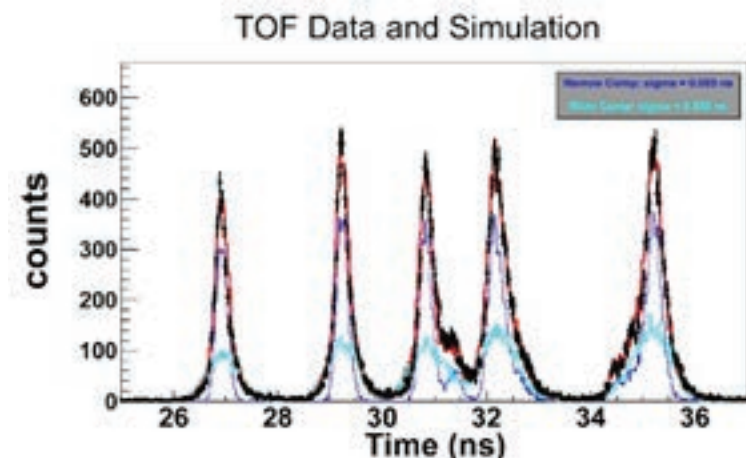


Figure 1. Time-of-flight measurement of alpha-particles from a Th-229 calibration source (black points) overlap the simulation (red line). The time resolution was determined to be 190 ps (full width at half maximum [FWHM]) based on this measurement.

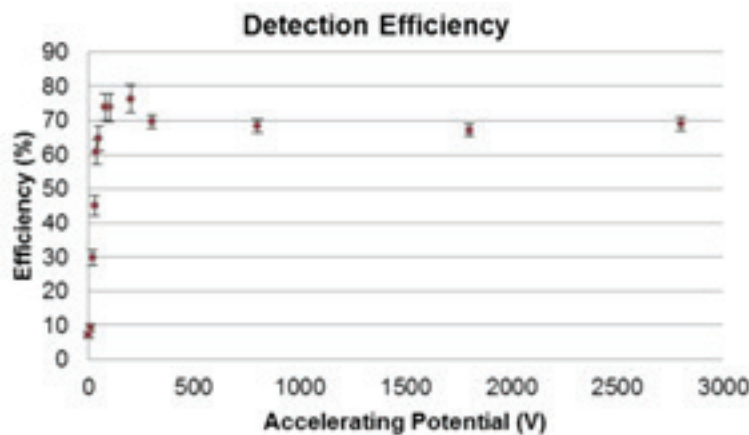


Figure 2. Efficiency of the timing detectors for alpha-particles as a function of accelerating potential on the electrostatic mirror.

# High-Fidelity Thermal Hydraulic Fuel Assembly Simulations for Nuclear Reactors

This project engages in cross-code verification of the high-fidelity computational fluid dynamics (CFD) models applied to nuclear reactor core flows. The aim is to systematically cross-verify the models of the four partner institutions in nuclear reactor core geometries characterized by either rod bundles or pebble beds, using common data shared among team members. A more reliable methodology can reduce arbitrary safety margins and the need for testing new designs and lead to improved design efficiency. However, proposed methodologies must be thoroughly verified and validated. There is currently a scarcity of useful experimental data to validate high-fidelity computations in complex geometries such as those in reactor cores.

At Argonne National Laboratory, the Simulation-based High-efficiency Advanced Reactor Prototyping (SHARP) project is a multi-divisional collaborative effort to develop a modern set of design and analysis tools for advanced nuclear reactors. With the SHARP suite, users construct highly detailed component models using high-fidelity methods or complex virtual reactor models that accurately reproduce the multi-physics behavior of nuclear reactor cores. The Nuclear Research and Consultancy Group employs primarily the commercial STAR-CCM+ finite volume CFD code, while Ghent University and SCK•CEN both use the ANSYS suite of codes. These codes will be compared using commonly agreed benchmarks.

The project objectives are to 1) systematically verify high-fidelity computational tools in the two geometries under examination (rod bundles and pebble beds) and 2) identify potential experiments to be used in validation exercises. By exchanging information and benchmark results, the researchers will be able to identify discrepancies or concerns with current predicting technologies. With these concerns identified, the team will then propose an experimental plan for validation.

## **The project involves three major tasks:**

- Verification of large eddy simulation (LES) or direct numerical simulation (DNS) CFD codes for rod bundle flows and related analysis. Rod bundles in nuclear reactors are typically spaced by

Project Number: 2012-001-E

**PI (U.S.):** Elia Merzari, Argonne National Laboratory

**PI (Euratom):** Ferry Roelofs, Nuclear Research and Consultancy Group

**Collaborators:** Ghent University, SCK•CEN (Belgian Nuclear Research Centre)

**Program Area:** Reactor Concepts RD&D

**Project Start Date:** October 2012

**Project End Date:** September 2015

rigid mechanical devices such as wires or grids. The presence of such devices complicates the flow considerably, and the lack of detailed experiments makes CFD validation problematic. The participants will work toward verifying numerical simulations pertaining to rod bundle flows.

- **Verification of DNS/LES CFD code for pebble bed flows and related analysis.** Participants will simulate pebble bed core flows and compare results. Future work will focus on finding efficient ways to accurately compute the flow in a realistic random pebble bed.
- **Experimental plan for validation of LES/DNS codes for rod bundles and pebble beds.** Based on the results of the two tasks above, the research team will devise a separate effects experimental plan to validate high-fidelity CFD codes.

As part of the first task, In the first year, a benchmark simulation campaign of the flow in a 7 pin rod bundle with wire-wrappers was conducted. The wire-wrapped bundle is a complex configuration for which few data are available for verification and validation of new simulation tools. The European collaborators performed their simulations with commercially available computational fluid dynamics (CFD) codes. High-fidelity large-eddy simulations (LES) were performed at Argonne with Nek5000, the open-source, high-performance CFD tool part of the Simulation-based High-efficiency Advanced Reactor Prototyping (SHARP) suite. Comparisons were conducted at Argonne National Laboratory and summarized in an Argonne Report [1]. A meeting of the three institutions was also conducted in Ghent (Belgium).

Comparison of the results obtained by the three institutions with Nek5000 results has shown good agreement, at least for the cross-flow data (Fig. 1). The collaborators are analyzing the results further and will define additional simulations, with the objective of a comprehensive journal publication.

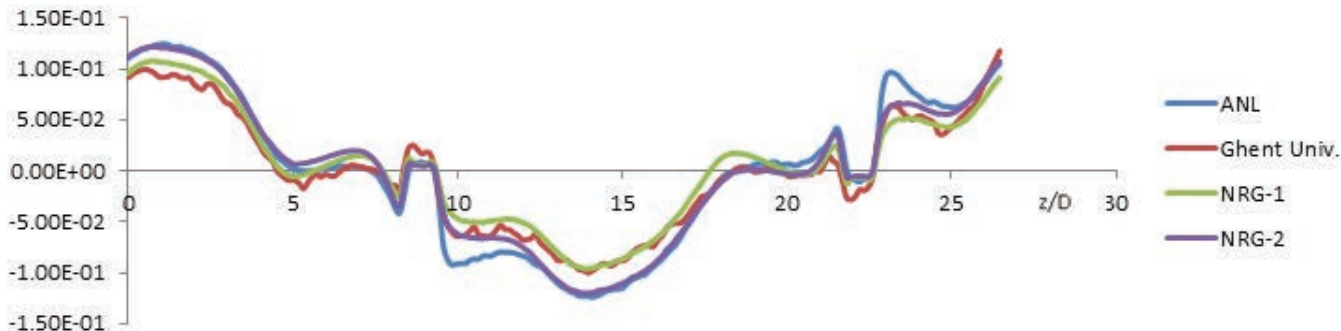


FIGURE 1. One of the cross flow comparisons in the 7 pin rod bundle benchmark – Central pin. Cross flows are normalized by  $U_{bulk}^*g$  (where  $g$  is the gap size without wire).

For the fiscal year 2013-2014, the collaborators continue working on wire-wrappers simulation. In particular the focus is on a conjugate heat transfer benchmark (i.e., heat transport is being simulated both in the coolant and the cladding) for a 19-pin rod bundle. The benchmark features geometry characteristics similar to the MYRRHA fuel assembly design. High fidelity calculations will again be performed at Argonne while the European counterpart will perform calculations with commercial software. Comparisons will be conducted at NRG, and a meeting of the participants is currently planned for September 2014 in Brussels.

For the fiscal year 2013-2014, the collaborators continue working on wire-wrappers simulation. In particular the focus is on a conjugate heat transfer benchmark (i.e., heat transport is being simulated both in the coolant and the cladding) for a 19-pin rod bundle. The benchmark features geometry characteristics similar to the MYRRHA fuel assembly design. High fidelity calculations will again be performed at Argonne while the European counterpart

will perform calculations with commercial software. Comparisons will be conducted at NRG, and a meeting of the participants is currently planned for September 2014 in Brussels.

As part of the second task, a set of pebble bed simulations have been conducted at Argonne National Laboratory (Fig. 2) and compared with available DNS data from NRG. The new data produced at Argonne represents a very high resolution DNS dataset. Velocity, turbulence statistics and turbulence "budgets" have been collected at various Reynolds numbers. This data will be invaluable for further verifying lower fidelity models such as Reynolds averaging Navier-Stokes (RANS) and LES-based simulations. In particular, this is the first instance turbulence budgets have been collected for pebble geometries to our knowledge. This type of data is invaluable for RANS model development, as it allows verification and improvement of specific terms in the modeling of the transport equations for the turbulent kinetic energy.

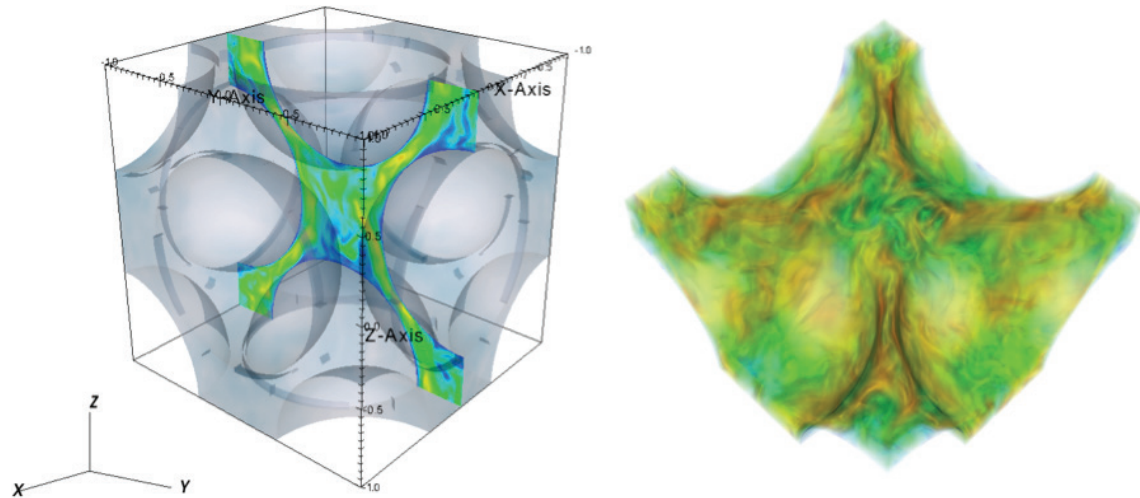


FIGURE 2. Pebble bed simulations at Argonne. (left) View of the computational domain and cross section with snapshot of the instantaneous velocity magnitude (right) volume rendering of the velocity field.

The new data confirms the presence of an asymmetry in the flow field. Moreover the velocity profile was proven to depend upon the Reynolds number, with an increasing degree of asymmetry at higher Reynolds numbers. Linear stability calculations performed at Argonne hint that this phenomenon might be due to the presence of a fundamental asymmetric mode in the transition from laminar to turbulent flow [2].

For the present year, work on the second task continues at Argonne on the simulation of pebble beds with different parameters and domain sizes. Simulations of single pebble domains continue to be conducted at different Reynolds number while simulations are being extended to multiple-pebble domain with groundbreaking DNS simulations.

[1] E. Merzari, P. Fischer, "BENCHMARK EXERCISE FOR FLUID FLOW SIMULATIONS IN A LIQUID METAL FAST REACTOR CORE", Technical Report ANL/NE 13-20, Argonne National Laboratory, 2013

[2] P. Ward, E. Merzari, Y. Hassan and P. Fischer, "DIRECT NUMERICAL SIMULATION AND LINEAR STABILITY ANALYSIS OF THE FLOW IN A PEBBLE BED", Proceedings of FEDSM2014 (accepted)

# Novel Technology For Synthesis of Nuclear Fuels

This project investigates advanced net shaping technology for nuclear fuel/target applications. The U.S. contribution to this collaborative research effort will be performed under the DOE Fuel Cycle Research and Development (FCR&D) program. The EURATOM contribution will be performed under Euratom FP7 and HORIZON 2020 programs on Safety of Nuclear Fuel

This project will advance the field of novel compaction technology for advanced fuel systems where conventional routes are not viable. Advanced fuels being studied for enhanced accident tolerance and for actinide transmutation often have unique characteristics which make conventional sintering routes undesirable for or incapable of yielding the required fuel pellet characteristics. For illustration, one example is UO<sub>2</sub>-composite fuels with second phases for increased thermal conductivity that have deleterious reactions with the UO<sub>2</sub> fuel above operating temperatures but below temperatures required to sinter a high quality fuel pellet. A second example is nitride fuels/targets which require such high temperatures for traditional sintering that there is an undesirably high loss of both Pu and Am due to volatilization during the sintering steps. Advanced compaction techniques, such as field assisted sintering and spark plasma sintering, offer the potential to generate these advanced fuel systems at reduced temperatures such that the damaging reactions and material loss are avoided.

Work on this project will focus on employing novel sintering techniques for several advanced fuel systems. The collaboration will enable efficient development and communication of not only process/structure relations for a set of ceramic fuel compositions but will also facilitate enhanced understanding of the effects of applied field and current on the processing behavior for advanced ceramic fuels, including oxide, nitride, carbide, silicide and boride based fuel systems. Finally, this collaboration will also enhance the necessary understanding for efficient assessment of process limiting interactions and therefore understanding when alternatives to conventional sintered should be employed.

Project Number: 2013-001-E

PI (U.S.): Kenneth McClellan, Los Alamos National Laboratory

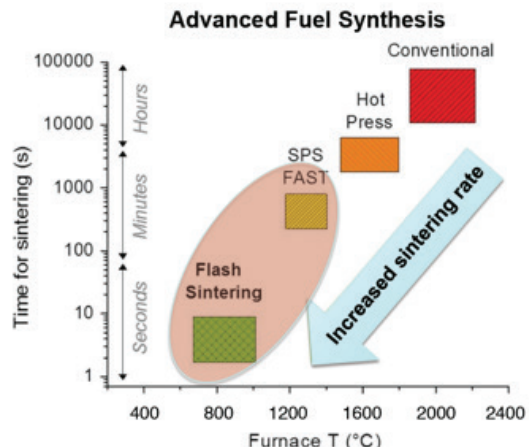
PI (Euratom): Joseph Somers, Joint Research Center-Institute for Transuranium Elements

Collaborators: Idaho National Laboratory, Oak Ridge National Laboratory, University of Florida

Program Area: Fuel Cycle R&D:

Project Start Date: October 2013

Project End Date: September 2016



This project will integrate the various embryonic advanced processing activities ongoing at each participating institution which will in turn allow this effort to encompass several field assisted sintering techniques employed for a range of ceramic systems. The primary techniques and materials systems for each institution are:

**Los Alamos National Laboratory:** Compare and contrast process/structure/property relations of multi-component, multi-phase advanced (high fissile density, U-based) ceramic fuel systems fabricated by both field assisted sintering and conventional sintering.

**Idaho National Laboratory:** Spark plasma sintering, microstructural characterization and property optimization of high fissile density ceramic-based fuels.

**Oak Ridge National Laboratory:** Thermodynamic and thermo-kinetic assessment of composite fuel interaction to inform advanced processing parameters.

**University of Florida:** Spark plasma sintering, microstructural characterization and property optimization of UO<sub>2</sub>/nano-diamond fuels with enhanced thermal conductivity.

**Joint Research Center- Institute for Transuranium Elements:** Adaptation of spark plasma sintering to plutonium environment for the comparison of oxide, nitride and carbide materials compaction using conventional press and sinter routes

# Phase Equilibria and Thermochemistry of Fission Products in Urania Fuel

The specific objective of the proposed I-NERI is to develop data and models for complex urania solid solutions and secondary phases with fission products (FPs). For example, a complete data set for RE FPs in urania is lacking, and there has yet to be a definitive study as to how molybdenum behaves in fuel and does the element indeed provide control over oxygen potential. It is the oxygen potential generated in the oxide fuel that is the source of the oxidation of the inner surface of cladding. As alternative cladding concepts are explored, understanding this relationship will be key to determining oxidation of the metals. New and literature reported measurements of chemical activities and determination of phase equilibria will be coupled with development of solid solution representations, most notably the compound energy formalism for fluorite structure urania containing additional metals. The thermodynamics of the dissolution of FPs in urania, including representation of oxygen potential-composition-temperature relations and consideration of potential secondary phases of selected fission products will be developed. The data will be used to generate optimized solid solution models, and determine formation of secondary phases. This information will allow development of an inclusive thermodynamic datafile for oxide fuel undergoing burnup, including the various solid solutions in addition to fluorite structure urania. Such thermochemical datafiles will be usable in fuel performance codes currently under development.

## The project involves the following tasks:

- **Modeling Urания-Yttria.** Extensive literature review and data-mining will be undertaken to obtain current phase equilibria and thermodynamic values for urания-yttria. The data will be assessed to determine a self-consistent set of information and a database will be generated. The base models for urания and uranium phases from Gueneau et al. (2011) will be used. Critical measurements that are needed to model the urания-yttria system will be identified and a series of TGA experiments

Project Number: 2013-002-E

**PI (U.S.):** Theodore Besmann, Oak Ridge National Laboratory

**PI (Euratom):** Rudy J. M. Konings, Joint Research Centre-Institute for Transuranium Elements

**Collaborators:** Advanced nuclear fuels and materials

**Program Area:** Fuel Cycle R&D

**Project Start Date:** October 2013

**Project End Date:** September 2016

will be developed to determine the needed values. The data along with literature values will be used directly in computing constituent free energies and solution interaction parameters in optimizations. (ORNL)

- **Modeling Urania-Praseodymia:** The task described above for urania-yttria will be repeated for the urania-praseodymia system. (ORNL)
- **Modeling Molybdenum Compounds in Urania Fuel:** The literature on the thermodynamic properties relevant molybdenum compounds (binary oxides and ternary oxides with cesium and barium) will be collected and reviewed and recommended data will be presented. The evaluation and applied models will be consistent with other databases for nuclear materials. (JRC-ITU)
- **Modeling Ruthenium/Zirconium Compounds in Urania Fuel:** The task described above for urania-yttria will be repeated ruthenium and zirconium. (JRC-ITU)
- **Development of Joint ORNL-JRC-ITU Datafile:** A datafile for use with the FactSage thermochemical software will be generated, initially using the already obtained urania models. This will serve as the baseline set of models into which the various FP elements can be included. The datafile will also be made available to the OECD-Nuclear Energy Agency project on Thermodynamic of Advanced Fuels – International Database. (ORNL – JRC-ITU)



Petten High Flux Reactor  
Photo courtesy of Euratom

## 4.2 United States–Republic of Korea Collaborative Projects

Director William D. Magwood IV of DOE-NE signed the first bilateral I-NERI agreement on May 16, 2001, with Director General Chung Won Cho with the ROK, signing for the ROK Ministry of Science and Technology. The first U.S.–ROK collaborative research projects were awarded in FY 2002, with a total of 49 projects awarded to date.

Areas of mutual interest between the two countries cover next-generation reactor and fuel cycle technology concepts that increase efficiency, safety, reliability and proliferation resistance; innovative nuclear plant design, manufacturing, construction, operation, maintenance and decommissioning activities; reactor safety; and fundamental nuclear sciences. Ongoing projects and fuel cycle R&D will be completed; however, any new collaborative efforts in these specific will be consolidated under the U.S.–ROK Joint Fuel Cycle Study.

Four U.S.–ROK projects were completed, while efforts continued on five projects. Three new projects were selected for award, and started in 2013.

Table 1 is an overview listing of completed, on-going, and new I-NERI U.S.–ROK projects, followed by summaries of their FY 2013 accomplishments and overviews.

Project Number**	Project Title	Completion Year
2010-001-K	Investigation of Electrochemical Recovery of Zirconium from Spent Nuclear Fuels	2013
2010-002-K	Science-Based Approach to Nickel Alloy Aging and its Effect on Cracking in Pressurized Water Reactors	2013
2010-003-K	Low-Loss Advanced Metallic Fuel Casting Evaluation	2013
2010-004-K	Development and Characterization of Nanoparticle-Strengthened Dual-Phase Alloys for High-Temperature Nuclear Reactor Applications	2013
2011-001-K	Atomic Ordering in Alloy 690 and Its Effect on Long-Term Structural Stability and Stress Corrosion Cracking Susceptibility	2014
2011-002-K	Development of Microcharacterization Techniques for Nuclear Materials	2014
2011-003-E	Verification and Validation of High-Fidelity Multi-Physics Simulation Codes for Advanced Nuclear Reactors	2014
2011-004-K	Development of Diagnostics and Prognostics Methods for Sustainability of Nuclear Power Plant Safety Critical Functions	2014
2011-005-K	Fully Ceramic Microencapsulated Replacement Fuel for Light Water Reactor Sustainability	2014
2013-001-K	Generation of Physics Validation Database and Analysis of Fast Reactor Depletion Capability	2016
2013-002-K	Science-Based Approach to Nickel Alloy Aging and Its Effect on Cracking in Pressurized Water Reactors	2016
2013-003-K	Low-Loss Advanced Metallic Fuel Casting Evaluation	2016

\* Completed in FY 2013

# Investigation of Electrochemical Recovery of Zirconium from Spent Nuclear Fuels

## Research Objectives

This project uses both modeling and experimental studies to design optimal electrochemical technology methods for recovery of zirconium from used nuclear fuel rods for more effective waste management. The objectives are to provide a means of efficiently separating zirconium into metallic high-level waste forms and to support development of a process for decontamination of zircaloy hulls to enable their disposal as low- and intermediate-level waste. Modeling work includes extension of a 3D model previously developed by Seoul National University for uranium electrorefining by adding the ability to predict zirconium behavior. Experimental validation activities include tests for recovery of zirconium from molten salt solutions and aqueous tests using surrogate materials.

## Research Progress

To investigate dissolution and deposition behavior of zirconium in molten salt, cyclic voltammetry, chronopotentiometry, and anodic stripping voltammetry were conducted with molten salts consisting of LiCl-KCl-ZrCl<sub>4</sub>, LiCl-KCl-UCl<sub>3</sub>, and LiCl-KCl-UCl<sub>3</sub>-ZrCl<sub>4</sub> at 500°C. Details of the oxidation and reduction reactions for each peak were defined based on an electrolysis experiment and previous cyclic voltammetry results from literature. For the zirconium reduction, Zr(IV), is reduced to ZrCl rather than Zr metal when cathode potential is not negative enough. Therefore, to directly recover zirconium metal, the cathode potential should be maintained at less than -1.5V (vs. Ag/AgCl). From the electrochemical tests performed, key physical properties (diffusion coefficient, standard reduction potential, and activity coefficient) were measured.

Project Number: 2010-001-K

**PI (U.S.):** Michael Simpson, Idaho National Laboratory

**PI (ROK):** Il-Soon Hwang, Seoul National University

**Collaborators:** Korea Atomic Energy Research Institute, University of Idaho

**Program Area:** Fuel Cycle R&D

**Project Start Date:** December 2010

**Project End Date:** November 2013

Table 1 summarized the values for these properties measured for U(IV), U(III), Zr(IV), and Zr(II).

	Diffusion coefficient, D (cm <sup>2</sup> /s)			Apparent standard reduction potential, E* (V vs Cl <sub>2</sub> /Cl <sup>-</sup> )			Activity coefficient, γ
	450 °C	500 °C	550 °C	450 °C	500 °C	550 °C	
U(IV)	---	6.72×10 <sup>-6</sup>	---	---	-1.448	---	0.00236 – 0.0109
U(III)	---	1.04×10 <sup>-5</sup>	---	---	-2.568	---	4.86×10 <sup>-5</sup> – 4.42×10 <sup>-4</sup>
Zr(IV)	5.85×10 <sup>-6</sup>	5.05×10 <sup>-6</sup>	7.88×10 <sup>-6</sup>	-2.012	-1.972	-1.914	---
Zr(II)	4.73×10 <sup>-5</sup>	6.87×10 <sup>-5</sup>	6.33×10 <sup>-5</sup>	-2.234	-2.190	-2.138	---

Table 1. Summary of Electrochemical and thermodynamic properties of UCl<sub>3</sub> and ZrCl<sub>4</sub> in LiCl-KCl.

Cobalt is the impurity of interest in the zircaloy cladding. Cyclic voltammetry for cobalt was conducted, and it was revealed that oxidation and reduction reactions of cobalt are much simpler than zirconium. Cobalt is also more reductive than zirconium. In addition, lab-scale electrorefining of Zircaloy-4 was performed and results are summarized in Table 2. Anode potential was controlled to prevent dissolution of all elements except zirconium. Composition of cathode deposits was evaluated by ICP-MS analysis. Zirconium of 99.7 wt% was recovered on the cathode with Fe and Cr impurities. Since Fe and Cr came from the initial molten salt, it is speculated that pre-purification of the molten salt could lead to achieving almost 100% Zr purity on the cathode.

Zircaloy-4 specimen		Deposits with LiCl-KCl		Deposits except LiCl-KCl	
Element	wt%	Element	wt%	Element	wt%
Zr	98.6	Zr	79.1	Zr	99.7
Sn	1.104	Sn	0	Sn	0
Fe	0.1595	Fe	0.1	Fe	0.2
Cr	0.0830	Cr	0.1	Cr	0.1
Co	0.0016	Co	0	Co	0
Li	N/D	Li	1.2	Li	-
K	N/D	K	19.4	K	-

Table 2. Composition of Zircaloy-4 specimen and cathode deposits.

Two pilot scale Zircaloy cladding electrorefiners were designed. One is an electrorefiner including auxiliary electrode, and another is a rotating drum cell electrorefiner. Characteristics of each electrorefiner were simulated via a three-dimensional multi-species electrodeposition model. It was predicted that a very high purity zirconium can be deposited on the main cathode, and most of the other elements can be dissolved from the anode and deposited on an auxiliary cathode. Furthermore, it is expected that zirconium metal rather than ZrCl<sub>4</sub> can be obtained on the cathode, since its potential can be controlled to be more negative than -1.5V (vs. Ag/AgCl). For the rotating drum cell electrorefiner, uniform contacting of cladding hulls with the molten salt can be achieved, and chlorine gas can be readily collected from the anode.

Table 3. Typical material balance after casting of U-10Zr-3RE fuel pins.

	Melting/casting part	Weight (g)	Fraction (%)
Before casting	Crucible	2,647	100.0
After casting	Crucible assembly	317	12.0
	Mold assembly	2,228	84.2
Fuel loss		102	3.8

	Melting/casting part	Weight (g)	Fraction (%)
Before casting	Crucible	2,490	100.0

A process has also been designed with the objective of selectively recovering zirconium from the Mark-IV ER. It involves electrorefining excess U metal followed by oxidizing residual U metal to UCl<sub>3</sub>. Then further oxidation would occur to convert a fraction of the Zr metal to ZrCl<sub>4</sub>. Then it is hypothetically possible to electrorefine purified Zr from the cadmium pool to the cathode. Two models were run to assess the viability of this process. As noted in Table 3, both predicted that high purity Zr cathode deposits could be achieved even with relatively high UCl<sub>3</sub> concentrations in the salt, provided that no U metal is in contact with the salt.

### Planned Activities

None. The project has been completed.

# Science-Based Approach to Ni-Alloys Aging and Its Effect on Cracking in PWRs

Project Number: 2010-002-K

**PI (U.S.):** Chi Bum Bahn and Ken Natesan, Argonne National Laboratory

**PI (ROK):** Ji Hyun Kim, Ulsan National Institute of Science and Technology

**Collaborators:** Korea Atomic Energy Research Institute, Seoul National University

**Program Area:** Reactor Concepts RD&D

**Project Start Date:** December 2010

**Project End Date:** September 2013

## Research Objectives

One of main objectives of this project was to investigate the effects of aging on the microstructure and SCC behavior of a dissimilar metal weld. Advanced instrumental analysis techniques were successfully applied, including in-situ Raman spectroscopy. The other objective was to fundamentally study the effect of Pb on Alloy 600 SG tube corrosion/cracking. In-situ oxide film study was also successfully conducted. Planned deliverables were completed as shown in a table below.

During the final year, microstructural analysis was conducted for the weld interface specimens aged at 400°C, which showed microstructures similar to those of specimens aged at 450°C. SCC testing was completed for the heat affected zone and weld interface specimens. In-situ Synchrotron X-ray analysis was conducted to observe the solid/liquid interface. X-ray reflectivity data was obtained at the Ni(NiO)/water interface. In-situ impedance spectroscopy showed the oxide evolution in the Pb-containing solution.

Milestone/Deliverable Description	Planned Completion Date	Actual Completion Date
Alloy 690/Alloy 152/LAS weld mock-up fabrication and aged weld sample fabrication	Nov./2013	Nov./2013
CGR testing at the weld/LAS interface	Nov./2013	Nov./2013
Aged weld sample characterization	Nov./2013	Nov./2013
Ni single crystal/water interface analysis by Synchrotron X-ray	Nov./2013	Nov./2013
Oxidation kinetics study for SG tube material in Pb containing solution	Nov./2013	Nov./2013

Korean participants from UNIST are still continuing the microstructural analysis work initiated under the I-NERI, focusing on Alloy 690 heat affected zone. ANL continues aging of the weld specimens at the lower temperature of 370°C.

The results obtained under this I-NERI program can be used to understand the long-term aging effect of structural materials in LWRs. In-situ synchrotron X-ray analysis and impedance spectroscopy can enhance the understanding of the basic corrosion phenomenon occurring at the interface between metal (metal oxide) and water.

# Low-Loss Advanced Metallic Fuel Casting Evaluation

## Research Objectives

The objective of this project is to develop methods of minimizing fuel losses and reducing waste streams during fabrication of metallic fuel pins for sodium-cooled fast reactors (SFRs). This work will enhance the technical readiness level of the metallic fuel fabrication process. This process has three phases: (1) fuel pin casting, (2) loading and fabrication of the fuel rods, and (3) fabrication of the final fuel assemblies. Most fuel losses and waste/recycle streams occur during fuel pin casting. Recycle streams include fuel pin rework, returned scraps, and fuel casting heels, which are of special concern in the counter-gravity injection casting process because of the large masses involved. Large recycle and waste streams lower the productivity and economic efficiency of the fabrication process.

The project team will evaluate fuel losses that occur during casting of U-Zr/U-TRU-Zr (uranium-transuranic-zirconium) fuel pins for an SFR. This will be accomplished by casting a considerable amount of fuel alloy in a furnace, and then quantitatively evaluating losses in the melting chamber, crucible, and mold. After identifying and quantifying materials at key process stages, the team will develop means of reducing losses, including permanent crucible coatings, permanent reusable molds, and advanced techniques such as continuous casting. The goal is to develop a coating technology for re-usable crucibles with good thermal cycling characteristics and excellent compatibility between fuel melt and coating layer. The scope of work consists of three major tasks:

- Casting development and mold loss comparison
- Coating development and characterization
- Continuous casting technology

## Research Progress

### Casting Development and Mold Loss Comparison

The research team at Korea Atomic Energy Research Institute (KAERI) cast batches of U-10Zr-1,3,10RE (weight basis), where the RE alloy is made up of 53% Nd, 25%Ce, 16% Pr, 6% La, on approximately a 2.5 kilogram scale.

Project Number: 2010-003-K

**PI (U.S.):** Randall Fielding, Idaho National Laboratory

**PI (ROK):** Dr. Ki-Hwan Kim, Korea Atomic Energy Research Institute

**Collaborators:** None

**Program Area:** Fuel Cycle R&D

**Project Start Date:** December 2010

**Project End Date:** December 2013

Chemical composition and mass balance of both batches were measured and used to determine fuel loss levels. All batches cast well. Mass balances for each composition are shown in the following tables:

Table 1. Typical material balance after casting of U-10Zr-1RE fuel pins.

	Melting/casting part	Weight (g)	Fraction (%)
Before casting	Crucible	2,647	100.0
After casting	Crucible assembly	317	12.0
	Mold assembly	2,228	84.2
Fuel loss		102	3.8

Table 2. Typical material balance after casting of U-10Zr-3RE fuel pins.

	Melting/casting part	Weight (g)	Fraction (%)
Before casting	Crucible	2,490	100.0
After casting	Crucible assembly	78	3.1
	Mold assembly	2,380	95.6
Fuel loss		32	1.3

Table 3. Typical material balance after casting of U-10Zr-10RE fuel pins.

	Melting/casting part	Weight (g)	Fraction (%)
Before casting	Crucible	2,325	100.0
After casting	Crucible assembly	35	1.5
	Mold assembly	2,285	98.3
Fuel loss		6	0.2

A considerable amount of dross and melt residue remained in the crucible after melting and casting; however, most charge materials were recovered after casting of the fuel pins. The amount of dross and melt residue in the crucible after fabrication of U-10Zr-1RE fuel pins was much higher than that of U-10Zr-3RE or U-10-10RE fuel pins. The large fuel loss in the U-10Zr-1RE fuel pins is likely caused by the melting and casting temperature of U-10Zr-1RE fuel being higher than that of U-10Zr-3RE or U-10Zr10RE. The higher melt temperature led to a greater amount of dross and residue in the crucible.

It was originally expected that there would be lower fuel losses for the lower (1-3%) RE containing fuel alloys as compared to the 10%RE alloy. Generally, RE elements are chemically active with the crucible so a higher fuel loss was expected, but it is thought that the lower losses in case of the U-10Zr-3,10RE fuel pins is related to crucible coating. The melting took place in a graphite crucible coated with a dense plasma-sprayed high-temperature ceramic material. These results show that gravity casting can be a feasible fabrication technology for producing a significant number of the fuel pins, which meet the goal of 0.1% fuel losses during fabrication.

Further experiments were carried out using manganese as a surrogate americium as the vapor pressure at the temperatures of interest are similar. These casting tests were done using the

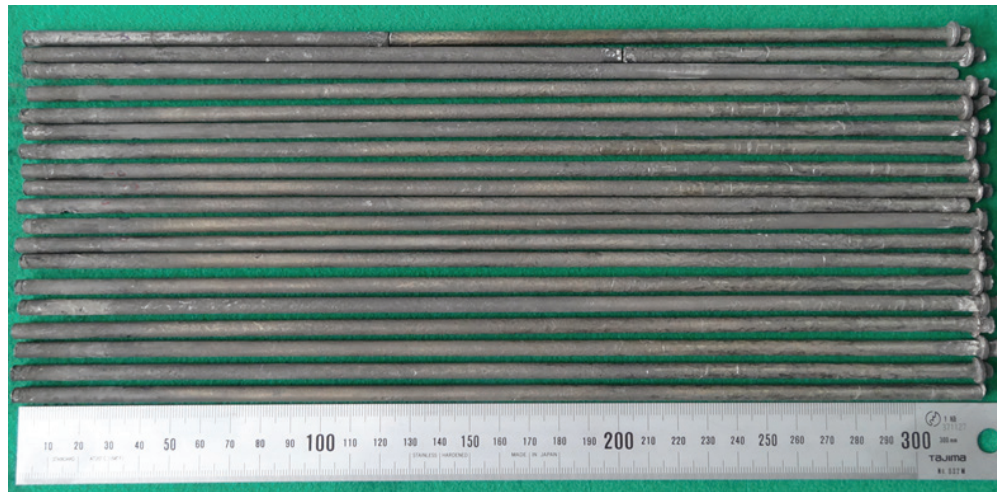
counter-gravity injection casting process as was used for the EBR-II fuel fabrication, however, the application of the vacuum was applied at different stages.

Figure 1 shows a typical batch of U-10Zr-1RE cast pins. As can be seen in the figure although some surface defects are present in general the pins are sounds and of full length. The material balance for the crucible and mold assembly after injection casting the S13-03 batch of U-10Zr fuel pins is shown in Table 4. Low fuel losses were expected because the injection casting process is simpler than that of the gravity casting method. As shown in the table, fuel losses after casting, relative to the initial charge of U-10Zr were very low, approximately 0.1%. These results show that injection casting can be a feasible fabrication technology for producing a significant number of the fuel pins, while meeting the goal of 0.1% fuel losses during fabrication.

The material balance for the crucible and mold assembly after injection casting U-10Zr-5Mn fuel pins, casting batch S13-04, is shown in Table 5. During casting, a reduced pressure was applied for only a short time before inserting the molds into the melt so little evaporation was expected. As shown in the table an increase of fuel loss due to evaporation of the Mn of only about 0.2% is observed compared to that of the U-10Zr fuel casting (S13-03).

The material balance for the crucible and mold assembly after fabrication of the S13-05 casting batch of U-10Zr-5Mn fuel pins is shown in Table 6. During casting, a vacuum was applied throughout the entire casting process, so a large amount of evaporation was anticipated. As shown in the table, an approximate 3.10% increase in fuel loss is observed compared to the U-10Zr fuel pins where the reduced pressure was applied for a short time only.

The material balance for the crucible and mold assembly after casting the S13-06 batch of U-10Zr-5Mn fuel pins is shown in Table 7. During this casting run a reduced pressure was not applied during the casting process so only a small amount of evaporation was anticipated. As shown in table, about a 0.2% increase of fuel loss is observed compared to the U-10Zr fuel pins.



**Table 4. Material balance after casting for the S13-03 batch of U-10Zr fuel pins.**

	Melting/casting part	Weight (g)	Fraction (%)
Before casting	Crucible	584.90	100.0
After casting	Crucible assembly	498.40	85.21
	Mold assembly	85.80	14.67
Fuel loss		0.70	0.12

**Table 5. Material balance after casting for the S13-04 batch of U-10Zr-5Mn fuel pins.**

	Melting/casting part	Weight (g)	Fraction (%)
Before casting	Crucible	655.00	100.0
After casting	Crucible assembly	573.80	87.60
	Mold assembly	79.30	12.11
Fuel loss		1.90	0.29

**Table 6. Material balance after casting for the S13-05 batch of U-10Zr-5Mn fuel pins.**

	Melting/casting part	Weight (g)	Fraction (%)
Before casting	Crucible	607.20	100.0
After casting	Crucible assembly	497.10	81.87
	Mold assembly	91.30	15.04
Fuel loss		18.80	3.10

**Table 7. Material balance after casting for the S13-06 batch of U-10Zr-5Mn fuel pins.**

	Melting/casting part	Weight (g)	Fraction (%)
Before casting	Crucible	608.20	100.0
After casting	Crucible assembly	538.70	88.57
	Mold assembly	68.20	11.21
Fuel loss		1.30	0.21

**Figure 1. U-10Zr-RE fuel pins.**

Casting activities at the INL included installation and testing of the GACS furnace in a transuranic capable glove box and initiation of transuranic bearing fuel casting development. Furnace design and mock-up testing occurred in previous years. Mock-up testing was particularly advantageous because many aspects of the design were modified or changed in order to provide an easier and more predictable operation. The GACS furnace is a bench scale casting system that can be used for either gravity or counter gravity injection casting. Figure 2 shows a schematic of the furnace and the furnace installed in the glovebox. The furnace has a capacity

of up to approximately 500 grams, but will usually be charged with approximately 200-300 grams. The current mold is configured to cast three pins at approximately 4.2 mm diameter and 250 mm long. The graphite mold and crucible are independently induction heated.

A small, 100 g, casting batch was used for the initial transuranic bearing casting. Table 8 shows the initial charge. It is noted that the zirconium feed was split between elemental zirconium and a Pu-Am-Zr alloy. The final charge composition was nominally U-7.4Pu-1.7Am-10Zr. This composition was chosen based on available transuranic feedstock and facility limits. All of the feedstocks were loaded in the crucible and heated to the casting temperature. The mold also was heated to approximately 500°C during the crucible heat up time but climbed to approximately 600°C from crucible heating during the crucible hold. After the material reached approximately 1450°C it was held for 10 minutes, after which the stopper rod was pulled and material flowed down into the molds. Pressure was maintained under a dynamic vacuum for the first five minutes of the run to allow for low-temperature, <350°C, degassing. After this time the pressure was increased to approximately 600-700 Torr (80.0-93.3 kPa) and maintained in that range for the duration of the casting process. The crucible was slurry coated with yttria and the mold cavities were slurry coated with zirconia.

The casting run resulted in three short pins being cast. Table 9 shows the resulting mass balance. The original charge was purposely made small, so the short length was expected. Two of the pins were approximately 100 mm in length while the third was approximately 75 mm in length with a large thinned section approximately 50 mm from the bottom. Figure 3 shows the three pins along with two "drips," or material that solidified on the wall of the pin mold before it could travel down and coalesce with the pin. Other than the previously mentioned thin section, the pins appeared to be sound and free from substantial surface flaws. A slight mismatch on the pin bottom results from the shape of the mold and shows the molten material did flow to the bottom of the mold and, in fact, started to fill the 0.6 mm groove leading to the 1.1 mm vent hole at the bottom of each pin cavity. A heel was retained in the crucible, resulting from molten material not fully draining into the mold. It is assumed that this material was retained due to surface tension and not

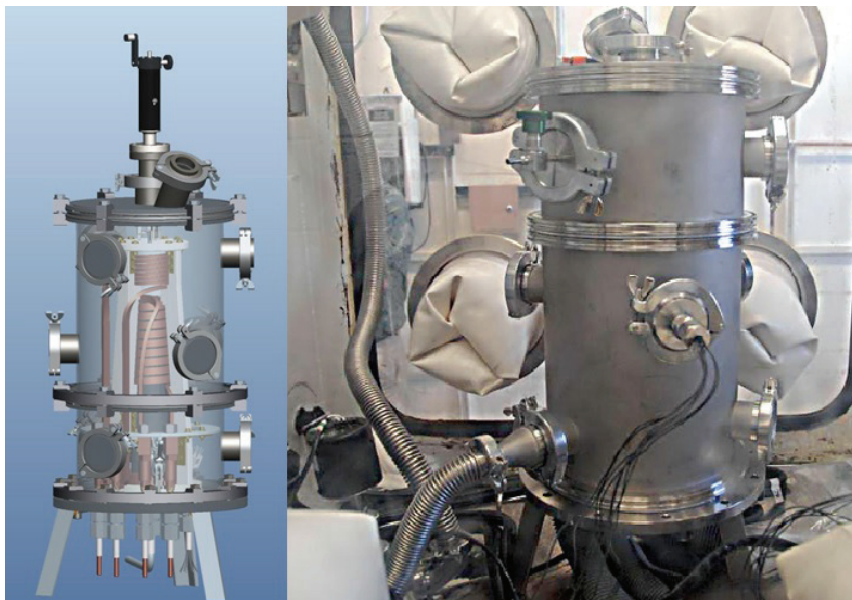


Figure 2. Schematic and photo of GACS configured for gravity casting. Note the linear actuator has been removed for the photo.

inadequate temperature because 1450°C is substantially above the melt point of the alloy. Also, of note, after the bulk of material drained, a small amount of liquid flowed over the 9.5 mm diameter casting orifice at the bottom of the crucible, closing off the hole. This behavior again shows a high surface tension of the melt leading to a substantial heel being left in the crucible. A substantial amount of dross was also present in the form of a loose powder adhering to the heel and monolithic slag/dross that adhered to the stopper rod.

**Table 8. Casting charge for the initial U-TRU-Zr casting.**

Charge Material	Mass (g)	Wt%
Uranium	80.66 <sup>a</sup>	80.96%
Zirconium	3.77 + Prealloy Zr	10.06% <sup>b</sup> (8.86% <sup>c</sup> )
Pre-Alloy TRU-Zr	15.22	—
Plutonium	7.45 <sup>b</sup> (6.03 <sup>c</sup> )	7.49% <sup>b</sup> (6.05% <sup>c</sup> )
Americium	1.49 <sup>b</sup> (1.21 <sup>c</sup> )	1.5% <sup>b</sup> (1.21% <sup>c</sup> )
Zirconium	6.25 <sup>b</sup> (5.05 <sup>c</sup> )	—

a. Chemical analysis of pre-alloyed TRU resulted in approximately .02g of uranium.

b. Calculated based on normalized chemical analysis data of prealloyed button.

c. Calculated based on the chemical analysis results not normalized to 100%.

**Table 9. Mass balance of cast product, assuming homogeneous Chemical composition of all products.**

	Net	U	Pu	Am	Zr	Ca	Mg	Wt. fraction
Initial Charge	99.633	81.898	7.448	1.225	8.917	0.028	0.042	100%
Pin 1	22.665	18.631	1.694	0.279	2.029	0.006	0.010	22.7%
Pin 2	21.221	17.446	1.586	0.261	1.90	0.006	0.009	21.3%
Pin 3	14.166	11.644	1.059	0.174	1.268	0.004	0.006	14.2%
Drip 1	7.600	6.247	0.568	0.093	0.680	0.002	0.003	7.6%
Drip 2	5.560	4.570	0.416	0.068	0.498	0.002	0.002	5.6%
Dross	2.231	1.834	0.167	0.027	0.200	0.001	0.001	2.2%
Heel	17.069	14.031	1.276	0.210	1.528	0.005	0.007	17.1%
Stopper material	9.071	7.456	0.678	0.112	0.812	0.002	0.004	9.1%
Process Loss	0.047	0.039	0.004	0.001	0.004	0.000	0.000	0.05%



Figure 3. Resuting pins and drips from the U-TRU-Zr casting experiment (claipers are set at 25.4mm)

After unloading of the furnace, each of the 4" pins were sampled from the top and bottom area of the pin. These samples were chemically analyzed using inductively-coupled plasma mass spectroscopy and optical emission spectroscopy. The resulting chemical analysis is shown in Table 10.

Table 10 showed that the cast product was axially chemically homogeneous to within the reported analysis error. This shows that the inductive forces during the melting are adequate to mix the melt homogeneously. This is an important result considering the short melting times and the disparity in component densities. In addition to this, when the input material composition is considered it can be seen that americium was retained throughout the melting process. As discussed above, because the TRU material was added as a TRU Zr pre alloyed feedstock, the initial input composition is calculated based on an assumed feedstock composition based on previous material accountability records. Normalized chemical analysis of pre alloyed TRU Zr shows it to be 48.96Pu 9.81Am 41.05Zr, which agrees well with material accountability records. However, during dissolution of the feedstock button, a black undissolved solution was first seen; this solid was treated with aqua regia. The black precipitate did begin to dissolve, but a yellow precipitate then formed that could not be further dissolved. The yellow precipitate was filtered out and the final solution analyzed. The results only showed a mass balance of 80.88. If it is assumed that the precipitate was another element not analyzed or a transuranic compound that was not dissolved, i.e. a ceramic or intermetallic, the pre-alloyed button composition changes to 39.6Pu 7.93Am 33.2Zr 19.12X, where X is another element or compound. If the undissolved solids were a TRU-bearing intermetallic or ceramic that could not be dissolved, it is likely that it would combine with the dross layer in the casting operation. When Table 10 is compared to the calculated charges, the Pu and Am numbers fall in between the two nominal charge calculations. Therefore, it may be possible that the undissolved solids were a Pu Am components that also may have come out as in the dross phase. These results indicates that the americium was retained during the casting process due to the fast heating cycle and inert overpressure.

Table 10. Chemical analysis results of the cast pins. Reported error at  $2\sigma$  is 5%

	Uranium	Plutonium	Americium	Zirconium	Calcium	Magnesium
Pin #1 Btm	82.0%	7.38%	1.25%	8.96%	.04%	0.08%
Pin #1 Top	84.2%	7.63%	1.24%	9.02%	0.00%	0.02%
Pin #2 Btm	81.7%	7.44%	1.24%	8.97%	0.01%	0.03%
Pin #2 Top	80.9%	7.45%	1.19%	8.85%	0.04%	0.04%
Average	82.2%	7.48%	1.23%	8.95%	0.02%	0.04%

As part of the casting development effort, the resulting cast product from the initial U-TRU-Zr casting was re-melted an additional two times and cast into an ingot as opposed to pins. A typical furnace temperature and pressure profile is shown in Figure 4. A surface oxide/dross was formed during the melting process and was present on the initial rods used as feedstock; however, the ingot was fully melted and coalesced as evidenced by the bottom of the ingot. The second ingot was made by breaking the first ingot into several pieces and re-melting. Many of the pieces of the first ingot were still visible in the second ingot, but there is also clear evidence of melting. Both ingots were analyzed to determine americium content; the resulting chemical analysis is shown in Table 11, with the reported error at  $2\sigma$  being 5%. As seen in Tables 10-11, americium content appears to be consistent between the two ingots and the initial casting, although one of the two samples from each ingot has a lower americium content and there is variability in the Zr content for the samples.

Table 10 shows the starting composition contained on average 1.23% americium. The two samples after the first melt showed americium levels were at 1.18% and 0.99%. The disparity between these two samples is not well understood. The samples were taken as random pieces from the broken ingot; therefore, some segregation may have occurred during melting i.e. the oxide dross phase may have contained a higher americium content which may not have been captured in the sample. However, the sample containing 1.18% americium is within the standard error of the starting material. After breaking the first ingot, it was remelted and sampled in the same manner again. This led to reported americium levels of 1.18% and 1.02%. Again, the disparity of the two samples is not well understood and cannot be addressed further, but the level of 1.18% remains within error of the originally sampled rod feedstock. Both melts were melted in an open crucible with a continuous argon purge of approximately 7 ft<sup>3</sup>/hr during the melting and soak cycle. The resulting ingot from the second volatility run did have a more pronounced oxide skin that may have interfered with the pieces fully fusing together, although, when the bottom of the second ingot is examined, it does appear that the ingot was fully molten. Despite the differences in the americium content between the two samples of each ingot, the americium levels from ingot to ingot stayed within the same range if reported error is taken into account. A logical conclusion from this is that some segregation may have occurred within the ingot that led to the difference in the samples, but the overall americium level was maintained in the ingot, despite being melted three times, if the original casting melt is included.

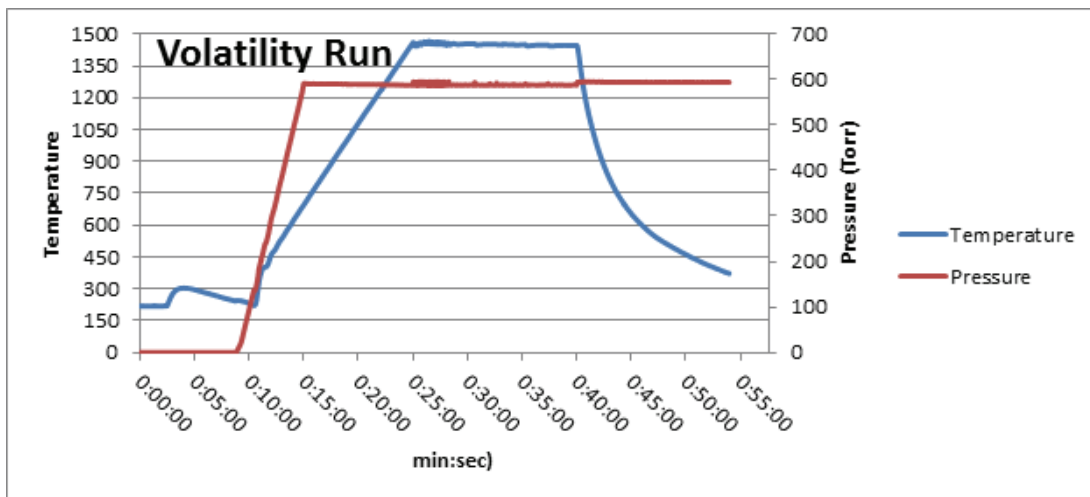


Figure 4. Typical furnace pressure and temperature profile for the volatility experiments.

### Coating Development and Characterization

Sample ID	Uranium	Plutonium	Americium	Zirconium
	Percent (%)			
Run 1 Sample 1	81.9	7.66	1.18	9.97
Run 1 Sample 2	83.5	7.64	0.99	8.66
Run 2 Sample 1	81.1	7.54	1.18	11.1
Run 2 Sample 2	83.5	7.48	1.02	10.2

Table 11. Chemical analysis of volatility runs.

Based on coating and U-Zr interaction results performed during previous years,  $\text{Y}_2\text{O}_3$ , TiC, and TaC coating materials were selected as promising coating materials for preventing the interaction between the coating layer and the U-Zr melt. In order to overcome the issue of thermal expansion mismatch between coatings and crucibles, various combinations of coating conditions such as coating thickness and multi-layer coating methods were investigated to find the optimal coatings and application parameters to withstand the thermal stresses. Based on the result from the interactions with U-10Zr and U-10Zr-5RE melt, single layer  $\text{Y}_2\text{O}_3$ (125), multi-layer TiC(100)- $\text{Y}_2\text{O}_3$ (100) and TiC(100)- $\text{Y}_2\text{O}_3$ (100) plasma-sprayed coating methods have been applied to graphite crucibles. Following coating injection casting experiments of U-10Zr and U-10Zr-5RE fuel slugs were performed to investigate the feasibility of re-use of the plasma-spray coated graphite crucibles. The graphite crucibles plasma-spray coated with a single-layered  $\text{Y}_2\text{O}_3$ (125), double-layered (100)- $\text{Y}_2\text{O}_3$ (100) and TiC(100)- $\text{Y}_2\text{O}_3$ (100) remained intact without an interaction layer with the melt after reusing the crucible for up to 2 casting cycles. Coupons of these coating compositions have been provided to INL researchers for testing in U-TRU-Zr melts at a later date.

### Continuous Casting

Earlier work on continuous casting development at KAERI showed that continuous casting of uranium is feasible and was carried out successfully. However, development with U-15Zr was not

as successful. In order to perform preliminary evaluations of fuel losses and feasibility of continuous casting of U-Zr alloy, the casting equipment was modified to account for the higher casting temperature and the more chemically aggressive nature of the U-15Zr alloy. Modifications included changing the design of the crucible and mold, or die, to allow a better flow of material during casting. In addition to these modifications, KAERI also has modified the coil, cast rod cooling system, and casting starting mechanism, including the starter-bar. The starting bar and mechanism was originally composed of copper alloys, which is a common industrial standard, and was adequate for pure uranium alloys. However, because of the aggressive nature of the U-Zr alloys, these materials would start to dissolve upon contact with the molten U-Zr melt. To overcome this issue the starting mechanism was re-designed using Type 304 stainless steel. Mo, Zr, and Inconel were used as the starter bar materials because the starter bar is in direct contact with the molten alloy and higher temperature materials were required. After the modifications were made, previous experimental results and procedures were reviewed and additional castings were attempted to produce U-15Zr pins.

Elemental zirconium and uranium were charged to the crucible and heated under vacuum until the melting point of uranium was reached. At the time of uranium melting the pressure was  $7.4 \times 10^{-3}$  Torr. Upon uranium melting argon was added to the chamber. A 8 mm starting rod was used to seal the melting chamber during heating and to withdraw the cast rod. Upon melting of the entire charge the starting bar is slowly withdrawn, allowing the molten alloy to contact the chilled walls of the die. The molten material solidifies upon contact and shrinks back from the die wall significantly decreasing the fuel rod diameter. During the withdrawal process a significantly higher withdrawal pressure or tension was generated than originally expected on the starting bar at which time the casting cycle was stopped to prevent product or equipment damage. After the casting process was terminated the cast rod was cut resulting in a rod approximately 147 mm in length. Based on these initial results fuel fabrication using continuous casting may be feasible, but would require substantial development to become a practical fabrication route. Also based on these results, because a vacuum pressure in not employed when the material is molten, it is thought that this process would also be expected to retain americium during the casting process.

### **Planned Activities**

Because of the cost and time required to install the GACS into a highly contaminated TRU qualified glovebox much of the planned work could not be carried out. This work will continue which includes U-TRU-Zr casting development which may also include incorporation of rare earth elements. In addition to casting development KAERI researchers have provided candidate mold/crucible coating materials for testing in TRU bearing alloys. These samples will be exposed to the molten alloy and characterized to determine optimized coating material.

# Development and Characterization of Nanoparticle-Strengthened Dual-Phase Alloys for High-Temperature Nuclear Reactor Applications

Project Number: 2010-004-K

**PI (U.S.):** Thak Sang Byun and David T. Hoelzer, Oak Ridge National Laboratory

**PI (ROK):** Ji-Hyun Yoon, Korea Atomic Energy Research Institute

**Collaborators:** None

**Program Area:** Fuel Cycle R&D

**Project Start Date:** December 2011

**Project End Date:** November 2013

## Research Objectives

The nanostructured ferritic alloys (NFAs) have been considered as primary candidate materials for both future fission and fusion reactors for their excellent creep strength and high dose irradiation resistance. In the past, however, the pursues of ultra-high strength NFAs commonly resulted in poor fracture toughness and ductility at high temperatures. The main objective of this research was to develop nanoparticle-strengthened alloys with excellent fracture toughness for application to high performance reactor core structures. This project also aims to produce a material property database for optimized materials, which includes tensile deformation data, fracture toughness data, high temperature deformation (including creep) data, and microstructural data for grain structure and distribution of nanoparticles.

## Research Progress

To achieve the primary goal, the researchers both at Oak Ridge National Laboratory (ORNL) and at Korea Atomic Energy Research Institute (KAERI) have combined the best processing practices for mechanical alloying and well-designed post-extrusion thermo-mechanical treatments (TMTs). To use the benefits of partial phase transformation in strengthening boundaries, the two atomized base alloys were chosen to have low chromium equivalents (in wt.%): Fe(bal)-9Cr-2W-0.4Ti-0.2V-0.12C (Cr-equivalent ~10%) and Fe(bal)-9Cr-2W-0.4Ti-0.2V-0.05C (Cr-equivalent ~11.5%), respectively, named 9YWTV-PM1 and 9YWTV-PM2 alloys. The TMTs after mechanical milling and consolidation were designed to strengthen the weak boundaries produced by powder-metallurgy. Attempts were made to effectively utilize the capability of computational simulation

for phase equilibrium and the feedbacks from microstructural and mechanical characterizations. Some TMTs such as 50% controlled rolling (CR) at 900°C resulted in excellent fracture toughness at high temperatures. Detailed characterization has been performed for the best performing CR-treated NFAs.

### Process Development

Researchers applied a variety of post-extrusion TMTs to the as-extruded (consolidation-processed) 9YWT-PM1 and 9YWT-PM2 alloys. To optimize the isothermal annealing condition, specimens were annealed at or near the intercritical temperatures (830°C–1000°C) for 30 minutes to 20 hours. This thermal annealing temperature range was determined according to the results of thermal stability calculation for phases. Further, researchers applied more intensive TMTs, i.e., controlled rolling (CR) for 20% or 50% reduction at 900°C–1000°C, to induce extensive deformation-recovery mechanisms in partial phase transformation condition, as illustrated in Figure 1. The research team characterized the thermomechanically treated materials to determine their microstructural and mechanical properties.

### Microstructural Characterization

Researchers analyzed the microstructures of the newly developed NFAs using an electron backscattered diffraction (EBSD) equipped in scanning electron microscope (SEM) and a high resolution transmission electron microscope (TEM). Grain maps for the two 9YWT-PM2 samples after 900°C 20% rolling and 975°C 50% rolling, which were generated using the EBSD band contrast, were presented in Figure 2. The band contrast maps show discrete distribution of brightness between grains and grain boundaries. Small and near-equiaxed grains are observed in the 20% rolled NFA, while more elongated grains are observed in the 50% rolled NFA. The grains show a common preferred orientation of <110> along the extrusion (and rolling) direction. The vast majority of grain sizes for the NFA in as-extruded condition were in the range of 100–300 nm. It is recognized therefore that during CR treatments the grains grew by about three times to 300–900 nm, confirming that the new NFAs after final TMTs are still nanograin materials.

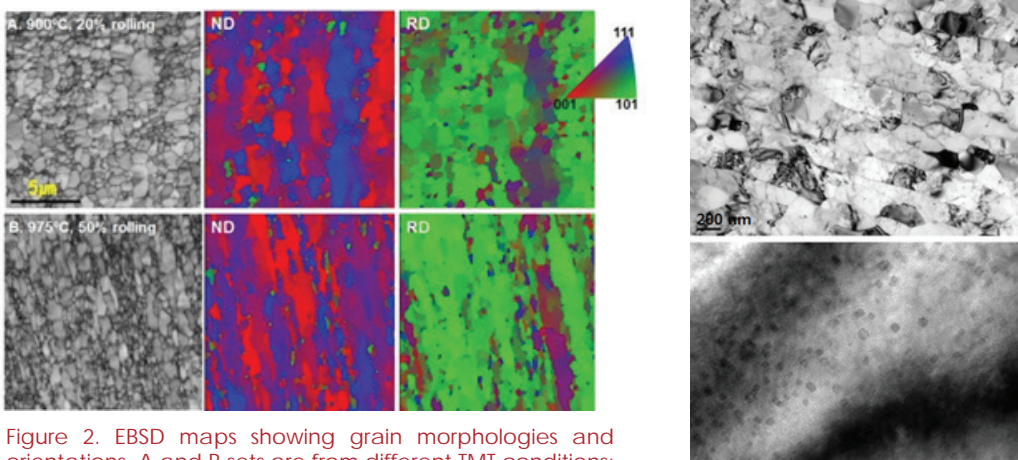


Figure 2. EBSD maps showing grain morphologies and orientations. A and B sets are from different TMT conditions: 900°C 20% rolling and 975°C 50% rolling, respectively

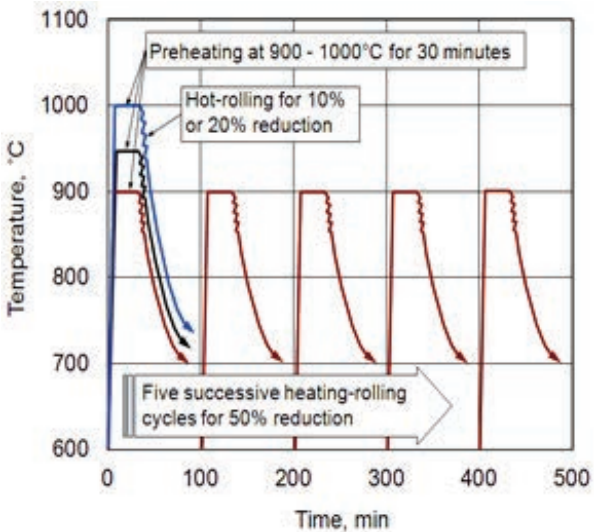


Figure 1. Schematics of controlled rolling (CR) treatments applied to Fe-9Cr base NFAs.

Transmission Electron Microscopy (TEM) micrographs for the 9YWTW-PM2 after 50% controlled rolling at 975°C are shown in Figure 3. Highly elongated grains and substructures are observed in the CR-treated material in Figure 3 (top). The subgrain structures contain high density of dislocations. A high density of nanoparticles is observed in Figure 3 (bottom); their sizes are mostly in the range of 1–4 nm. Prior to TMT, the grains in the base NFA had highly preferred orientation {110} to the extrusion direction and were mostly ferrite. Nanoparticles within the ferrite grains were almost evenly distributed and their nominal diameter was about 2 nm; particles bigger than 10 nm existed rarely. Therefore, Figure 3 showing equally small particles indicates that the nanostructure of the NFA has not been significantly coarsened during the TMT.

### Mechanical Characterization

Researchers have completed a comprehensive fracture resistance (J-R) testing and analysis to compare the effects of various TMT conditions and to demonstrate the improvement of fracture toughness in the new NFAs by the controlled rolling (CR) treatments. Cracking resistance at or near the initiation is usually defined as the fracture toughness (critical K or J value) and is considered as the most important fracture parameter. KJQ values were converted from the JQ values which are determined at the intersection of the 0.2 mm shifted blunting line and J-R curve.

While thermal annealing greatly improved fracture toughness for 9YWTW-PM2, the controlled hot-rolling resulted in even more significant increases. In Figure 4 the temperature dependence of KJQ over a wide range of temperature up to 700°C is displayed for the CR-treated NFAs. In the 9YWTW-PM2 alloy the improvement of fracture toughness by CR treatments is significant and consistent. The room temperature KJQ values were in the range of 150–280 MPa√m and the CR-treated PM2 alloy retained similar level of fracture toughness up to at least 300°C. Obvious decrease with temperature started above 300°C, but the sudden decrease of fracture toughness in 200–300°C region, which is often observed in high strength NFAs including the reference materials, did not occur in the CR-treated 9YWTW-PM2. At the highest temperature of 700°C the KJQ value after 20% rolling at 900°C and 50% rolling at 950°C decreased slightly below 100 MPa√m. Except for a few data points at room temperature and 700°C, the fracture toughness data of the CR-treated 9YWTW-PM2 fall within the band of non-NFA FM steels. Among the CR-treatments the 50% rolling at 900°C resulted in the highest fracture toughness, after which high KJQ values of >150 MPa√m were retained over the entire test temperature range. The specimens with 50% rolling at 925°C, 950°C, 975°C, and 1000°C also showed similar KJQ values throughout the test temperature range.

The main reason for such high toughness is believed to originate from high fracture strength combined with appropriate ductility. By the CR-treatments, the nanoscale fracture mechanism changed from a low energy grain boundary decohesion to a shear fracture after high plasticity. No fracture surface after a CR treatment indicated the low-energy detachment of grain boundaries which is a common high-temperature fracture mechanism in the high strength NFAs. For example, the 9YWTW-PM2 after 50% CR-treated at 900°C and tested at 700°C displays highly deformed flake-like features in its fracture surface, Figure 5. These flake-shaped units should correspond to highly deformed nanograins as their sizes are in a few to several hundred nanometers.

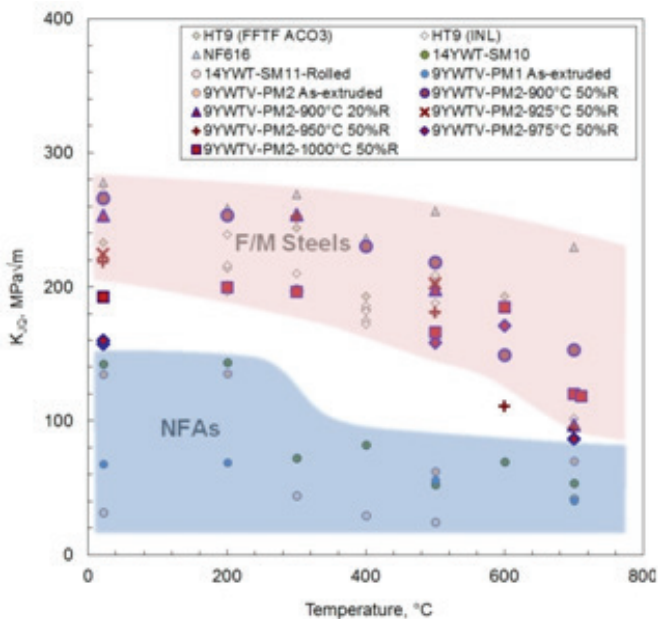


Figure 4. Fracture toughness data of 9YWTV-PM2 after hot-rolling at 900°C, 925°C, 950°C, 975°C, and 1000°C, compared to the data for FM steels and other NFAs.

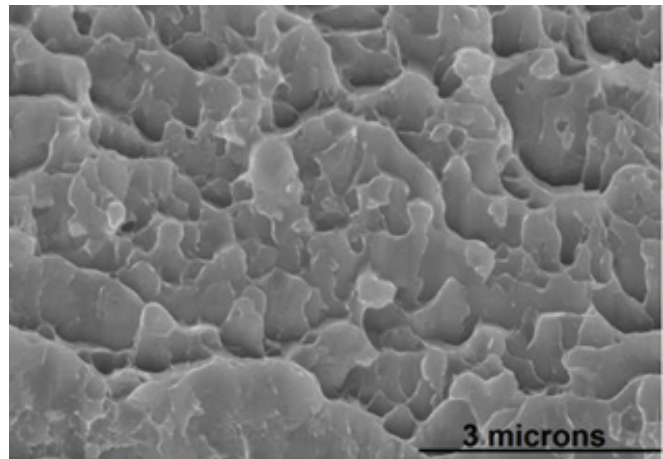


Figure 5. Fracture surface of 9YWTV-PM2 tested at 700°C after 50% hot-rolling at 900°C.

## Planned Activities

It was the final year of this I-NERI project. The project team has already published key findings in a few research articles and will continue to publish in coming years. Further, although the activities planned in the project ended as the I-NERI collaboration for the topic is closed, further studies on the new NFAs will be continued for more scientific or application purposes in the FC R&D and Fusion Materials Programs. Currently, basic study on irradiation effect in a base material is carried out in Fusion Materials Program, and high dose irradiation experiment is being pursued in FC R&D project. Upon execution of this project we realized that the delayed phase transformation in nanostructured materials and the stability of nanoclusters during TMTs have not been understood. Pursuing answers to these questions should be part of our future researches.

# Atomic Ordering in Alloy 690 and Its Effect on Long-Term Structural Stability and Stress Corrosion Cracking Susceptibility

Project Number: 2011-001-K

**PI (U.S.):** Michael Kaufman, Colorado School of Mines

**PI (ROK):** Young Suk Kim, Korean Atomic ENergy Research Institute

**Collaborators:** University of North Texas and University of Michigan

**Program Area:** Reactor Concepts RD&D

**Project Start Date:** December 2011

**Project End Date:** December 2014

## Research Objectives

Alloy 690 is being used as a possible replacement for Alloy 600 for certain applications in light water reactors. Although Alloy 690 is known to be more resistant to primary water stress corrosion cracking (PWSCC), it is not immune to PWSCC. Furthermore, an Electric Power Research Institute (EPRI) coordinated international program has demonstrated that crack growth rates as high as those encountered in Alloy 600 have occurred in high temperature deaerated primary water in thermally treated Alloy 690 subjected to 20-30% cold work. To address this issue, a better understanding of the PWSCC mechanism in Alloy 690 is required, which is the principal aim of this proposed study. Alloy 690 is prone to the formation of multiple chemical-ordering reactions leading to the formation of embrittling precipitates, such as Ni<sub>2</sub>Cr type ordering at 420°C and Fe<sub>3</sub> Ni/Ni<sub>3</sub> Fe type ordering at even lower temperatures. These ordering reactions can presumably occur under light water reactor (LWR) operating conditions and adversely affect the long-term structural stability and mechanical properties of this alloy. In other words, these ordering reactions involving Ni, Cr and Fe atoms, the main components of Alloy 690, cannot be avoided whenever they are exposed to high temperatures and stresses, which may be a critical factor to govern the life time of the structural components made of Alloy 690 in reactors. The objective of this project is to examine atomic ordering in Alloy 690 under PWR operating conditions and its effect on mechanical integrity and intergranular stress corrosion cracking (IGSCC) susceptibility of Alloy 690 and to extend the life time of Alloy 690 over 60 years.

## Introduction

Alloy 690 reportedly undergoes an ordering transformation after long-term exposure at a temperature range between 350 and 475 °C to form Ni<sub>2</sub>Cr long range ordered precipitates.

This ordering ultimately results in a degradation of properties. While this long-range ordering is well recognized in the literature, the transformation to LRO from the parent matrix is not well understood. One school of thought is that the LRO forms from a short-range order (SRO) structure that may develop after water quenching or in the first few hours of annealing of Ni-Cr alloys [1]. The nature of this SRO and its effect on properties has been the initial focus of this collaborative research project between the Colorado School of Mines, the University of Michigan and the University of North Texas on the U.S. side and KAERI on the Korea side. In total, 36 thermo-mechanical processing (TMP) conditions of Alloy 690 were prepared by KAERI and some of these were provided to the U.S. collaborators in this project. These conditions included combinations of solution anneal, cold work, thermal treatment, low (8.64 wt. %) and high (10.21 wt. %) iron contents, and varying aging times (3000 and 10,000h) and temperatures (350, 420, 475 and 550°C).

## TEM ANALYSIS

Evidence of Short Range Order in Alloy 690 TEM analysis of a number of the low Fe content KAERI specimens has been conducted since the inception of this project. Significantly, regardless of the thermomechanical processing (TMP) history, certain selected area diffraction patterns (SADPs) contained diffuse intensities purportedly due to the presence short-range order (SRO) [2]. Examples of the observed diffuse intensities are shown in Figure 1; as can be seen, there is intensity in the kinematically-forbidden  $\{422\}$  positions in  $\langle 111 \rangle$  patterns and  $\frac{1}{2}\{311\}$  reflections in  $\langle 112 \rangle$  patterns. The fact that the diffuse intensities did not appear to depend on the TMP condition suggests that the diffuse intensity might be the result of something besides SRO. Some of the possible explanations considered to date include: (1) thermal diffuse scattering (TDS) [3], (2) spiking of higher order Laue zone (HOLZ) reflections to the zero layer, and (3) Kikuchi band intersections. In an effort to determine if any of these explanations have merit, experiments were conducted as follows: Thermal Diffuse Scattering: Conduct diffraction experiments using a cryogenic stage and compare SADPs at different temperatures. Spiking of HOLZ reflections: (a) Determine if similar intensities are observed in related materials (pure Ni and a Co-Cr-Mo FCC alloy were selected). (b) Look at other zones in which the HOLZ effects would be more likely. (c) Examine the effects of thickness on the nature of the diffuse intensities. (d) Determine if there is any effect of accelerating voltage given its effect on the diameter of the Ewald sphere. Kikuchi Band Intersections: Look at thickness effects systematically. In addition, apply precession electron diffraction in order to produce more kinematic diffraction conditions [4]. In addition to these experiments, it was decided that if these intensities represent any sort of SRO, then they should be present in any zone that contains  $\{422\}$  and  $\{311\}$  reflections. Thus, tilting experiments were conducted in which specific zones were obtained that contained these reflections. The results of most of these experiments have been reported in our monthly reports during this past year. A summary of the results obtained is provided in Table 2.

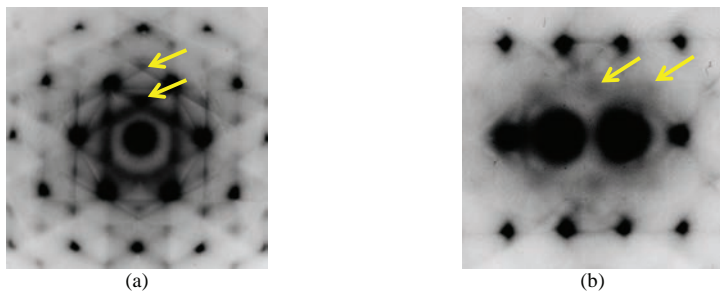


Figure 1: Typical selected area diffraction patterns (SADPs) from Alloy 690 showing diffuse scattering at the  $\{422\}$  positions in the  $\langle 111 \rangle$  pattern (a) and the  $\frac{1}{2}\{311\}$  in the  $\langle 112 \rangle$  pattern (b).

## MICROHARDNESS

Several authors have shown that hardness variations are a direct indication of atomic ordering in the Ni-Cr system [5]–[7]. As such, Vickers microhardness measurements were performed on Alloy 690 specimens, aged for up to 10,000h. A load of 500 gmf for 10s was used and the results are shown in Figure 2. As expected, the hardness after cold working is increased but, other than that, there appears to be essentially no hardness variation as a function of TMP history or aging treatment.

Figure 2: Vickers microhardness results for Alloy 690 samples aged up to 10,000 h.

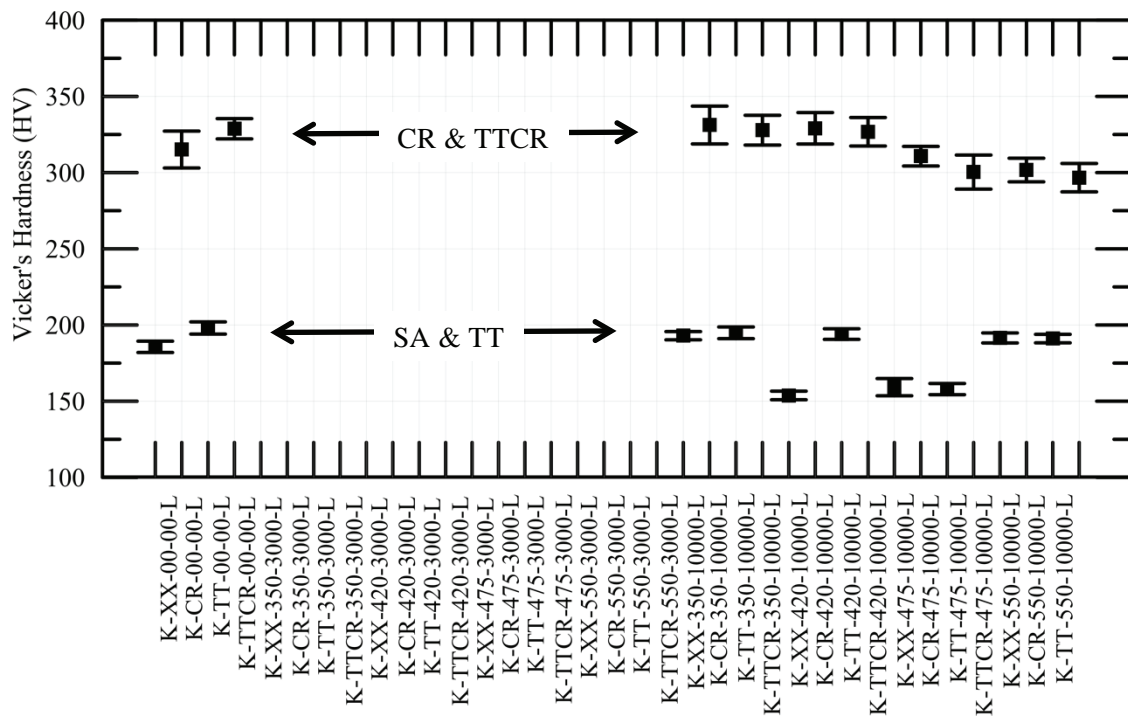
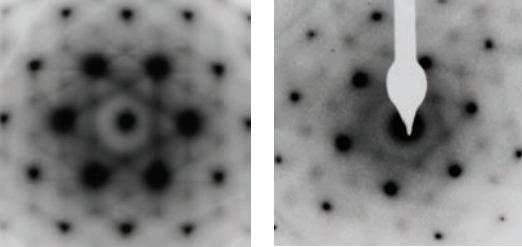
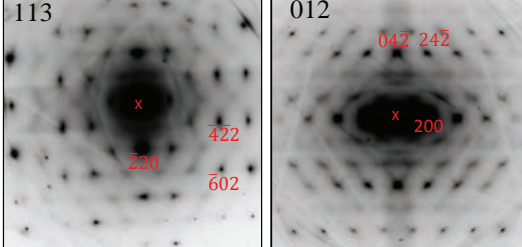
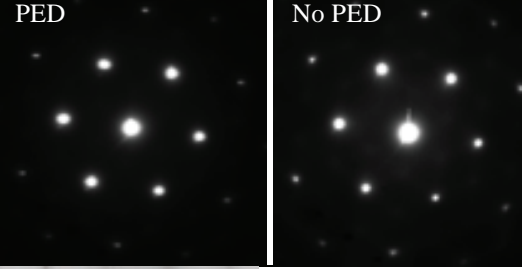
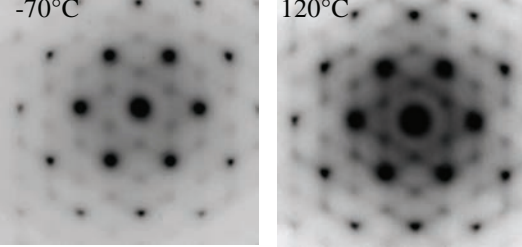
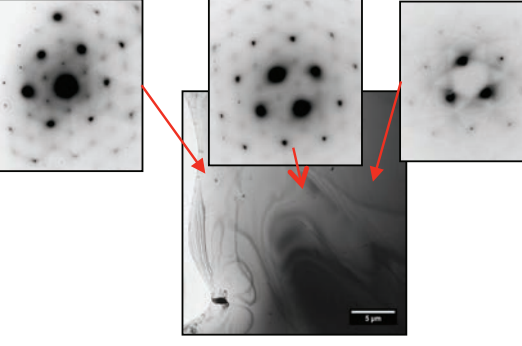


Table 1: Examples of TEM experiments that have been conducted in an effort to determine if the diffuse intensities from Alloy 690 (Figure 1) are due to SRO or some other effect.

Experiment	Results		Comments/Conclusions
<111> patterns from other materials for comparison	 <div style="display: flex; justify-content: space-around; width: 100%;"> <span>Pure Ni</span> <span>Co-Cr-Mo</span> </div>		Similar intensities seen in patterns from other materials suggesting that they are not due to SRO but, rather, to some diffraction effect.
SADPs from other zone axes containing 422 and 311 reflections	 <div style="display: flex; justify-content: space-around; width: 100%;"> <span>113</span> <span>012</span> </div>	The $\frac{1}{3}\{422\}$ and $\frac{1}{2}\{311\}$ reflections were usually not observed in other patterns containing 422 and 311 reflections. This suggests that these diffuse intensities are not due to SRO.	
Precession electron diffraction (PED) experiments	 <div style="display: flex; justify-content: space-around; width: 100%;"> <span>PED</span> <span>No PED</span> </div>		Loss of diffuse intensity occurs when using PED. This is inconsistent with SRO as it suggests that the effect is dynamical in nature.
Cryostage experiments	 <div style="display: flex; justify-content: space-around; width: 100%;"> <span>-70°C</span> <span>120°C</span> </div>	No significant differences observed as a function of temperature from -70°C to 120°C. Thus, TDS seems unlikely.	
Thickness effects on diffuse intensity in <111> SADPs	 <div style="display: flex; justify-content: space-around; width: 100%;"> <span></span> <span></span> <span></span> </div>		Spots became sharper as the thickness was decreased. This would be consistent with relrod spiking from HOLZ reflections and inconsistent with SRO.

## LATTICE PARAMETER CHANGES

### Lattice Parameter Changes in Ni-Cr

According to Taylor and Hinton [1], alloys exhibiting a high degree of order also have a smaller lattice constant compared to the fully disordered condition. For Alloy 690, this assumption was examined in the synchrotron at the Argonne National Lab to study the order-disorder transition in a Ni<sub>2</sub>Cr alloy and its relative effect on lattice parameter changes. Specifically, an in-situ heating test was conducted on a LRO Ni-Cr sample (initially water quenched and annealed for 8,000h at 475°C) by heating from room temperature at a rate of 0.5°C per second up to 800°C and data was recorded every 18 seconds. The same was done while cooling the sample in air. A graph of lattice constant vs. temperature is plotted in Figure 3, with the arbitrarily selected data points being analyzed. From this plot, it is clear that lattice expansion occurs during heating of the sample as expected due to thermal expansion. However, the slope change observed after 630°C (arrow) could be due to disordering of the LRO structure. During cooling, the slope is constant and almost linear in lattice parameter decrease. Furthermore, after heating and then cooling, the lattice constant near room temperature is somewhat larger than that from the initial LRO sample. Note that the lattice parameter difference is approximately 0.29%, which corresponds to the degree of lattice contraction due to the LRO structure [8].

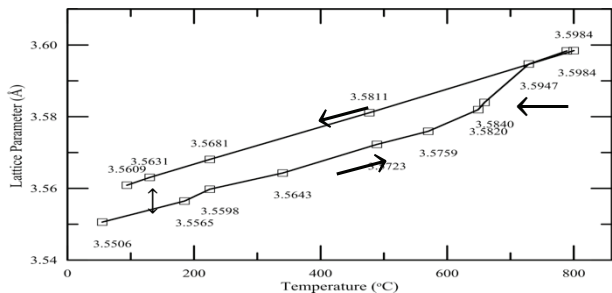


Figure 3: Lattice parameter as a function of temperature for a Ni<sub>2</sub>Cr sample initially aged for 8,000h at 475°C. This was conducted at the Advanced Photon Source (APS) at (ANL).

### Lattice Parameter Changes in Alloy 690

Two of the main manifestations of SRO are thought to be lattice contraction and increases in electrical resistivity. The lattice parameter variations of Alloy 690 were collected after various stages of heat treatment in the synchrotron at the Argonne National Lab. Table 3 shows the lattice parameters of Alloy 690 after a preliminary analysis of the synchrotron data. From Table 3, it can be seen that the lattice parameter changes after various stages of aging. Upon aging below 550°C, minimal lattice contraction is observed compared to the water quenched condition. After 550°C aging however, the matrix disorders and the lattice expands. None of the heat-treatment conditions showed any evidence of LRO; in the absence of LRO, the lattice contraction may be attributed to the formation of SRO.

Sample Condition	a <sub>0</sub> (Å)	Δa <sub>0</sub> (Å)	Δa <sub>0</sub> (%)
K-XX-00-00-L	3.5724	-	-
K-XX-350-10000-L	3.5700	0.0024	-0.0675
K-XX-420-10000-L	3.5657	0.0067	-0.1897
K-XX-475-3000-L	3.5711	0.0013	-0.0377
K-XX-550-10000-L	3.5733	-0.0008	0.0233

Table 2: Lattice parameter measurements of Alloy 690, determined using the synchrotron at ANL, showing changes in lattice parameter as a function of aging.

### 3-D ATOM PROBE TOMOGRAPHY

Atom probe tomography (APT) was performed on selected samples of both the Ni-Cr alloy and Alloy 690 to investigate the microstructure and to determine 3D chemical composition fluctuations. Through a data-mining algorithm called "clustering", inhomogeneity was detected in both aged Ni<sub>2</sub>Cr and Alloy 690. As a consistency check, water-quenched samples of both alloys were also analyzed, but no inhomogeneity was detected. It is probable that these inhomogeneities could be the manifestation of SRO that has a different composition from the matrix. Table 3 lists the results obtained from the various alloys and provides the average chemical compositions of these inhomogeneities. The bulk composition of Alloy 690 is Ni-35Cr-9Fe.

Sample Condition	Avg. Composition (at.%)
Ni <sub>2</sub> Cr WQ	Not detected
Ni <sub>2</sub> Cr aged 8,000 h, 475°C	Ni-17Cr
IN690 WQ	Not detected
IN690 aged 3,000 h, 475°C	Ni-15Cr-4Fe
IN690 aged 10,000 h at 475°C	Ni-16Cr-4.5Fe

Table 3: 3DAPT sample condition and resulting average composition using "clustering" data-mining algorithm.

### STRESS CORROSION CRACKING

All non-cold rolled conditions of the KAERI heat have been evaluated for their SCC initiation susceptibility. The gage section of each tensile bar was mechanically abraded up to #4000 grit and then electropolished. Slow strain rate tensile (SSRT) testing was used to strain the samples up to 7% plastic strain at 5×10<sup>-8</sup> s<sup>-1</sup> in 360°C high purity water containing 18 cc/kg H<sub>2</sub>. After the straining test, A JOEL JSM-6480 SEM was used to image more than 40 equally spaced areas at 1000X along the gauge section. The images were examined for intergranular cracks. For both SA and TT samples, significant serrations due to dynamic strain aging appear on the stress strain curve. It was found that the average stress amplitude of the serrations increased after aging treatments for both types of samples, which may be due to microstructural changes induced by aging. The cracking results are summarized in Figure 4. Figure 4a indicates that, for the SA samples, the differences of crack length per unit area between different aging conditions fall within the measurement errors and thus are not statistically significant. For TT samples aged for 3000 h however (Figure 4b), the crack length per unit area changes slightly. Significantly, as the aging time increases up to 10000 h, the crack length per unit area for the sample aged at 350°C increases significantly while that for the sample aged at 475°C decreases below the value for the non-aged sample.

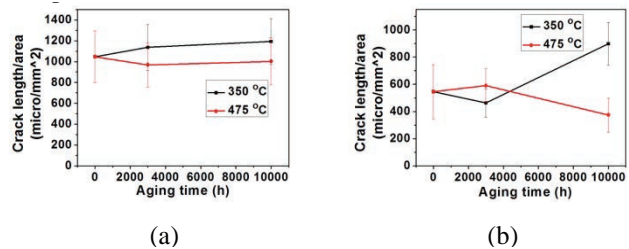
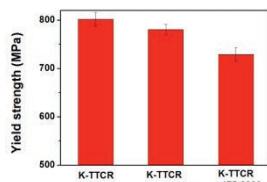


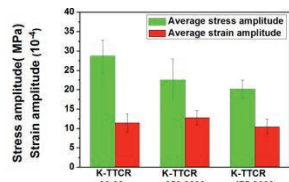
Figure 4: Crack length per unit area of (a) solution annealed and aged samples, and (b) thermally treated and aged samples which were strained to 7% at 5×10<sup>-8</sup> s<sup>-1</sup> in 360°C water containing 18 cc/kg H<sub>2</sub>.

Straining tests with thermally treated, cold rolled and aged samples have also been performed. It is very difficult to initiate SCC on cold rolled samples using the slow strain rate test technique due to the limited uniform elongation. K-TTCR-00-00 was strained to failure at 5×10<sup>-8</sup> s<sup>-1</sup> in 360°C

water containing 18 cc/kg H<sub>2</sub>. No significant SCC cracks could be found after the test. Thus, in the straining tests using K-TTCR-350-3000 and K-TTCR-475-3000 samples, both were strained to approximately 2% at a slower rate  $1 \times 10^{-8}$  s-1. The yield strengths are shown in Figure 5a. K-TTCR-350-3000 had slightly lower yield strength than did K-TTCR-00-00 while K-TTCR-475-3000 yielded at a much lower value than the other two samples. It is likely that aging at 475°C resulted in greater recovery, which causes greater softening in sample K-TTCR-475-3000. The average stress and strain amplitudes of the serrations are shown in Figure 5b. The data from K-TTCR-00-00 are also included for comparison although this sample was strained at  $5 \times 10^{-8}$  s-1. The results indicate that, in addition to significant softening, the average stress amplitude was reduced slightly. Such significant softening of cold rolled samples creates a concern that any possible effect of ordering on the SCC behavior would be masked by the reduction in residual cold work due to the thermal treatment.



(a)



(b)

Figure 5: (a) Yield strengths and (b) average stress and strain amplitudes of serrations of thermally treated and cold-rolled samples in the un-aged and aged conditions which were strained in 360 °C water containing 18 cc/kg H<sub>2</sub>

The cracking results of thermally treated, cold rolled sample are summarized in Figure 6. The crack length per unit area decreases as the aging temperature increases. Accordingly, it is thought that the residual cold work in those cold rolled samples plays a dominant role in SCC susceptibility over any possible formation of ordering.

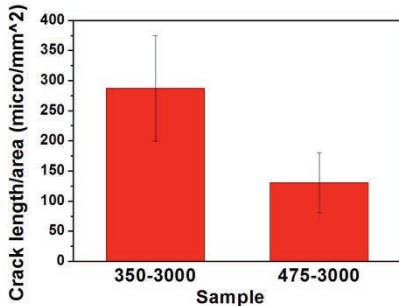


Figure 6: Crack counting results of cold rolled and thermally treated samples with two aging conditions which were strained to 2% at  $1 \times 10^{-8}$  s-1 in 360 °C water containing 18 cc/kg H<sub>2</sub>.

## REFERENCES

- [1] A. Taylor and K. G. Hinton, "A study of order-disorder and precipitation phenomena in Nickel-Chromium alloys," J. Inst. Met., vol. 81, pp. 169–180, 1952.
- [2] E. Lang, V. Lupinc, and A. Marucco, "Effect of thermomechanical treatments on short-range ordering and secondary-phase precipitation in Ni-Cr-based alloys," Mater. Sci. Eng. A, vol. 114, pp. 147–157, Jul. 1989.
- [3] D. B. Williams and C. B. Carter, Transmission Electron Microscopy: A Textbook for Materials Science, 2nd ed. New York: Springer, 2009.
- [4] C. S. Own, W. Sinkler, and L. D. Marks, "Prospects for aberration corrected electron precession," Ultramicroscopy, vol. 107, no. 6–7, pp. 534–42, 2007.
- [5] A. Marucco, "Atomic Ordering and  $\alpha'$ -Cr phase precipitation in long-term aged Ni<sub>3</sub>Cr and Ni<sub>2</sub>Cr alloys," J. Mater. Sci., vol. 30, pp. 4188–4194, 1995.
- [6] F. Delabrouille, D. Renaud, F. Vaillant, and J. Massoud, "Long range ordering of alloy 690," in 14th. Int. Conf. on Environmental Degradation of Materials in Nuclear Power Systems, 2009, vol. 690, no. 1988, pp. 888–894.
- [7] A. Marucco, "Atomic ordering in the Ni-Cr-Fe system," Mater. Sci. Eng. A, vol. 189, no. 1–2, pp. 267–276, Dec. 1994.
- [8] G. A. Young, J. D. Tucker, and D. R. Eno, "The kinetics of long range ordering in Ni-Cr and Ni-Cr-Fe alloys," in Proceedings of the 16th Annual Conference on the Environmentally Assisted Cracking of Materials in Nuclear Power Systems - Water Reactors, 2013, pp. 1–22.

# Development of Micro-Characterization Techniques for Nuclear Materials

Project Number: 2011-002-K

## Background

Since 2003, small scale mechanical testing has been available to the material science community. While a large amount of basic scientific knowledge has been obtained during this period, the application towards nuclear engineering issues is rather limited due to the limitations of engineering alloys as well as errors associated with the techniques and undeveloped procedures. The potential benefits and potential high impact of these techniques however, include but are not limited to:

- Reduced amount of radioactive material per sample to make sample handling easier and more time and cost effective.
- Being able to sample small components from reactors as well as specific areas of interest (welds, joints, bend areas, etc..)
- Making mechanical property data available on ion beam irradiated materials as "surrogates" for neutron irradiated samples.
- Obtaining large amount of statistics from small materials irradiated in reactors and being able to cross calibrate the large number of small scale mechanical testing data with the limited number of large scale mechanical testing data.
- Due to limited archived materials, the materials testing can often times only be conducted at a limited number of conditions (temperature, strain rate, environment) increasing the number of possible tests by downsizing the individual specimen size on the same material will allow to maximize the number of data from irradiated library samples.

Due to the large number of substantial benefits of new mechanical testing techniques, the intention of this project is to evaluate the existing small-scale testing techniques to improve and adapt them for engineering alloys or develop new techniques and evaluate the limitations for engineering alloys. One of the main questions is when and under what condition can bulk properties be measured using small scale mechanical testing. In the current program with KAERI we investigate exactly this issue using microcompression testing on irradiated and not

**PI (U.S.):** Peter Hosemann, University of California, Berkeley

**PI (ROK):** Chansun Shin, Korea Atomic Energy Research Institute

**Collaborators:** Lead, Korea Atomic Energy Research Institute (KAERI) and Los Alamos National Laboratory

**Program Area:** Reactor Concepts RD&D

**Project Start Date:** December 2011

**Project End Date:** December 2014

irradiated structural materials. In the current work stainless steel, ODS alloys and copper has been tested with well selected microstructural features and conditions. Different thermo mechanical treatments were applied to those materials to achieve a different grain structure. Subsequent systematic micro compression testing was performed in order to evaluate when the material deviates from its original bulk data. In addition, ion beam irradiated materials (Stainless steel, ODS alloys as well as F/M steels) are subject of investigation to evaluate the property changes due to displacement damage.

### **Current Project Status Summary**

The project plan of this I-NERI describes the systematic development and investigation of small-scale material testing on structural materials for nuclear application. These rather novel methods have the potential to evaluate irradiation-induced mechanical property changes from rather small-sized samples. The advantage of these testing techniques is to access ion beam irradiated materials and allow one to gain mechanical testing data on 10-20 $\mu\text{m}$  deep irradiated samples. In addition, the sample size required for reactor irradiated materials is rather small so that radioactive samples can be handled in a university setting without the need for hot cells. While these techniques have clear benefits to irradiated materials, they also allow the testing of mechanical properties from specific areas such as welds and surface near regions of interest.

The three-year project was started on November 2011, on the basis of a collaboration of three organizations (UCB, KAERI, LANL). While we had frequent exchange via online meetings between KAERI, UCB and LANL, we also had a visit in Korea in 2013. Peter Hosemann visited KAERI for a week in March 2013 and detailed discussions together with actual hands on demonstrations were done. Peter Hosemann demonstrated the at UCB developed technique of micro bend bar testing on edges as it was conducted for the bend bar testing from the last report.

Also, several joined publications are either published or under review as direct results of this project while two more publications are currently under preparation at UC Berkeley.

### **Narrative Results:**

Fabrication of micro/nano-scale testing samples and initial multiscale materials testing (not irradiated).

Compression Testing of Ultrafine Grain Copper Nanopillars: A "Strength Determining Features" Study

Contributors: C. Howard, P. Hosemann

Scope: In order to evaluate scaling effects, an ultra-fine grained Copper sample was selected to conduct thorough scaling studies with varying grain sizes. Many micro compression samples were manufactured and tested. The tests were carried out on as processed specimens with a very fine grain size as well as on annealed specimen with larger grain size. The specimen grain sizes are shown as function of heat treatment in Figure 1. It can be seen that the grains of the sample grow rapidly as a function of annealing time and temperature. Both extreme cases (as processed with the samples grain size) as well as the large grained material were selected for conducting micro compression tests. All tests conducted are summarized in the Plots in Figure 2. The micro compression data and YS measured are directly compared to tensile test data of the same material. It was found that no change in yield stress as a function of specimen geometry was found.

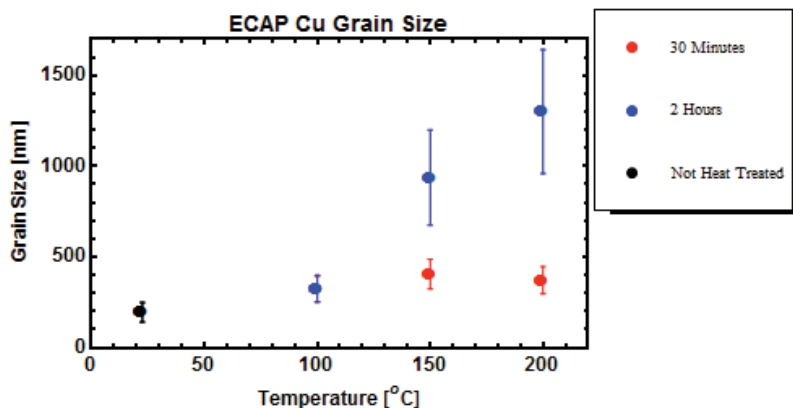


Figure 1: Grain size as a function of heat treatment measured using Scanning electron Microscopy and the intersect methods.

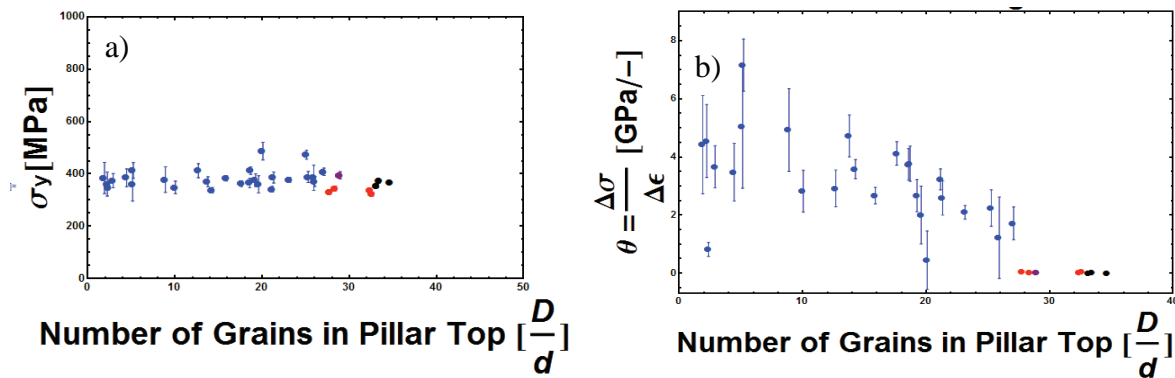


Figure 2: Yield stress as a function of pillar diameter to grain size ratio of the as processed sample with 200nm grain size. The black and red dots are the data points measured by macroscopic tensile testing. It is found that no change in yield stress is observed a). Work hardening as a function of pillar diameter to grain size ratio. A decrease in work hardening can be observed with sample size.

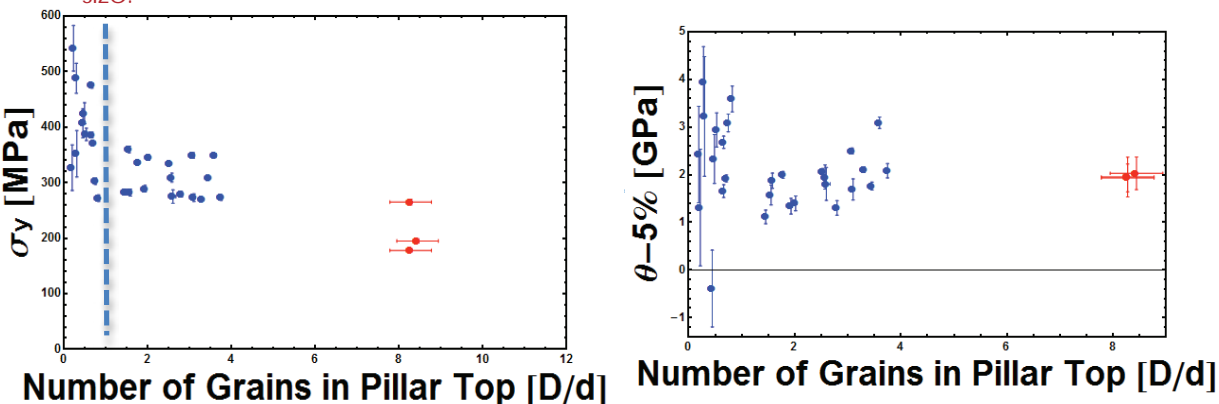


Figure 3: Yield strength as a function of the ratio of pillar diameter vs. grain size. It can be seen that these samples do show a size effect. Again the red data points are the tensile test data. B) work hardening as a function of the ratio of pillar diameter vs .grain size.

In our tests it was found that small grains in the order of 200nm or less do allow one to measure identical yield stress compared to macroscopic tensile testing. Larger grained and annealed structures do show evidence of a size effect. We can say that small scale testing allows one to probe polycrystalline samples with no size effect at small microstructural length scales. Larger microstructural features show a size effect but pillars of sufficient size can mitigate this effect.

### Materials testing of the ion beam irradiated samples.

#### Compression Testing of Ion Irradiated K3 ODS materials

Contributors: C. Howard, S. Parker, A. Lupinacci, P. Hosemann, W. Choi, M. Fluss.

Ion beam irradiated samples are made available to us and thorough mechanical testing studies have been conducted. We conducted nanoindentation as well as micro compression testing on ion beam irradiated materials. The samples have been irradiated via triple ion beam irradiation and different depth of the irradiation profile show different dose or ion concentration (He<sup>+</sup>, H or self ions) as indicated by the sketch in Figure 4.

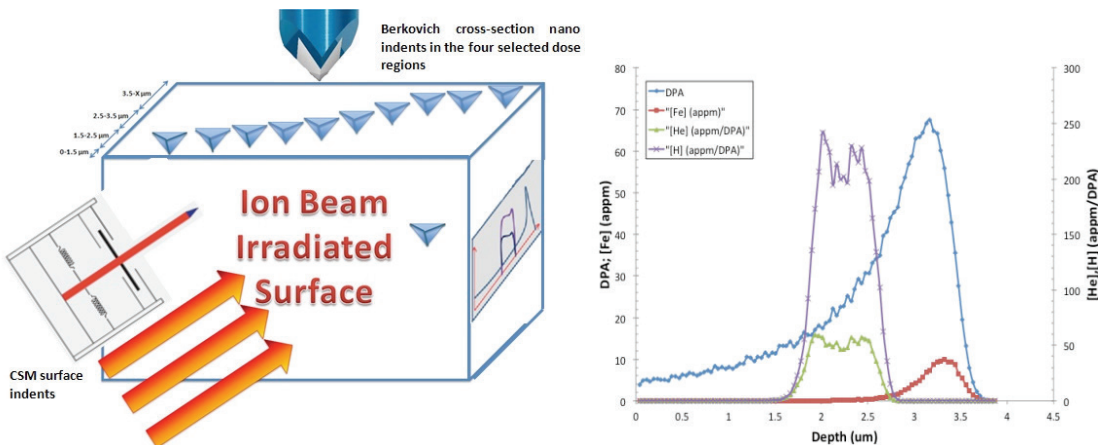


Figure 4: Schematic sketch of the mechanical testing vs. ion beam irradiation profile on the triple ion beam irradiated samples.

Figure 5: presents the micro compression data obtained from different parts of the irradiation spectrum on the sample K3-ODS as well as Eurofer 97. It was found that the ODS alloys shows no change in Yield stress as a function of He, H and dpa while the Eurofer 97 sample does show a change and the implanted region shows the highest YS. In addition, it was observed that some pillars manufactured exactly in the He region show significant evidence of a brittle like failure where sudden shear of the pillars are observed. This shows that the ODS alloy experienced little change due to the harsh triple ion beam irradiation while the F/M steel does.

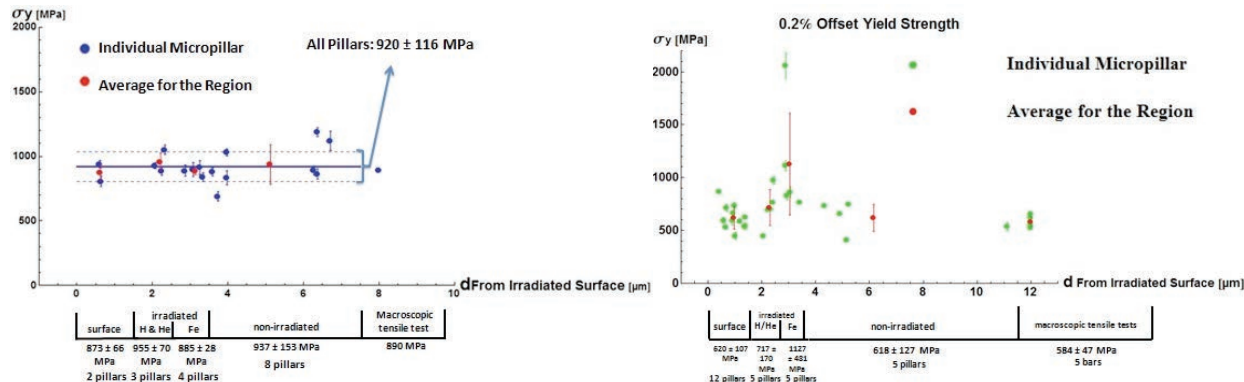


Figure 5: Triple ion beam irradiation profile on K3 ODS alloy a) and Eurofer 97 b) in different regions of the ion beam implantation.

#### Development of In-situ EBSD measurements.

Lage grained materials are heavily influenced by the grain structure and orientation of the specimen. A setup geometry was developed allowing in-situ Electron backscatter Diffraction (EBSD) measurements during in-situ pillar testing. This allows one to determine the critical resolved shear stress on a pillar in -situ during testing and one can compare the mechanical properties of different pillars manufactured in different grains.

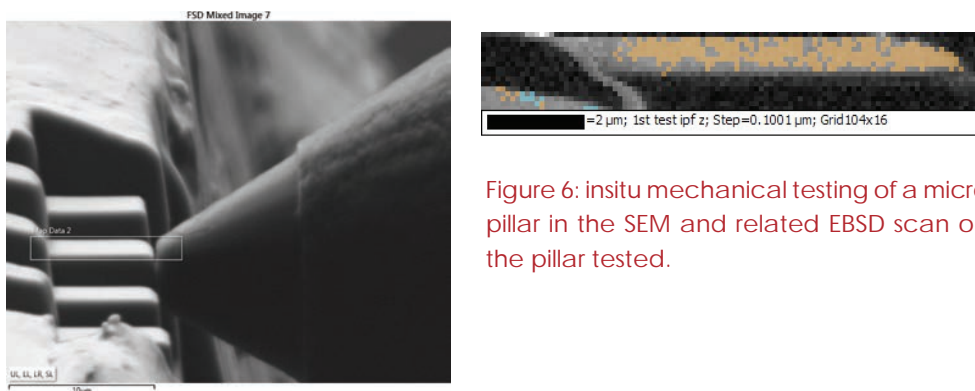


Figure 6: insitu mechanical testing of a micro pillar in the SEM and related EBSD scan on the pillar tested.

#### List of Publications

1. C. Shin, H.-ha Jin, W.-J. Kim, Ji-Y. Park "Mechanical Properties and Deformation of Cubic Silicon Carbide Micropillars in Compression at Room Temperature" J. Am. Ceram. Soc., 95[9] 2944-2950 (2012)
2. C. Shin, H.-h Jin, H. Sung, D.-J. Kim, Y.S. Choi, K. Oh "Evaluation of Irradiation Effects on Fracture Strength of Silicon Carbide using Micropillar Compression Tests" Exp. Mech., DOI 10.1007/s11340-012-9678-1
3. C. Shin, C. , S. Lim, H-H. Jin, P. Hosemann, J. Kwon; Development and testing of micro compression for post irradiation characterization of ODS steels; J. Nucl. Mat. 444 (2014) 43-48

# Verification and Validation of High-Fidelity Multi-Physics Simulation Codes for Advanced Nuclear Reactors

## Research Objectives

The objective of this project is to verify and validate a suite of high-fidelity multi-physics simulation methods and codes developed during a previous I-NERI project. The team compares results against Monte Carlo solutions and experimental measurements for light water reactor (LWR) and very high-temperature reactor (VHTR) cores. The main focus for FY 2013 was: to verify the DeCART neutronics code against numerical benchmark problems such as two-dimensional (2D) problems of PMR200 and HTTR cores; to improve code capabilities in terms of cross-section library group structure optimization, fundamental and generalized adjoint equation solver, cylindrical boundary treatment, improved ray tracing, and direct resonance integral table method for resonance treatment; and, to develop the generalized cross section library and application programming interface (API) which can be applied to various reactor types including LWR, VHTR, and sodium-cooled fast reactor (SFR).

## Research Progress

### Verification and Validation of the DeCART Neutronics Code for the VHTR

The project team has prepared many numerical benchmark problems based on PMR200 and HTTR cores for integral-effect tests of DeCART. From the tests, it was found that the DeCART cross section library for VHTR underestimates the multiplication factor up to -750pcm for some pin cell problems. In the depletion benchmark with the burnable poison (BP) loaded 2D PMR200, DeCART underestimated the multiplication factor at the beginning of cycle but overestimation was introduced with depletion, resulting in the error of up to 350 pcm at the middle of cycle. In the 2D HTTR benchmark, DeCART overestimated the multiplication factor for the fresh core by about 500 pcm, which is inconsistent with the PMR200 benchmark results. These errors will be investigated when updating DeCART and its cross section library next year.

Project Number: 2011-003-K

PI (U.S.): Changho Lee, Argonne National Laboratory

PI (ROK): Hyun Chul Lee, Korea Atomic Energy Research Institute

Collaborators: None

Program Area: Reactor Concepts RD&D

Project Start Date: October 2011

Project End Date: November 2014

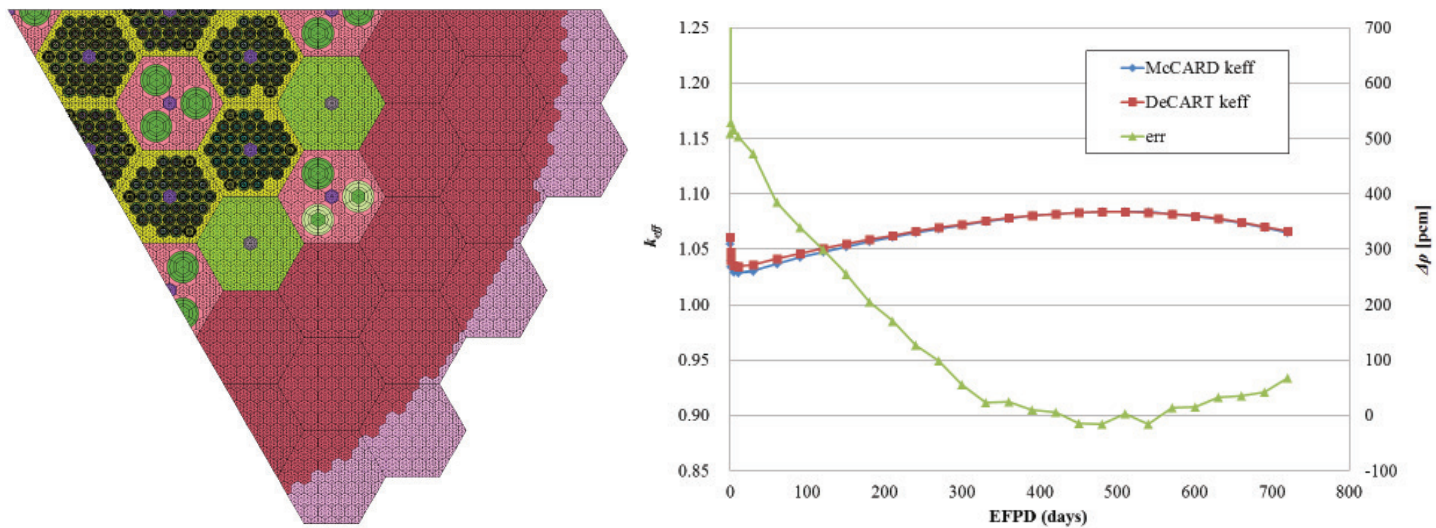


Figure 1. DeCART 2D 1/6 Core Model and Depletion Calculation Results for HTTR

A validation test of DeCART was initiated this year using the HTTR experimental benchmark. Prior to DeCART calculations, reference solutions were obtained by the McCARD Monte Carlo code with ENDF/B-VII.0 or VII.1 data. It was noticed that the McCARD results with ENDF/B-VII.1 were much closer to the experimental results than those with ENDF/B-VII.0. Since the updated data of the HTTR start-up core was recently obtained, the 3-D DeCART and McCARD models will be revised next year to compare simulation results with the experiment data.

A methodology was developed this year to optimize the neutron energy group structure for the cross section library. Preliminary results showed that the optimization produced less number of fast groups, more number of resonance groups, and similar thermal group structures, compared with the existing HELIOS 190-G structure. It was also found that the more number of groups were placed at the peaks of resonances and the less number of groups were located at the valleys of resonances. The resulting optimized group structure will be used to improve the accuracy of the cross section library next year.

Several new features were implemented into DeCART this year. Fundamental and generalized adjoint flux solvers were implemented for sensitivity and uncertainty analysis. A new boundary model was developed to accurately treat the cylindrical boundary. The Gaussian azimuthal angle discretization developed last year was implemented into DeCART to reduce the error associated with the azimuthal angle discretization. The direct resonance integral table (RIT) method for resonance treatment was implemented to remove the difficulties in generating the subgroup data.

Verification of the DeCART/CORONA code system for the VHTR multi-physics simulation was initiated this year. As an initial effort, a preliminary calculation of CORONA for the OECD/NEA MHTGR-350 neutronics/thermal fluid coupled benchmark was carried out. A coupled analysis of DeCART/CORONA for the MHTGR-350 coupled benchmark will be carried out next year.

#### Generation and verification of the generalized cross section library for thermal and fast reactors

In FY13, Argonne tasks have been modified since the focus of the NEAMS program supporting the I-NERI project was changed from LWR to SFR and accordingly the work scope of Argonne

had to be altered. A new task was created by expanding Task 2F (generation of a generalized cross section library) to include verification activities as well as development of the cross section API. Instead, the tasks associated with LWR were removed.

A generalized cross section methodology and library was developed for application to various reactor types including LWR, VHTR, and SFR. The ultrafine group (2158 groups) cross section library including the resonance integral tables was produced by the GeneCS code using the cross section data generated from MC2-3 and NJOY. The resonance integral tables were formulated for absorption, nu-fission, and scattering cross sections. The ultrafine group cross section library can be condensed to a broad group library for specific use on a target reactor. This is accomplished using the group condensation optimization algorithm which uses a representative neutron spectrum and various homogeneous or pin cell compositions for the reactor type of interest. The number of the broad groups for the reduced library is determined by a group condensation error criterion.

For verification tests of the developed cross section library, seven different compositions of SFR were selected. Reference solutions were generated using MCNP5 and MC2-3. The maximum difference in eigenvalue between the two codes is 144 pcm. The eigenvalue solutions from the RI table method with the 2158 group library (using the Bondarenko iteration for resonance self-shielding) agreed well with MCNP5 solutions within 196 pcm. The group optimization resulted in the broad group libraries with 383, 219, and 142 groups depending upon the criterion of  $\Delta k$  set to 5, 20, and 50 pcm. The eigenvalues from the broad group libraries agreed with the MCNP5 solutions within 225, 230, and 327 pcm  $\Delta k$ , respectively.

For LWR, the broad groups resulted from the group condensation optimization process were 204, 120, and 78 groups for a  $\Delta k$  criterion of 5, 20, and 50 pcm, respectively. These broad groups have the smaller number of groups than those for SFR. This is because coarser groups were determined in the high energy range which are more important to SFR but less important to LWR. The eigenvalues from the broad group libraries with 204, 120, and 78 groups were off from the MCNP5 solutions by maximum 186, 144, and 183 pcm  $\Delta k$ , while the eigenvalue from the ultrafine group library agreed with the MCNP5 solution within 198 pcm  $\Delta k$ .

For VHTR, the resulting broad groups were 198, 113, and 76 groups for different  $\Delta k$  criteria. Similar to LWR, the resulting numbers of broad groups with the same stopping criteria for determining group boundaries are smaller than those for SFR. In addition, the number of broad groups for VHTR is similar to those for LWR, even though the allocation of group boundaries are somewhat different each other. The eigenvalues from the ultrafine group (2158), 198, 113, and 76 broad group libraries were off from the MCNP5 solutions by maximum 174, 195, 244, and 317 pcm  $\Delta k$ , respectively. Further verification tests will be performed for various heterogeneous problems next year.

The cross section application programming interface (API), as shown in Figure 2, was developed to make it easier to implement the cross section generation tool into any transport code. The subgroup method option was created as a cross section generation method of the cross section API. The generalized cross section method will be another option of the cross section API next year. The cross section API requires the transport solver with the fixed source problem to obtain the region-wise escape cross sections for resonance self-shielding. The fixed source solver should be provided by the transport code to which the cross section API is implemented. The subgroup API has been connected to the Argonne unstructured finite element mesh based neutronics code PROTEUS as well as DeCART. Preliminary test results with pin cell and small lattice problems indicated its successful implementation to the transport code.

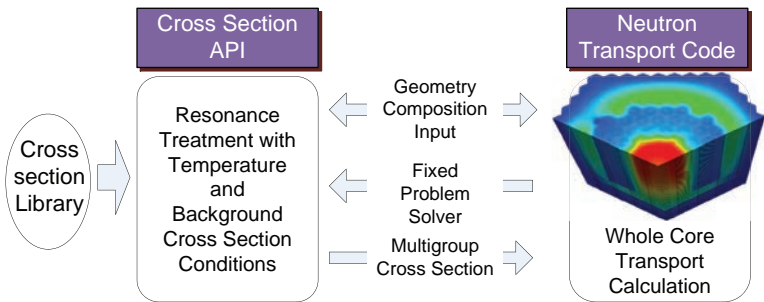


Figure 2. Interaction between Cross Section API and Neutron Transport Solver

## Planned Activities

In the last project year, the research team will complete the remaining Tasks 1, 3, and 4.

### Task 1 (Verification and Validation of Neutronics Code for VHTR)

- Analyze numerical and experimental benchmark problems for VHTR to complete the assessment of the accuracy of DeCART. Further improve accuracy and computational efficiency of DeCART.
- Update and test the multi-group cross-section library for VHTR.

### Task 3 (Verification of Multi-physics Simulation Code System for VHTR)

- Verify the DeCART/CORONA coupled code system for VHTR multi-physics simulation against the OECD/NEA MHTGR-350 neutronics/thermal fluid coupled benchmark problem. Initiate efforts to verify the multi-physics simulation.

### Task 4 (Generation and Verification of the Generalized Cross Section Library for Fast and Thermal Reactors)

- Verify the generalized cross section library using DeCART for various benchmark problems of LWR, VHTR, and SFR.
- Test the cross section API integrated into the PROTEUS neutronics code for various reactor types.

# Development of Diagnostics and Prognostics Methods for Sustainability of Nuclear Power Plant Safety Critical Functions

Project Number: 2011-004-K

**PI (U.S.):** Belle R. Upadhyaya and J. Wesley Hines, University of Tennessee

**PI (ROK):** Jung-Taek Kim, Korea Atomic Energy Research Institute

**Collaborators:** Chungnam National University, Kyung-Hee University, Pacific Northwest National Laboratory

**Program Area:** Reactor Concepts RD&D

**Project Start Date:** November 2011

**Project End Date:** November 2014

## Research Objectives

The objective of this I-NERI project is to develop and demonstrate advanced plant monitoring, diagnostics, and prognostics methods during beyond design-basis accidents. Such events, marked by loss of residual heat removal and other safety-critical plant functions, coupled station blackout and degradation of critical monitoring instrumentation, are difficult to mitigate without reliable information on critical parameters. This project is developing self-powered sensors that will provide plant information during extreme conditions, along with sensor networks incorporating these devices into plant communications, data transmission, and remote actuation systems. This effort includes demonstrating a remote sensing system consisting of a small number of self-powered sensors and processors in the form of a sensor network. Using dynamic simulation of a typical nuclear plant's operations, the U.S. and Korean collaborators will generate data needed to validate the proposed technical approach. Figure 1 shows the project organization and management diagram.

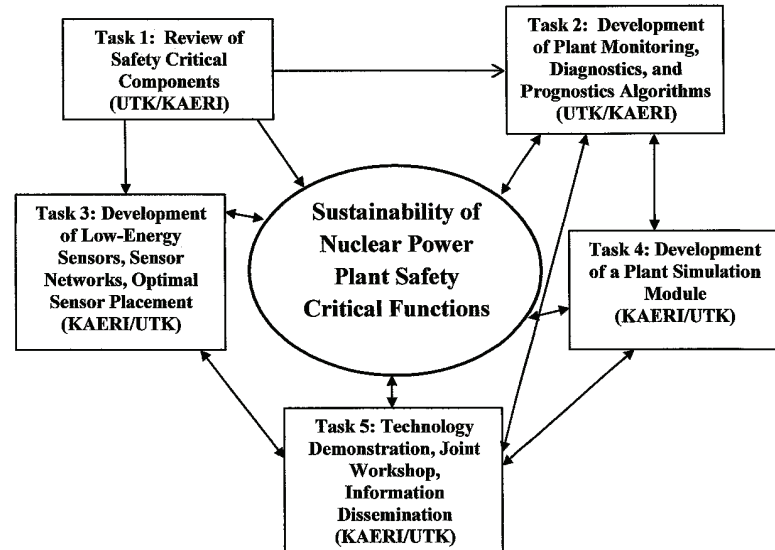


Figure 1. Project organization and management diagram.

The I-NERI project consists of the following tasks:

1. Review operability of safety-critical functions and components in light water reactors (LWRs).
2. Develop algorithms for plant monitoring, diagnostics, and prognostics.
3. Develop low-energy, self-powered process sensors and networks, and determine optimal placement strategies.
4. Develop plant simulation models to generate normal operational and faulty condition data.
5. Demonstrate the integrated technology.

The integrated system consists of a monitoring, diagnostic & prognostics module, remote sensing, sensor network, and self-powered sensing modules. The various modules are being demonstrated in a remote sensing system, consisting of a small number of self-powered detectors and processors in the form of a sensor network.

A Memorandum of Understanding (MOU) between the University of Tennessee and KAERI was signed in March 2014. This would facilitate future collaborative research between the two organizations.

## Research Progress

### Task 1: Review of Operability of Safety Critical Functions and Components

Collaborators at Korea Atomic Energy Research Institute (KAERI) reviewed safety critical functions and components of typical LWRs in Korea, while the University of Tennessee (UT) conducted a parallel review for U.S. nuclear reactors. The objective was to collect input parameters related to critical safety functions. Both reviews considered the critical safety function and indication parameters found in Nuclear Regulatory Commission (NRC) Regulatory Guide 1.97, "Instrumentation for Light-Water Cooled Nuclear Power Plants to Assess Plant and Environs Conditions During and Following an Accident." These functions are keys to preventing core melt and minimizing radiation releases to the public. In addition to evaluating a standard LWR, KAERI conducted a similar review of the SMART modular reactor and outlined a plan for demonstrating techniques and algorithms in the ATLAS thermal-hydraulic test facility. The following key sub-tasks have been completed.

- Review of Critical Safety Functions and Components, and Operational History in Wooljin Units 3 and 4 of Korea Standard Nuclear Power Plants (KSNP).
- Review of the monitoring parameters in ShinGori Units 1 and 2 (KSNP).
- The U.S. team developed suggestions for instrumentation and supporting technology necessary to monitor beyond design basis accidents, applying the latest guidance in RG 1.97 that establishes a strategy for selecting system parameters to monitor during accident conditions.

Figure 2 shows the location of monitoring points in the KSNP units as developed by the KAERI investigators.

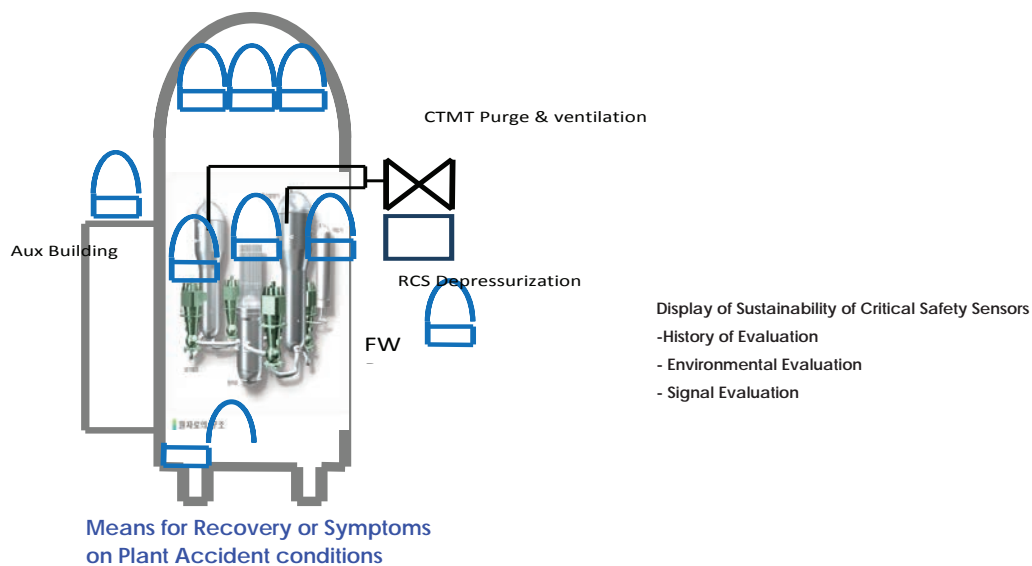


Figure 2. Identification of monitoring points for critical safety functions and components (KAERI).

## Task 2: Development of Plant Monitoring, Diagnostics, and Prognostics Algorithms

The following important subtasks were accomplished during Year 2 of the project

- One week Workshop at the University of Tennessee on MDP algorithms and toolboxes. Process and Equipment Monitoring (PEM) and Process and Equipment Prognostics (PEP) Software Toolboxes were transferred from UTK to KAERI.
- Development of data-based models and algorithms for characterizing the cause-effect relationship among a set of features and for feature prediction. PWR simulation data from KAERI were used in this sub-task.
- Development of inferential data-based models for estimation (Process & Equipment Monitoring/ PEM) and for signature trending and estimating remaining useful life (RUL) of equipment (Process & Equipment Prognostics/PEP) were accomplished by KAERI.

Researchers at Kyung-Hee University (KHU) identified requirements, methodologies and resources for the development of a safety index monitoring during severe accidents (SIMSA) system. Their research has resulted in the development of a virtual parameter network toolbox. The following are the key accomplishments:

- To provide an alternative (virtual, redundant) parameter, a correlation -based sensor network to predict the missing safety parameter due to failure of sensor related to critical safety functions.

- To evaluate goodness-of-sensor installation and assess the safety critical parameters from other statistically related parameters during a severe accident.

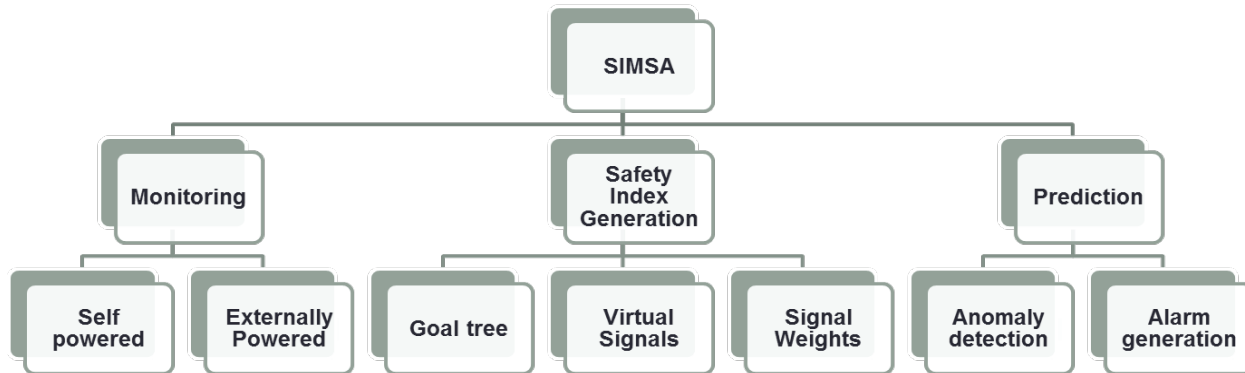


Figure 3 is an overview of the analysis toolbox being developed by KHU.

Figure 3. Virtual Parameter Network Toolbox (KHU)

Other accomplishments by the University of Tennessee are contributions from the on-going DOE NEUP project on in-situ monitoring of small modular reactors (SMRs) and lifecycle prognostics of nuclear plant systems.

**Remote Monitoring of SMRs:** Following are the major objectives of this task.

- Identify critical in-vessel SMR components for remote monitoring and development of their low-order dynamic models, along with a simulation model of an integral pressurized water reactor (iPWR).
- Develop an experimental flow facility with motor-driven valves and pumps, incorporating data acquisition and on-line monitoring interface
- Develop stationary and transient signal processing methods including the development of a data analysis toolbox.

Physics models of an integral reactor, main coolant pump and motor unit were developed for simulating equipment faults. An experimental flow control loop was developed at the University of Tennessee to demonstrate the methods being developed for this task.

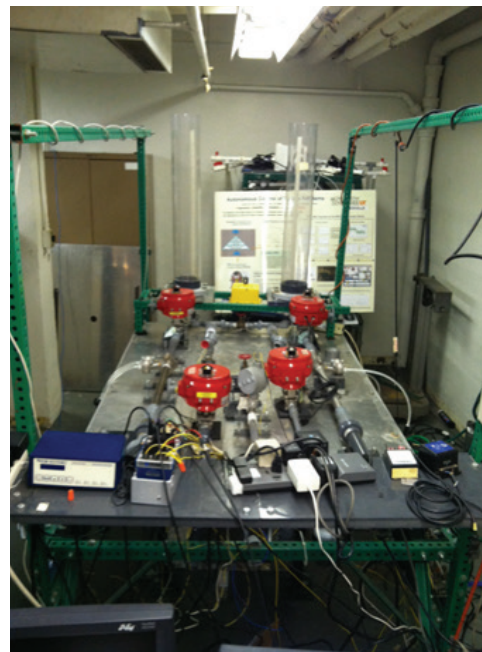


Figure 4. Experimental flow control loop at the University of Tennessee.

Figure 4 shows a photograph of this facility. The data from the tests were used relate pump motor power, flow rate, and pump discharge pressure.

### Lifecycle Prognostics of Plant Equipment

Generally, an approach for prognostics involves the monitoring of a given piece of equipment or a device and uses the measurements of parameters that reflect its degradation for prognostics or for estimating its remaining useful life (RUL). Figure 5 shows the progression in achieving this goal. The University of Tennessee is a leader in this area. The basic prognostics methods are outlined below:

- Type I models work exclusively from historic time to failure data and are generally expected to predict the average failure time of the average unit in average conditions.
- Type II expands upon this and also incorporates environmental and stressor based information. These models work for the average unit in some specific set of conditions.
- Type III models utilize information collected directly from the query unit. This most specific model type is the most precise and is used to predict the specific behavior of a query unit as it progresses to failure. This natural progression of the model types lends itself to lifetime system prognostic transitioning as more information becomes available.

Figure 6 illustrates the transitions between information types and lists some examples of the prognostic algorithms that utilize each information class.

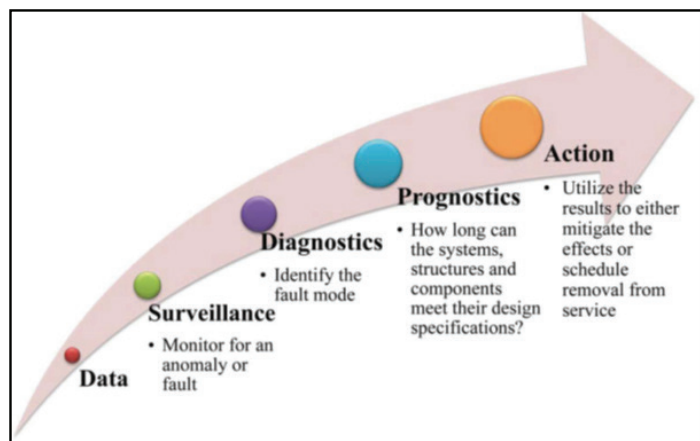


Figure 5: Stepwise application of data analysis for maintenance applications.

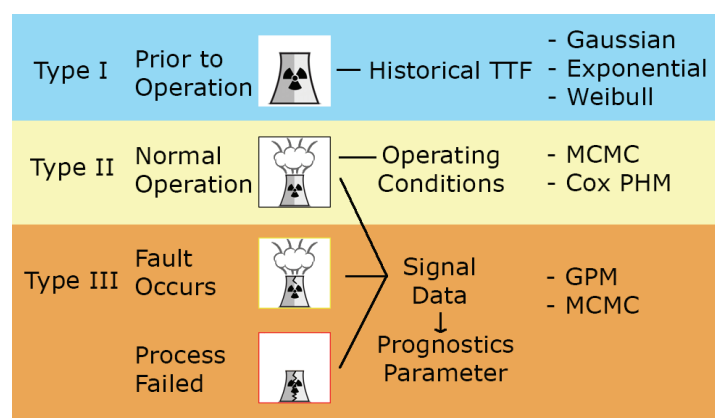


Figure 6. Transition between information types as part of a lifecycle prognostics approach.

The prognostics algorithms have been evaluated using data from several test beds that provide equipment degradation data.

#### Task 3: Development of low-energy self-powered process sensors, sensor networks, remote monitoring, and optimal sensor placement strategy

KAERI is investigating low-energy sensors (solar, photo-voltaic, thermoelectric, and piezoelectric or electromagnetic vibration devices) for harvesting ambient light, heat, vibration, and electromagnetic energy from sensor surroundings and converting it into usable electrical energy to power portable electrical devices without batteries.

UT researchers are investigating remote monitoring systems for critical equipment in small modular reactors (SMRs). They upgraded an existing experimental flow control loop with instrumentation

designed to demonstrate the relationship between remotely-measurable electrical signatures and process variables. Preliminary results show a strong correlation between motor power and pump flow rate (see Figure 7). This relationship, with proper calibration, can be used for monitoring reactor flow rate remotely.

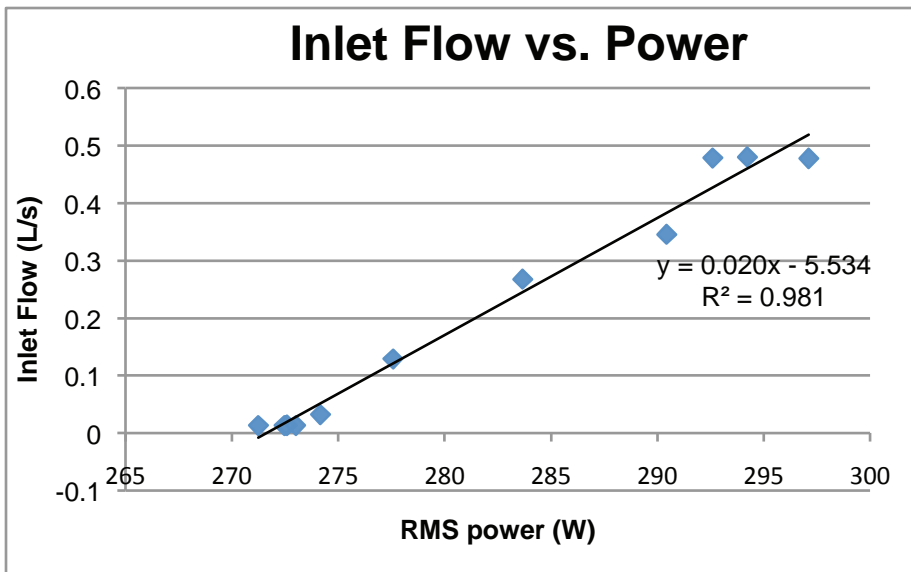


Figure 7. The RMS power drawn by the pump increases as the flow rate increases

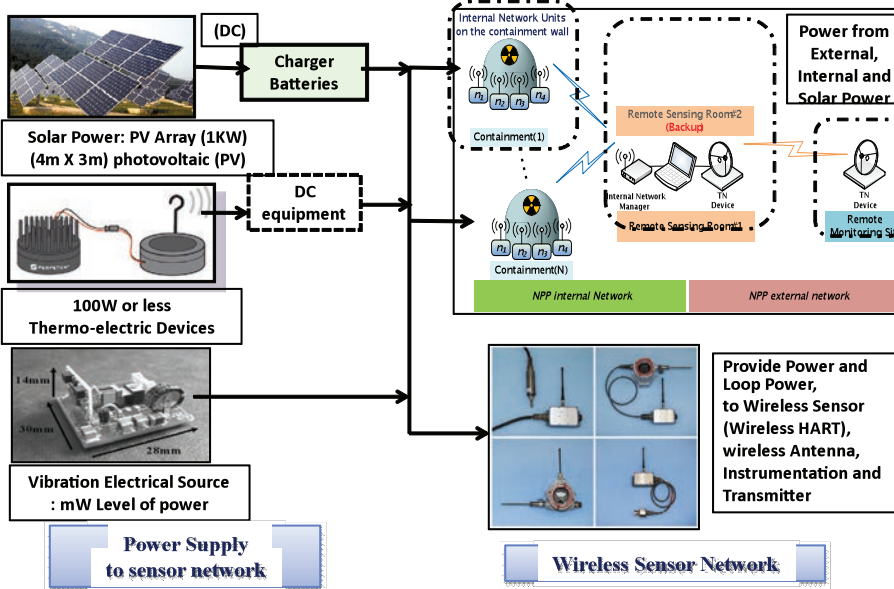
Researchers at Chungnam National University (CNU) are developing and demonstrating wireless technologies for condition monitoring during a station blackout. Design issues identified include line of sight, frequency, antenna type (e.g., directional vs. omnidirectional), interference, modulation/demodulation, topologies, and network size. The team narrowed findings to the recommended network shown in Figure 6, consisting of three parts: the internal network, external network, and remote sensing room. Digital signals acquired from wired sensors inside the containment are combined in an internal network unit (INU) using a multiplexer to increase the efficiency. INUs placed on the outer wall of the containment (to avoid the harsh radio environment and to minimize damage during accidents) wirelessly transmit diagnostic information to the internal network manager (INM) located in a remote sensing room, which in turn sends data to remote monitoring sites through an external network. A design framework has been developed to optimize sensor allocation based on detection and isolation of faults.

KAERI and Chungnam National University (CNU) are performing the following research related to sensor development:

- Fabricate a prototype low-energy self-powered instrumentation considering solar cells, thermo-electric devices, vibration sources as energy harvesting techniques (KAERI).
- Develop a prototype low-energy self-powered self-mapping wireless sensor network (CNU).

These tasks are important for monitoring beyond design-basis accidents (BDA). Figure 8 shows the various technologies brought together for developing low-energy self-powered

## Task 3-1 Low-Energy Self-Powered Instrumentation



instrumentation with wireless communication. These tasks require a large investment in human resources and involve the use of existing and new technologies under development.

Figure 7. Development of low-energy self-powered detectors and wireless communication.

### Planned Activities

Task 1 is complete. During FY 2013, the research team has completed the development and testing of monitoring and prognostics software and the associated toolboxes. These are R&D activities associated with Task 2. The planned activity under this task includes the application of prognostics tools to new data being acquired from test beds at the University of Tennessee and at KAERI. Some of these results are being compiled for publication in scientific journals and conference proceedings. The continuing R&D at KAERI involves testing low-energy self-powered instrumentation. This will help identify failure modes and aging mechanisms of these devices.

Task 3 planned activities include the following:

- Manufacture a prototype low-energy self-powered instrumentation system using solar cells, thermo-electric devices, and vibration sources as energy harvesting methods (ROK).
- Develop prototype self-powered self-mapping wireless sensor networks (CNU).
- Field Performance testing (rated power, rated load efficiency, switch-over, etc.) under harsh environments.
- Incorporating optimal sensor placement approach for low-energy self-powered instrumentation and developing optimal sensor allocation (ROK & UTK)
- Demonstration of remote and inferential measurement methods with applications to integral light water reactors (UTK).

A final project report will be submitted to the U.S. Department of Energy and the Ministry of Science, ICT and Future Planning, ROK, in November 2014.

# Fully Ceramic Microencapsulated Replacement Fuel for Light Water Reactor Sustainability

Project Number: 2011-005-K

**PI (U.S.):** Lance Snead, Oak Ridge National Laboratory

**PI (ROK):** Won-Jae Lee, Korea Atomic Energy Research Institute

**Collaborators:** Ultra Safe Nuclear Corporation, Inc.

**Program Area:** Fuel Cycle R&D

**Project Start Date:** October 2011

**Project End Date:** September 2014

## Research Objectives

This project is assessing the feasibility of replacing conventional uranium oxide ( $\text{UO}_2$ ) fuel assemblies in the existing fleet of light water reactors (LWRs) with accident-tolerant fully ceramic microencapsulated (FCM) fuel assemblies. FCM fuel is a TRISO-based dispersion fuel consisting of ceramic-coated microspheres of low-enriched uranium embedded in dense, uniform silicon carbide (SiC) matrix fuel pellets with similar geometry to conventional  $\text{UO}_2$  pellets.

In order to replace conventional  $\text{UO}_2$  fuel, FCM fuels must achieve comparable energy generation and heat transfer levels, as well as acceptable neutronic, thermal-hydraulic, and fuel performance characteristics. Acceptable designs must meet the limiting design basis accident (DBA) envelope for the plant and satisfy beyond design-basis accident (BDBA) criteria. The team will also model and qualify FCM fuel properties under irradiated conditions to ensure acceptable accident tolerance.

The project consists of four tasks:

1. Core neutronics exploration
2. Core thermal-hydraulics assessment
3. Safety assessment
4. Fuel qualification

The project has selected two reference pressurized water reactor (PWR) cores for demonstration: the U.S. team will focus on a Westinghouse 1000-MWe core with 17×17 fuel assemblies,

## Research Progress

In this second year of the project, five FCM FA design candidates proposed from the FA-level study in the 1st year (Figure 1) were evaluated for their compatibility in OPR-1000 transition cores. It is assumed that the core is initially fully-loaded with the FCM FAs. The core neutronic performance in the transition cores from initial to equilibrium cycles was explored for each candidate. An optimum FCM FA design was then screened based on a combination of the core neutronic, TH, mechanical and safety performance. Detailed core follow analysis from the initial to equilibrium cores was carried out for the selected design to quantify core physics parameters such as power distributions and reactivity coefficients. Using these core physics parameters, the core TH, safety and coated particle fuel performance were assessed to demonstrate the compatibility and enhanced accident tolerance of the FCM FA. In parallel, design models and methods were developed for mixed transition cores where the FCM and UO<sub>2</sub> FAs coexist.

Basic fuel fabrication work involving uranium mononitride (UN) kernels was performed at Oak Ridge National Laboratory (ORNL) to produce kernels of density as high as possible. The manufacture of silicon carbide (SiC) compacted pellets was continued using nano-powders and sintering agents. The initial irradiation of compacts with and without fuel particles was performed at the High Flux Isotope Reactor (HFIR) to test swelling and property changes during irradiation. Some post irradiation examination was performed on samples irradiated in the previous year.

The following sections summarize results in each task area.

### Task 1: Neutronic Exploration

Using the DeCART2D and MASTER neutronics codes, the project team performed explorative studies searching for an optimum core loading pattern. Five feasible OPR-1000 cores loaded with candidate FCM FAs were

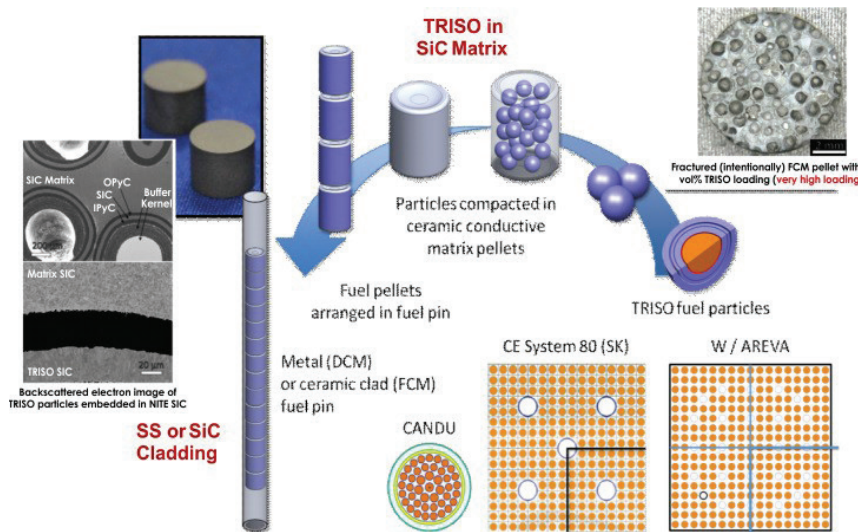


Figure 1. FCM replacement fuel design.

Candidate	BP Type	TRISO Packing Fraction
16×16-SS	Admixed	45%
12×12-SS	BISO	42%
16×16-SiC	BISO	42%
12×12-SiC	Admixed	45%
16×16-ZC	BISO	45%

(a)

L	H	L	H	L	H	L	H
L	H	L	H	L	H	L	H
L	H	L	H	L	H	H	L
L	H	L	H	L	H	H	L
				L	H	L	H
				L	H	L	H
				L	H	L	H
				H			

H: High or Fresh

L: Low or Once Burned

(b)

Figure 2. (a) Summary of OPR-1000 candidate FCM fuel assembly designs, and (b) assumed OPR-1000 loading pattern.

investigated through a multi-cycle analysis from the initial to equilibrium cores. Candidate cladding materials included SiC, stainless steel (SS), and SiC-coated zirconium-alloy. The five FA design candidates were 16×16 arrays clad with SS (16×16SS), SiC (16×16-SiC), or SiC-coated zirconium-alloy (16×16-ZC) and 12×12 arrays clad with SS (12×12-SS) or SiC (12×12-SiC). Calculations assumed a 2 batch fuel management scheme with an 18-month cycle length and used typical design criteria to search transition and equilibrium core loading patterns. Figure 2 summarizes the FA candidates and depicts the OPR-1000 low-leakage loading pattern used.

For each core design, core physics parameters including reactivity, critical boron concentrations, power distributions, reactivity coefficients, shutdown margin, and fast neutron fluence were quantified for thermal-hydraulic, safety and fuel performance assessment. FCM fuel with SiC-coated zirconium-alloy cladding in a 16×16 FA configuration was selected as a reference design based on neutronic performance. Figure 3 shows power peaking factors calculated during these analyses.

Displacement per atom (DPA) cross sections using 47 and 190 energy groups were developed based on molecular dynamics simulations by SRIM/TRIM and implemented in DECART2D to estimate irradiation damage of FCM fuel materials. DPA calculations for SiC and pyrocarbon (PyC) coating layers were provided for fuel performance analysis. DPA cross sections and results are shown in Figure 4.

#### Task 2: Core Thermal Hydraulic Assessment

In order to model the cross flow in heterogeneous gaps between FCM and OPR-1000 FAs in a mixed transition core, a lateral loss coefficient model was developed with the aid of a computational fluid dynamics (CFD) model and implemented in the MATRA core TH/subchannel code. Core pressure drop ( $\Delta P$ ) and departure from nuclear boiling ratio (DNBR) performance were evaluated for a mixed transition core and used to confirm TH compatibility. Sample findings are provided in Figure 5.

A two-step core TH and subchannel analysis method was developed for core thermal margin analysis. This method consists of 1) a core-wise assembly analysis step and 2) a hot-assembly subchannel analysis step. The thermal margin in the transition cores fully loaded with the 16×16 FCM FAs with SiC-coated zirconium-alloy cladding was then assessed by employing the quantified core physics parameters. Figure 6 shows the two-step core TH method, quarter-core power distributions used for thermal margin analysis, and minimum DNBRs (MDNBRs) calculated for transition cores fully loaded with FCM FAs.

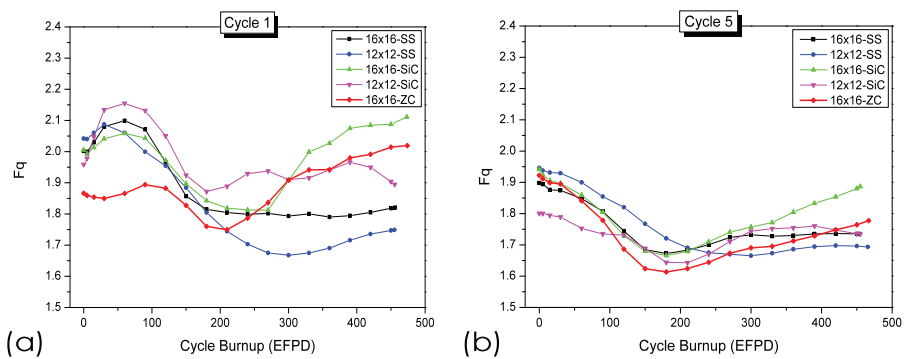


Figure 3. Power peaking factors for OPR-1000 FCM replacement fuels in (a) Cycle 1 and (b) Cycle 5 (equilibrium cycle).

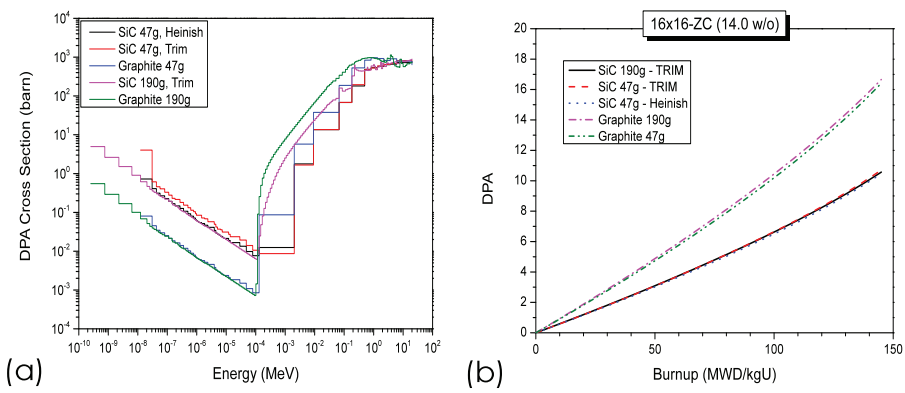
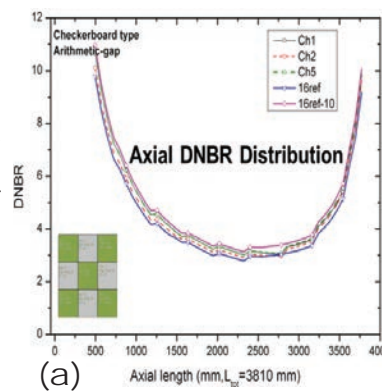


Figure 4. DPA results for Power peaking factors for OPR-1000 FCM replacement fuels in (a) Cycle 1 and (b) Cycle 5 (equilibrium cycle).



	16x16 (OPR)	Limit	16x16 (FCM)
DNBR	2.79		3.13
$\Delta P$ (bar)	1.33	1.45	1.57

Figure 5. Mixed transition core compatibility analysis of (a) axial DNBR distribution and (b) standard and FCM DNBR and  $\Delta P$  results and limits.

The thermal margin in the transition cores fully loaded with the 16×16 FCM FAs with SiC-coated zirconium-alloy cladding was then assessed by employing the quantified core physics parameters. Figure 6 shows the two-step core TH method, quarter-core power distributions used for thermal margin analysis, and minimum DNBRs (MDNBRs) calculated for transition cores fully loaded with FCM FAs.

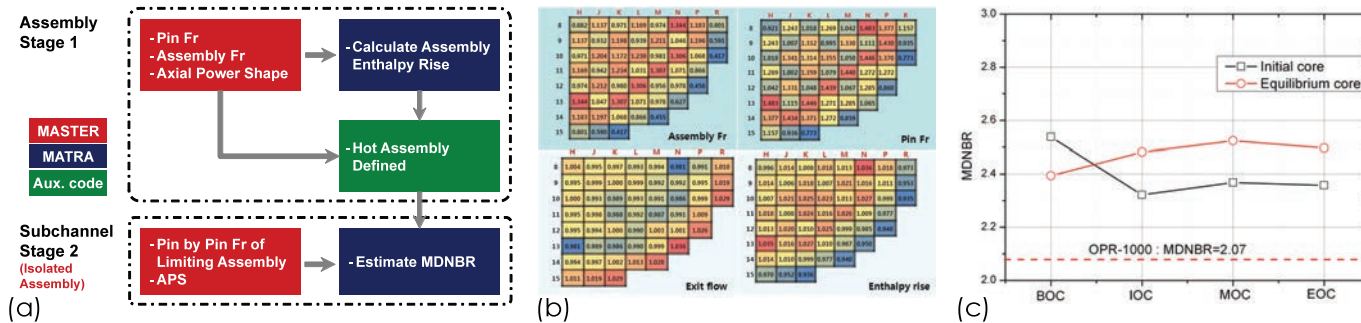


Figure 6. Core TH assessment (a) two-step method used for margin analysis, (b) quarter-core power distributions used for TH calculations, and (c) MDNBRs calculated for transition cores fully loaded with 16×16 FCM FAs

### Task 3: Safety Assessment

A thermal conductivity model for nano-infiltration and transient eutectic-phase (NITE) SiC pellets was incorporated into the MARS code to account for the effect of irradiation temperature measured by ORNL. Preliminary scoping analyses carried out for various cladding material candidates showed 16×16-ZC to be the most promising candidate. Analyses of limiting DBAs and BDBAs analyzed using core physics parameters from fully FCM transition cores found safety margin of the FCM core for DBAs and greatly enhanced accident tolerance for FCM cores during BDBAs, permitting more time for operator actions. Figure 7 shows results from these safety assessment analyses.

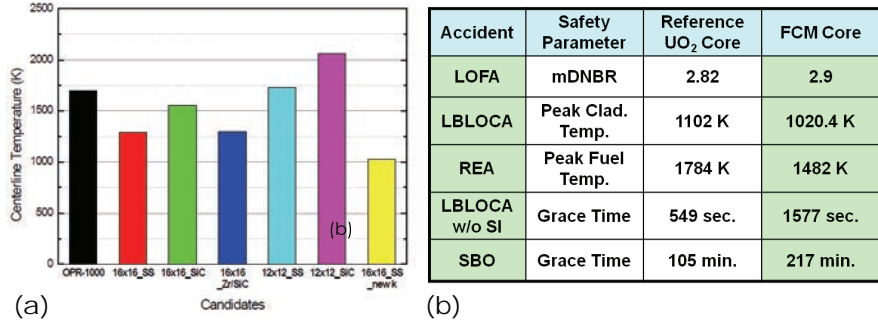


Figure 7. (a) Results from initial stored energy analyses and (b) enhanced accident tolerance for 16×16-ZC FCM FAs for limiting DBAs and BDBAs.

### Task 4: Fuel Qualification

UN kernels were fabricated and characterized at approximately 90% of theoretical density with kernel diameters around 830 µm. Uranium oxide-carbon microspheres were produced using an internal gelation process. They then underwent carbothermic conversion to become UN kernels, with vacuum conversion of uranium oxide-carbon producing an intermediate composition that was converted to UN through a single-stage conversion/sintering process using a nitrogen environment or mixed gases containing nitrogen.

Irradiation experiments using a “rabbit capsule” in HFIR at ORNL for FCM fuel pellets containing TRISO particles with surrogate ZrO<sub>2</sub> kernels investigated irradiation stability of the SiC nano-powder-based matrix and TRISO particle coating layers at LWR-relevant conditions of temperature and fluence. Monolithic (particle-free) SiC nano-powder-based matrix pellets were also irradiated to examine irradiation stability of the SiC matrix without fuel particle perturbations. Results showed that surrogate fuel compacts and ceramics derived from the SiC nano-powder hot pressed with yttria and alumina sintering aids exhibit an as-irradiated swelling somewhat greater than that of CVD SiC. Thermal conductivity degradation was consistent with known CVD SiC values considering the added irradiation-induced swelling. Irradiation near 300°C had no apparent adverse effect on the particle coating layers and post-irradiation examination did not find any

gross cracking or debonding between layers. Furthermore, no reaction was observed between the SiC nano-powder matrix and Zircaloy-4 cladding material.

A COPA/HSC analysis system was established and used to evaluate FCM coated particle fuel performance. A PyC irradiation-induced dimensional change (IIDC) model and failure models for PyC and SiC layers were developed based on CEGA models. Preliminary fuel performance analyses found fission gas pressure (including noble gases and vapor species) at LWR operating conditions are small enough not to influence the SiC layer mechanical stresses. Stresses on the PyC and SiC layers are mainly challenged by PyC IIDC, which is not well quantified at fluences over 4 dpa. Refinement of the IIDC model based on new irradiation data is needed.

Mechanical integrity of the FCM FAs by maximum cross flow of 0.6 m/s in a mixed transition core was assessed. It was demonstrated that sufficient margin is available against flow-induced vibration both for 12×12 and 16×16 FA configurations.

## Planned Activities

In the third project year, the research team will perform core neutronics, thermal-hydraulics, safety, and fuel performance analyses for FCM FAs with FeCrAl cladding and for mixed transition and equilibrium cores. FCM fuel manufacture and irradiation will continue as planned. Researchers will conduct the following activities specific to each task:

### Task 1 (Neutronics Exploration)

- Search and optimize mixed transition core loading patterns to achieve core neutronics performance comparable with conventional fuel. FeCrAl cladding will be considered along with other cladding options in these analyses.
- Generate core physics parameters for both mixed transition and equilibrium cores and supply them for core TH, safety, and fuel performance analysis

### Task 2 (Core T/H Assessment)

- Analyze core and subchannel TH compatibility of the FCM FAs in mixed transition and equilibrium cores. Assess core thermal margin using parameters from neutronics results.

### Task 3 (Safety Assessment)

- Develop methodology for safety analysis of mixed transition cores
- Perform scoping analysis of DBA and BDBA scenarios for mixed transition cores
- Perform feasibility analysis of accident-tolerant cladding materials
- Develop accident tolerance analysis of FCM SiC pellet for severe accidents

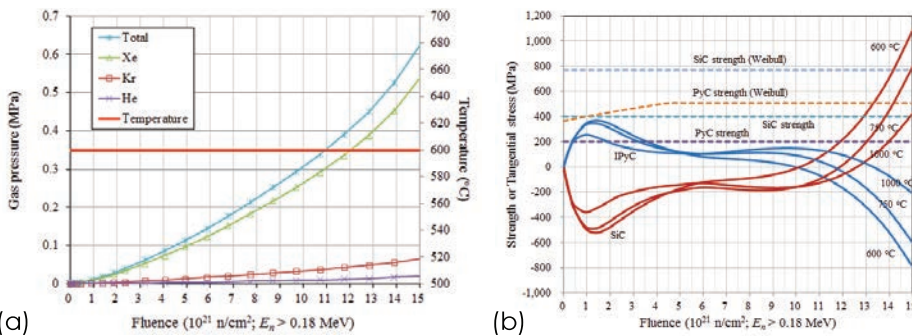


Figure 7. (a) Fission gas pressure in TRISO at 850°C and (b) stress at TRISO layers at 850°C.

#### Task 4 (Fuel Qualification)

- Continue development of FCM fuel fabrication.
- Prepare FCM fuel samples for future irradiation experiments, possibly in the Advanced Test Reactor (ATR) at the Idaho National Laboratory (INL).
- Improve fuel performance analysis models and validate using irradiation test results when possible.
- Assess fuel performance in the mixed transition and equilibrium cores will be assessed.

# Generation of Physics Validation Database and Analysis of Fast Reactor Depletion and Core Characteristics Calculations Using MC2-3/DIF3D/REBUS-3

Project Number: 2013-001-K

**PI (U.S.):** Changho Lee & Richard R. Lell,  
Argonne National Laboratory

**PI (ROK):** Sang Ji Kim, Korea Atomic Energy Research Institute

**Collaborators:** N/A

**Program Area:** Reactor Concepts  
RD&D

**Project Start Date:** December 2013

**Project End Date:** November 2016

## Research Objectives

The objective of this project is to archive and evaluate the integral experiment data, analyze the experiments, and prepare computational models for validating a suite of fast reactor design and analysis tools being used at ANL and KAERI. During the project, the ANL team will retrieve and analyze core follow data of metallic-fueled driver assemblies and blanket assemblies inserted into EBR-II. A series of mockup experiments conducted for a 330 MWe Integral Fast Reactor (IFR) under the ZPPR-15 program, known as the IFR Benchmark Physics Test Program, will also be retrieved and analyzed. The KAERI team will compile and analyze the new BFS-109-2A experiments carried out as mockup experiments of the 100 MWe metallic-fueled core at the Russian BFS-1 facility. In addition, the as-built models of the Monte Carlo (MCNP) and deterministic (MC2-3/DIF3D/REBUS-3) codes for ZPPR-15 and EBR-II experiments of ANL and BFS experiments of KAERI will be generated based on the ENDF/B-VII data.

## Planned Activities

The project was started from December 2013 at KAERI and late March 2014 at ANL. In the first year, the project team will focus on the following four tasks.

Tasks 1 and 2: MCNP Monte Carlo models for the selected ZPPR-15 experiments will be generated based on as-built experiment data. Corresponding deterministic models will be created using the MC2-3/DIF3D codes and will be compared with MCNP results.

Task 3: As-built MCNP Monte Carlo models for the BFS-109-2A physics experiments performed by KAERI in 2012 will be generated and analyzed.

Task 5: Deterministic models using MC2-3/DIF3D/REBUS for the BFS-109-2A, BFS-73-1, BFS-75-1, and BFS-76-1A physics experiments available will be generated and compared with MCNP results.

# Development of Oxidation Protective Coating Technology on Graphite for VHTR Core Support Structure

## Research Objectives

This project is assessing the feasibility of applying novel deposition designs to develop oxidation reducing SiC coatings on nuclear graphite structural components. The graphite support components used in the High Temperature Reactor (HTR) or design can undergo significant oxidation during off-normal (accident) events which can compromise the core structure integrity. Development of oxidation protective coatings on the outside of the graphite support structure will prevent excessive oxidation of these critical components. This research will focus on developing an adhesion enhanced dense SiC coating process with the aid of an ion beam process.

During an air ingress event such as D-LOFC (Depressurized-Loss of Forced Convection), oxygen can and will attack the graphite support components at temperatures  $< 400$  °C. During a long reactor shutdown, the graphite components will be at high temperatures allowing the potential for significant oxidation of the support components with a corresponding loss of mechanical strength. Significant oxidation of the graphite and subsequent loss of mechanical strength could lead to the loss of core integrity, a severe accident event. Reducing the oxidation rate of these critical graphite components is highly desirable.

Silicon Carbide (SiC) is a candidate material for high temperature oxidative protection for graphite support components and an accepted nuclear core material. SiC does not oxidize at the highest temperatures expected during a HTR accident event (1400°C - 1600°C). Consequently, a protective SiC coating on the graphite components could assist in preventing oxidation. Normally, irradiation-induced dimensional changes in the graphite (shrinkage followed by swelling) would provide internal stresses capable of delaminating the coating from the graphite eliminating this coating as an option. However, for the lower plenum area where the support column structures are located, the dose level is minimal, eliminating most internal irradiation induced stresses. The prime concern becomes the adhesion of

Project Number: 2013-002-K

PI (U.S.): W.E. Windes, Idaho National Laboratory

PI (ROK): Jae-Won Park, Korea Atomic Energy Research Institute

Program Area: Reactor Concepts RD&D

Project Start Date: October 2013

Project End Date: September 2016

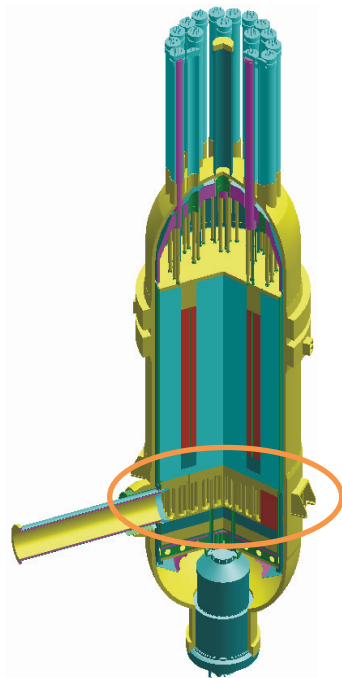


Figure 1. Schematic of a VHTR design illustration the core support region.

the SiC coating at the expected elevated temperatures during an accident event which is dependent on the interfacial properties.

The interface property of SiC coating on graphite is quite different from that of the coating on metallic materials. Graphite is formed from stacked layers of graphene planes with relatively weak bonds between the planes (metallic or Van der Waals bonding). Several factors must be considered when forming a SiC coating on the graphite components including the difference in the thermal expansion at elevated temperature (CTEgraphite (1100 °K):  $8.6 \times 10^{-6}$  K-1 and CTESiC (1100 °K):  $5.5 \times 10^{-6}$  K-1), thermodynamic compatibility, and the inherent weak bond nature of the bonding between graphene planes. The difference in thermal expansion between the two dissimilar materials and thermodynamic incompatibility (i.e. lacking chemical reaction) often lead to bonding failure at elevated temperatures for many coating/host materials. Although the interfacial reaction is thermodynamically favored, the problem of the inherently weak bonding nature of graphite basal planes still remains.

To resolve these problems, a functionally graded layer at the interfacial region is being developed applying various techniques such as CVD, CVI+CVR, slip/packing coating and so on. In the case of CVI + CVR technique, for instance, the molten silicon is evaporated and infiltrates the surface of the graphite substrate through the micro-pores on the surface and thus the silicon carbides are formed by the reaction between infiltrated Si and the host graphite, enhancing adhesion force of the SiC coating formed and the graphite substrate. However, SiC formed by the infiltration reaction contains a certain amount (~10 - 20%) of free Si. For the CVD process, a functionally graded layer having the graded compositional ratio of SiC-Si-C can be formed by controlling the concentrations of the volatile precursors and the carrier gases. Therefore, the interface tailoring is of importance in case of SiC coating on graphite.

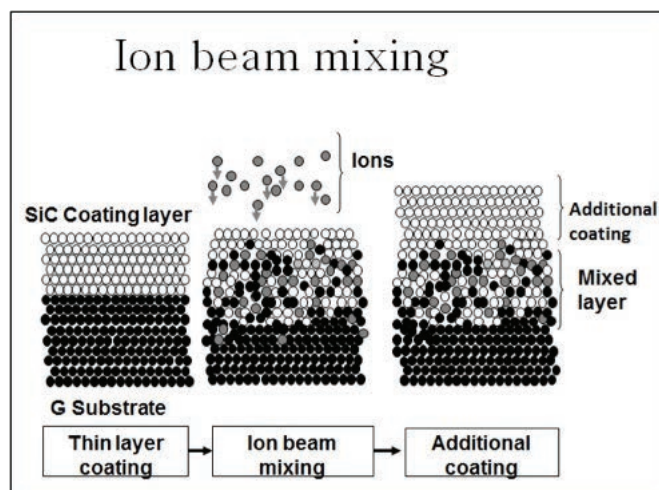


Figure 2. Schematic illustrating the ion beam mixing processes.

Once the gradient coatings have been established on initial graphite interfaces, the technique will be applied to small graphite specimens which will be irradiated in the Idaho National Laboratory (INL) Advanced Graphite Creep (AGC) experiment. The coatings will be characterized and analyzed non-destructively before irradiation to ascertain the viability of the coatings. After irradiation, the coatings will be re-examined and tested for adherence to the graphite substrate, cracking, spallation, or other degradation issues experienced while being irradiated.

### Research Progress

In this first year project, researchers at Korean Atomic Energy Research Institution (KAERI) have been developing the ion beam processing with a state-of-the-art coating technology. The INL has been designing and fabricating the next AGC irradiation test train (AGC-4) for insertion and irradiation into the Advanced Test reactor (ATR) in November 2014.

The following sections summarize results in each task area.

#### Task 1: CFD calculations in case of air ingress (INL)

The INL's HTR program has been developing computational fluid dynamics (CFD) models for a variety of HTR designs including Pebble Bed and Prismatic designs. The PIs for this study have been in discussions with the HTR Methods group to ascertain the various ingress accident scenarios including air and water. The sophisticated ingress accident models will be exploited in further development of future oxidation protective coatings once the coating technique has been proven.

An air-ingress accident is the most aggressive oxidation condition and the CVD models pertaining to this event are being actively researched with the HTR Methods program. However, while not included within the original proposal, it has become apparent through discussions with the HTR Methods group that a water ingress event has a high probability, especially when a water-based heat exchanger is included within the design. The effects of water on the SiC coating must be addressed as well as the air oxidation resistance. There are no anticipated issues with water on the SiC coatings but testing under moist conditions will be one of test variables.

#### Task 2: Modeling and weight loss testing of SiC coated graphite (INL/KAERI)

Initial work in modeling accident conditions has begun. However, testing of the SiC coated graphite specimens is awaiting the development of initial coatings.

##### Task 2a: Theoretical simulation

First-principles density-functional theory (DFT) calculations are being developed to obtain the optimal parameters and conditions for the SiC coating layers on a graphite substrate. Calculations as well as ab-initio molecular dynamics simulations are being performed for the following subjects: (1) oxidation of graphite; (2) oxidation of SiC; (3) structure of the SiC/graphite interface; (4) graphitization process in the SiC/graphite interface; (5) oxidation of the SiC/graphite interface.

These calculations and simulations will be fully utilized once the initial deposition techniques have been established. The conditions and experience gained from the initial coating development will assist in creating the optimal deposition parameters for a graphite component. An iterative feedback for the reaction rate processes based upon the coating test results will enhance the coating technique for these hybrid structures.

##### Task 2b: Oxidation experiment

Oxidation experiments will be conducted once sample development has produced acceptable coatings (Task 4).

#### Task 3: Pore structure and strength variation of SiC graphite (KAERI/INL)

Pore structure and strength variation experiments will be conducted once sample development has produced acceptable coatings (Task 4).

##### Task 3a: Thermal test

Thermal testing will be conducted once sample development has produced acceptable coatings (Task 4).

### Task 3b: XRD analysis

XRD analysis will be conducted once sample development has produced acceptable coatings (Task 4).

### Task 3c: Surface and interface analysis

Cracks, pores, and pinholes on the coating layer will be observed by HR-SEM and OM once sample development has produced acceptable coatings (Task 4).

### Task 3d: Mechanical property analysis

Compression strength, surface hardness, and sonic velocity will be measured for the oxidation-tested specimens once sample development has produced acceptable coatings (Task 4). The interfacial responses under the compressive loading will be examined by means of digital image correlation method.

### Task 4: Development of oxidation protective coating (KAERI)

The development of an adherent and robust SiC coating on graphite specimens utilizing the improvements inherent to ion beam mixing is the primary task of this project. Basically, an ion beam is focused onto a thin SiC deposited film, mixing the Si and C atoms together in the film and the interface. This is followed by additional SiC coating to a desired thickness. One of the merits of ion beam mixing (IBM) is that the surface pretreatment is not imperative as in conventional diffusion bonding because a forceful intermixing by the energetic ions mitigates the effect of the initial surface conditions. Ion beam processed coatings create improved interfacial properties utilizing graded ion-mixing with ramped ion energy, employ multiple ion beam mixed deposition processes to build up the thickness of protective layer, and can inject various compound forming species during deposition. The ion beam process can produce not only a graded interface but also improve the bonding property in the near surface layers of the graphite. These coating attributes are to be investigated during this project.

The majority of activity on the project has been concerned with this task. Equipment purchase, apparatus assembly, and preliminary coating technique development has been initiated over the past 7-8 months since the beginning of this project, Figures 3-6. The SiC film is being deposited on right cylindrically shaped, isotropic nuclear grade graphite specimens. The coating will be deposited to a thickness of 50 – 100 nm by e-beam evaporation, followed by ion beam mixing with Ar ion. The coating and ion beam mixing system operates in high vacuum. For optimal mixing and subsequent interfacial strength, the ion energy deposition will be maximized at the interfacial region. Stopping Range of Ions in Matter (SRIM) software may be employed to assist with the ion beam mixing process. After ion beam mixing, additional SiC film will be deposited up to the designed thickness. The coating and the ion beam bombardment is repeated to produce a less abrupt interface and to increase the film density by ion hammering.

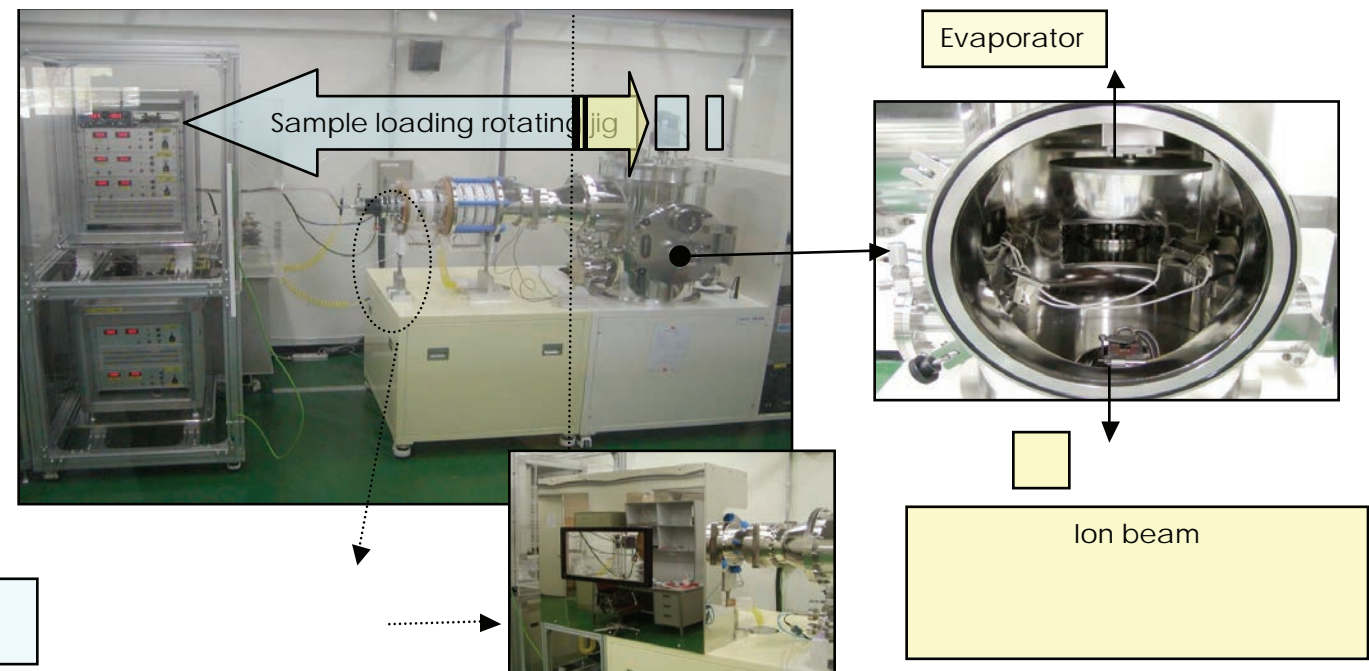


Figure 3. The e-beam evaporative deposition device is equipped with a 100 keV ion implanter, aiming the . . .

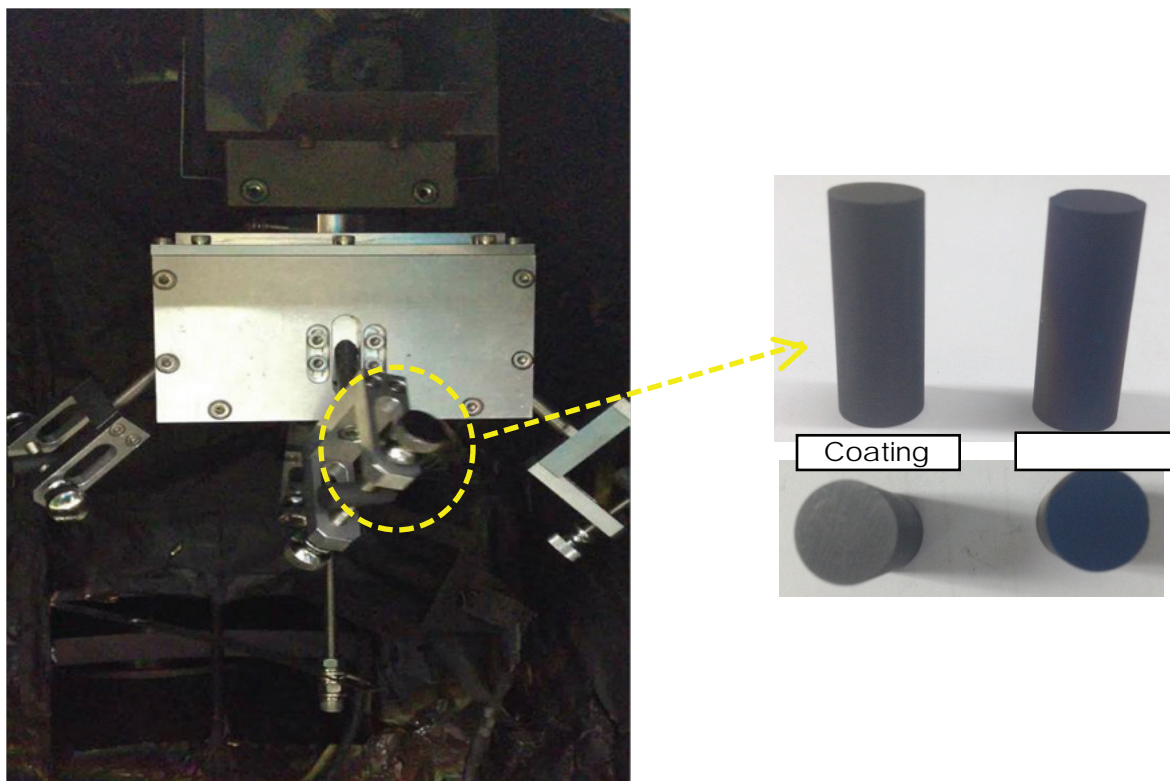


Figure 4. Image of rotating jig inside the coating/ion mixing chamber. The 360° rotation allows uniform coating of entire specimen.

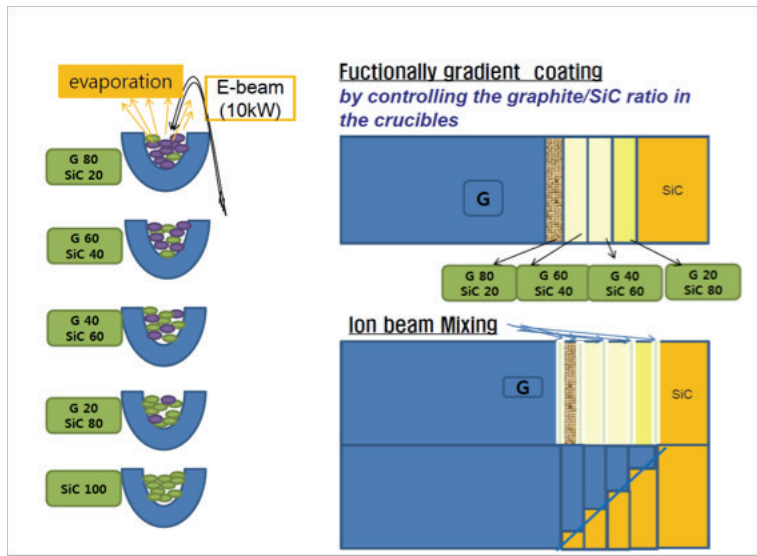


Figure 5. Schematic of E-beam evaporative coating deposition process. A functionally graded coating is created by melting and depositing successive layers with different compositions of materials as illustrated by the different materials on the left side of the graphic. Ion beam mixing is used between successive deposits to create a gradual gradient rather than a step-wise gradient of material compositions.

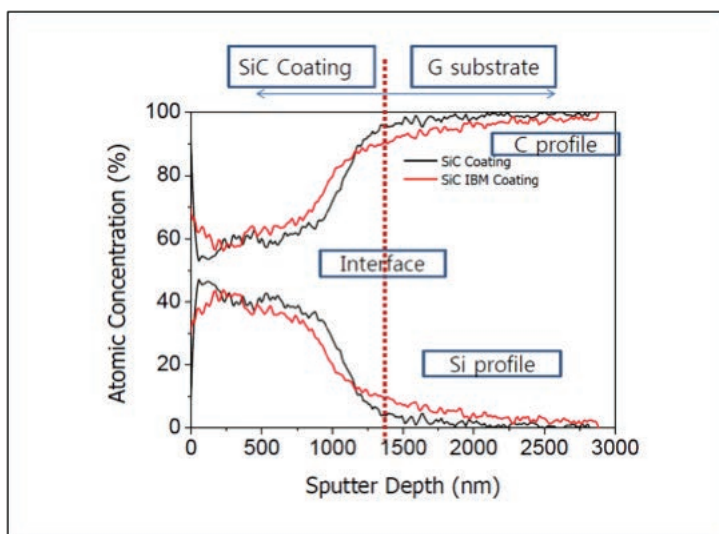


Figure 6. Auger analysis of initial SiC coating. The coating with IBM shows more broadened interface than a coated interface without ion beam mixing. Analysis illustrates functionally gradient coating resulting from IBM.

#### Task 4a: E-beam SiC coating and Ion beam mixing

During initial coating the SiC material will be applied in a  $\sim 1\mu\text{m}$  thick deposit on the graphite specimens. After analyzing the interface and the deposited thin film, larger deposition thicknesses are used to build up the thickness of the protective layer.

#### Task 4b: SiC formation by CVI+ CVR and Ion beam mixed SiC coating

Vapor infiltration and vapor reaction (CVI & CVR) coatings are formed using the following steps: (1) substrate surface is bombarded with  $\text{Ar}^+$  ions to eliminate surface contaminants and open any closed micro-pores near the surface, (2) Solid poly-silicon is thermally evaporated and reacted with the graphite substrate to form SiC on the surface of the substrate, (3) Ions beam mix the deposited, thin coating to mix the surface layers.

#### Task 4c: CVD on the ion beam mixed SiC layer

Chemical vapor deposition (CVD) is also carried out on the ion mixed coating layers in order to create thicker SiC coating layers rapidly.

#### Task 4d: Analysis of the protective coating

The thickness, density, phase content and microstructure of the SiC coating layers are examined after each deposition. The relation between these characteristics and the physical parameters of the coatings during oxidation testing (in air) will be conducted at 1000°C and 1500°C. Furthermore, thermal cyclic tests between 500°C and 1000°C will be conducted.

#### Task 5: Thermal heating and low dose irradiation of the coated specimens (INL)

The NGNP Graphite R&D program will provide irradiation and high temperature oxidation testing for the SiC coated graphite specimens based upon the expected conditions during an air accident event (Task 1). The NGNP Graphite R&D program is currently in the process of designing and building the fourth Advanced Graphite Creep irradiation test train (AGC-4). The AGC-4 irradiation capsule will expose a set of graphite specimens to temperatures of 800 °C and a neutron dose range of 2-7 dpa. The central stack area of each test series capsule has been made available for experimental VHTR materials such SiC coated-graphite, as shown in Figure 7. Approximately 12 SiC coated graphite specimens will be irradiated in the central column along with other graphite specimens.

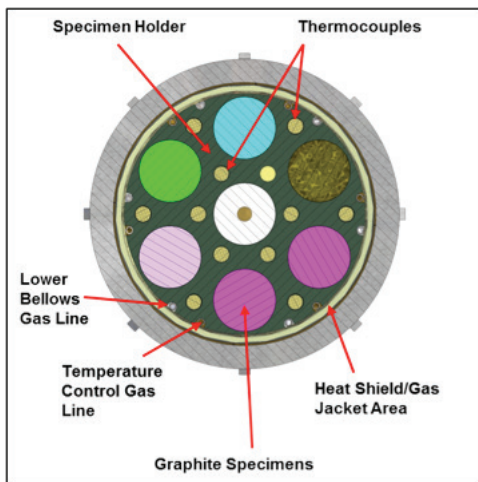


Figure 7. AGC irradiation test train cross-section illustrating specimen columns. Six outer columns are tested under a mechanical load while the central column is unloaded. SiC coated specimens will be irradiated in the central unloaded column.

Since the application for SiC coated graphite is for low fluence graphite support columns, the specimens will be placed in low dose positions within the AGC test train. The coated specimens will be irradiated in graphite "cans" which will contain any coatings that may fail during irradiation. The SiC coated specimens will be required to meet the interior dimensions of the irradiation cans - 10mm diameter X 6mm in length. Depending upon the position within the test series capsule the specimens can be expected to achieve end of life dose levels (1-2 dpa). No mechanical load will be placed upon these initial test specimens. This irradiation test will provide the final proof that the coating can survive the expected conditions inside a VHTR design.

In addition to coating examination (Post irradiation examination – PIE), oxidation testing of the specimens will be provided by INL. Oxidation rates of the coated and irradiated specimens will be compared to uncoated, irradiated and unirradiated specimens that have been previously been tested at INL's Carbon Characterization Laboratory (CCL). Any damage to the coatings or significant weight loss during oxidation testing will be investigated. The anticipated outcome of this project is a verified and validated oxidation protective coating process on the graphite with computational and experimental data to use for VHTR design.

Depending upon the progress made with the coating technique, large enough specimens may be coated which could allow INL to perform mechanical testing after the oxidation mass loss experiments. Mechanical strength results for the SiC coated specimens can then be directly compared to uncoated specimens that have been previously tested for acute air-ingress accident conditions. Preparations are being made at the CCL to mechanically test irradiated specimens. The testing equipment has been purchased, received, set-up, qualified, and preliminary mechanical testing on unirradiated specimens is being conducted. Once the proper techniques have been developed the irradiated specimens will be tested.

### **Planned Activities**

In the second project year, the research team will optimize the IBM coated specimen coatings, test the new coatings both mechanically and thermally, and initiate irradiation testing of the initial coated specimens. Researchers will conduct the following activities specific to each task:

#### **Task 1: CFD calculations in case of air ingress (INL)**

Discussions with the INL's HTR Methods Development team on computational fluid dynamics (CFD) models for a variety of HTR designs including Pebble Bed and Prismatic designs will continue. The conditions for both air and water ingress accident scenarios will be investigated and applied to post-coating testing methodologies.

#### **Task 2: Modeling and weight loss testing of SiC coated graphite (INL/KAERI)**

Modeling of oxidation weight loss under accident conditions will continue. The modeling results will be augmented with data from weight loss testing results. Modeling efforts (and weight loss testing) will be conducted on optimized coatings utilizing the analysis of the microstructure developed by functionally graded deposition and ion beam mixing.

#### **Task 2a: Theoretical simulation**

First-principles density-functional theory (DFT) calculations will continue. Calculations based upon detailed microstructure as well as chemical profiling within the graded coatings will assist in the development of more sophisticated models. Once the coating parameters have been more established, calculations as well as ab-initio molecular dynamics simulations will be performed for graphite & SiC coating oxidation rates. This will necessarily include understanding the oxidation behavior and rate of the graded SiC/graphite interface structure.

An iterative feedback process utilizing the results from these calculations and simulations along with the actual coating results has been initiated to create a more optimized coating. The conditions and experience gained from the initial coating development will continue to assist in this iterative process to create an optimal deposition parameter based upon the theoretical simulations of these hybrid structures.

### Task 2b: Oxidation experiment

Oxidation experiments will be conducted on the initial specimens. Results from these initial studies will provide feedback to the simulations, models and coating parameters of the graphite specimens. Oxidation experiments will continue on optimized specimens with corresponding feedback to the coating parameters.

### Task 3a-d: Pore structure and strength variation of SiC graphite (KAERI/INL)

Mechanical strength testing will be conducted on the initial coated specimens. Results from these initial studies will provide feedback to the coating process and the coatings will be optimized for future specimens. Thermal, XRD analysis, surface and interface analysis, and finally mechanical property testing will be conducted to ascertain the mechanical strength and structural integrity of the coatings.

### Task 4a-d: Development of oxidation protective coating (KAERI)

KAERI will continue to optimize the development of an adherent and robust SiC coating. The coating technique being developed has a wide variety of combinations utilizing different functionally graded deposition layer depths, layer compositions, amounts of mixing through ion beam interactions, and thickness of remaining CVD coating. Utilizing the information from the development of coating models and simulations along with direct data from testing and coating analysis will assist in developing an optimized coating.

The optimal coating process utilizing deposition thickness, gradient level, and coating material compositions will be ascertained during the second year of development. Utilizing the deposition chamber capabilities to alter the coating layers and feedback from post-deposition analysis the parameters for an optimal gradient coatings will be developed. In addition, to reduce the thermally induced stresses potentially present within the interface layers the ion beam parameters will be varied. The ion beam time, beam energy, and stages of application during deposition will be explored.

A number of SiC coated specimens will be fabricated for testing and analysis. Data from these tests will be used for model and deposition process improvements. In addition, right cylindrical shaped specimens will continue to be fabricated for irradiation and large mechanical testing.

### Task 5: Thermal heating and low dose irradiation of the coated specimens (INL)

The NGNP Graphite R&D program will begin irradiation testing of the initial SiC coated graphite specimens in the fourth Advanced Graphite Creep irradiation test train (AGC-4). While the initial coated specimens are not optimized we want to take advantage of the opportunity to irradiate coated specimens within the AGC experiment. These irradiations are effectively free since there is available space within the AGC-4 irradiation capsule. Approximately 12 SiC coated graphite specimens will be irradiated in the central column of the AGC-4. The AGC-4 irradiation test train will be irradiated from November 2014 to October 2016. Therefore, the AGC-4 capsule will not be available for any future optimized coated specimens during this time frame. Potential irradiation capsules for future specimens will be explored.

Thermal testing of the SiC coated specimens will be conducted in this second year of the program. Coated specimens will be subjected to normal and accident temperatures based upon CFD calculations (Task 1). A high-temperature furnace in the CCL will be used to test the coatings on the specimens followed by analysis of the coatings and graphite substrate. Analysis data from these inspections will be utilized for model, process, and coating improvements.

# Development of Advanced Long Life Small Modular Fast Reactor

Project Number: 2013-003-K

**PI (U.S.):** Changho Lee & Richard R. Lell,  
Argonne National Laboratory

**PI (ROK):** Sang Ji Kim, Korea Atomic  
Energy Research Institute

**Collaborators:** N/A

**Program Area:** Reactor Concepts  
RD&D

**Project Start Date:** December 2013

**Project End Date:** November 2016

## Research Objectives

The primary objective of this three-year collaborative research program is to develop an affordable and high-performance small modular reactor core concept aiming local small-size electricity grid markets (~100 MWe) without refueling for reactor lifetime.

A wide range of SMR core concepts has been proposed aiming for lower initial capital investment, scalability, and siting flexibility at a location where a large-scale plant is not accommodated. The majority of proposed SMR core concepts use light water as the coolant; however, fast reactor SMR technologies have potential inherent safety and nonproliferation benefits. The SMRs based on fast reactor technology could be fabricated and fueled in a factory, sealed and transported to sites for power generation or process heat, operated without refueling for reactor lifetime and then returned to the factory.

In this project, an affordable, high performance, and long-life small modular fast core concept will be developed by merging the sodium-cooled fast SMR core concept developed by Argonne National Laboratory (ANL) and the long-life breed-and-burn fast reactor core concept developed by Ulsan National Institute of Science and Technology (UNIST). The developed long-life SMR core concept from this project will meet the goals pursued by the U.S. Department of Energy's Office of Nuclear Energy (DOE-NE) SMR programs and increase the presence of U.S. and Korea industries in small-grid markets where a clean, secured and stable electricity resource is required.

## Planned Activities and Programs

### Feasibility Study of Long Life Fast Reactor Concepts.

The goal of this task is to evaluate the feasibility of long life fast reactor concepts and develop the design requirements. Table 1

shows primary design and core performance parameters of the selective long life fast reactor concepts, which include 100 MWe SMR (ANL-100) and 3000 MWt ultra-long life core concept (ULFR-3000) developed by ANL targeting capital and operational cost reductions and ultra-high burnup in a fast reactor system, long-life core concept (UCFR-1000) developed by UNIST, and Constant Axial shape of Neutron flux, nuclide densities and power shape During Life of Energy production (CANDLE) proposed by Sekimoto.

Table 1. Long Life Breed-and-burn Fast Reactors

Parameter	UCFR-1000 <sup>a)</sup>	ULFR-3000 <sup>b)</sup>	AFR-100 <sup>c)</sup>	CANDLE <sup>d)</sup>
Power, thermal/electrical [MW]	2600 / 1000	3000	250 / 100	3000
Refueling interval [year]	60	44	30	-
Fuel form	U-10Zr/SF-7Zr	U-Pu-Mo	U-10Zr	U-10Zr
Fuel density [% TD]	74.5	75	75	75
Active core height [cm]	240	175	110	800
Core diameter [cm]	600	600	300	400
Fuel volume fraction [%]	43.7	39.7	43.9	50
Initial heavy metal loading [t]	238	297	23.9	-
Specific power density [MW/t]	10.9	10.1	10.5	-
Specific power density [W/cc]	61	59	64.3	-
Avg. Linear power [kW/m]	159	24.4	15.2	-
Peak fast neutron flux fluence [ $10^{23}$ n/cm <sup>2</sup> ]	22	19.4	5.97	-
Avg. Burn-up, driver/blanket [GWd/t]	239	303/164	101	381
Overall Breeding ratio	1.1	1.081	0.8	-

a) Taewoo Tak, Deokjung Lee, and T. K. Kim, "Design of Ultralong-Cycle Fast Reactor Employing Breed-and-burn Strategy," Nuclear Technology, 183, pp.427-435, September (2013).

b) T. K. Kim and T. A. Taiwo, "Feasibility Study of Ultra-Long Life Fast Reactor Core Concept," PHYSOR-2010, Pittsburgh, PA (2010).

c) T. K. Kim, C. Grandy, and R. Hill, "A 100MWe Advanced Sodium-Cooled Fast Reactor Core Concept," PHYSOR-2012, Knoxville, TN (2012).

d) H. Sekimoto, K. Ryu, and Y. Yoshimura, "CANDLE: The New Burnup Strategy," Nuclear Science and Engineering, 139, 306-317 (2001).

The initial feasibility study on the long-life core concept was conducted using the CANDLE concept and additional feasibility studies for the non-water cooled reactor concepts are planned. Figure 1 shows the simplified conceptual schematic of the geometry of 8m-tall CANDLE concept. The CANDLE adopted the breed-and-burn strategy in axial direction: i.e., enriched uranium region located at the core bottom plays a role of an igniter and a blanket region in axial direction as a fissile breeder that utilizes natural or depleted uranium. The enrichment uranium region of total 1.2 m consists of three parts, which have different enrichment each, and it starts the burning and consequently causes the breeding. The diameter of this core is 4 m including radial reflector of 50 cm thickness and this reflector is also made of depleted uranium. All the fuel is a binary metallic fuel of U-Zr form. Figures 2 and 3 show the results of a core depletion calculation: the core multiplication factors and the axial power profiles as a function of depletion time, respectively. The fluctuation of the core multiplication factor is due to the nature of Monte Carlo calculations. It is noticed that there is a saturation region in the graph for the multiplication factors, which means a steady breeding is performed along the axial direction. Figure 3 presents the movement of maximum power position whose trend line tells that the propagation speed is 3.4 cm per year.

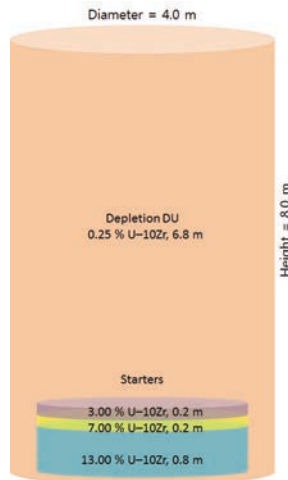


Figure 1. Conceptual Drawing of CANDLE Core

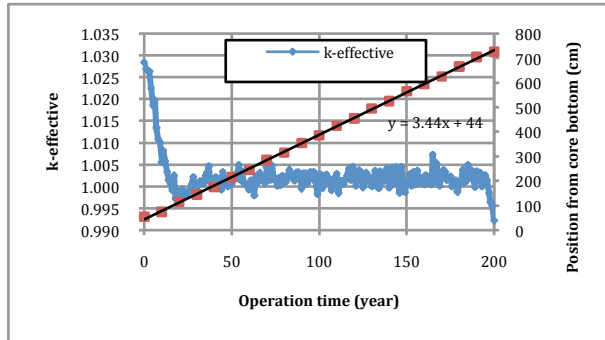


Figure 2. Feasibility Test of Breed-and-burn Core Concept with CANDLE Model

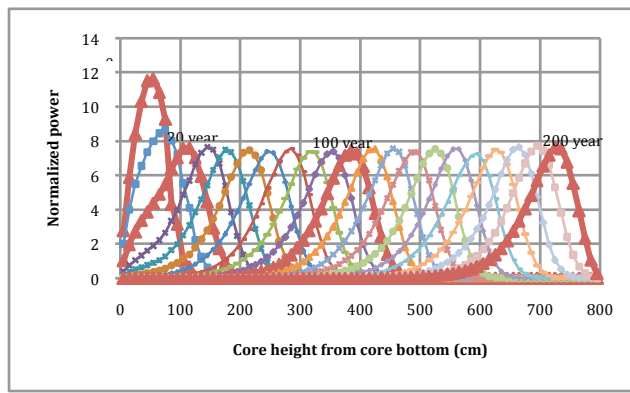
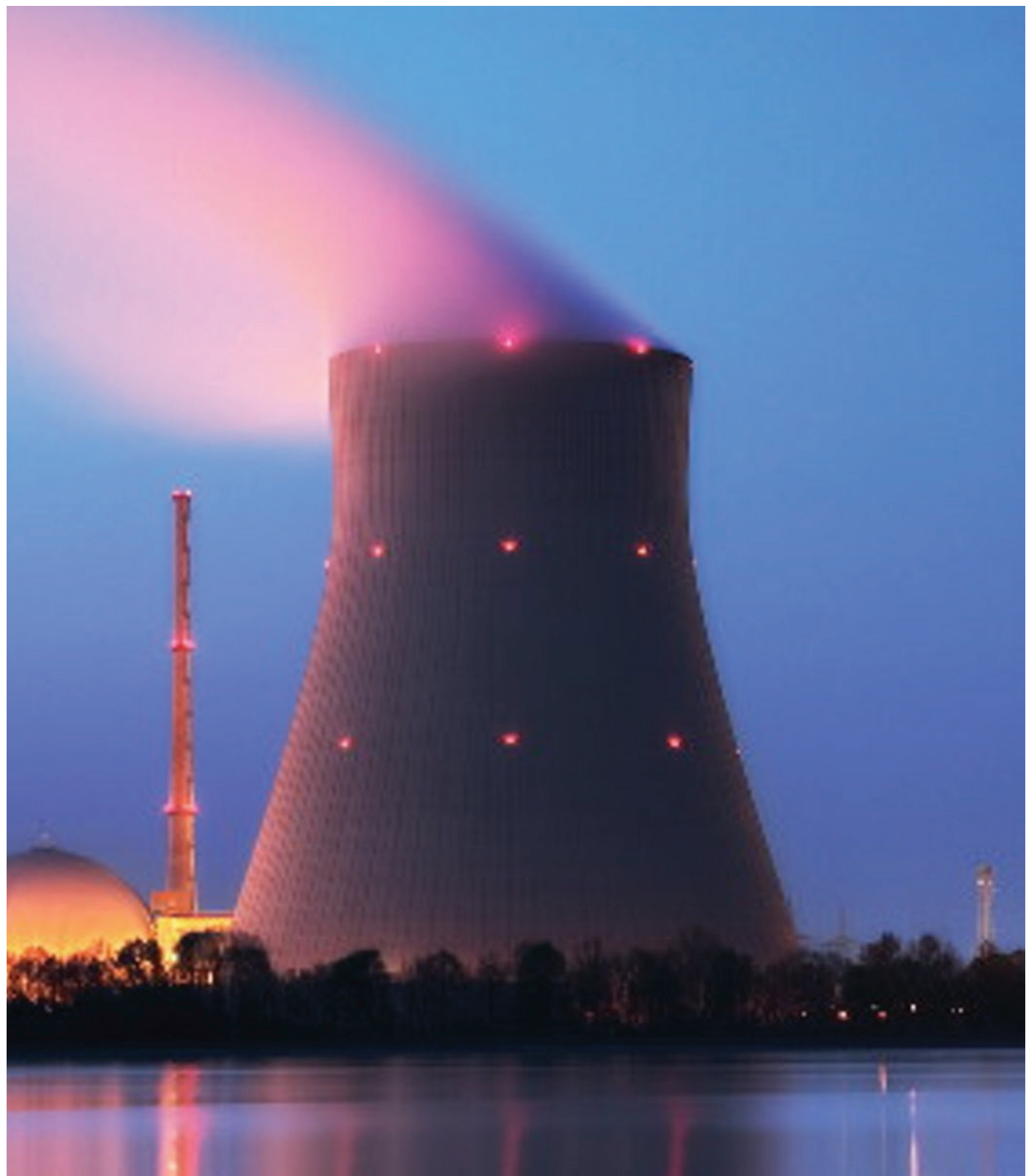


Figure 3. Propagation of Axial Power Profile in CANDLE

**Task 2: Conceptual Design Long Life Small Modular Fast Reactor.** The goal of this task is to develop a conceptual design of long-life small modular fast reactor. The new reactor concept will be based on the ANL's small modular reactor AFR-100 and UNIST's ultra-long life reactor concept UCFR- 1000. The new reactor design will be developed using ANL's fast reactor design code system and Monte Carlo depletion code systems, MCNPX and McCARD. Various design

parameters will be determined to meet the core design requirements developed in Task 1. The long life small modular fast reactor will use the breed-and-burn concept. Various propagation concepts of the depletion zone, such as axial (traveling wave) or radial (assembly shuffling) directions, will be assessed in this task.

**Task 3: Core Performance Analysis of Long Life Small Modular Fast Reactor.** The goal of this task is to evaluate the core performance characteristics and the safety features of the newly developed long life small modular fast reactor concept in Task 2. Core performance parameters such as reactor power, uranium enrichment, refueling interval, number of batches, active core height, specific power density, core average burnup, burnup reactivity swing, fissile breeding ratio, discharge burnup, peak fast flux, and linear heat rate will be assessed. The kinetics and reactivity feedback parameters will also be assessed. Finally, the inherent fast features will be assessed using the integral reactivity parameters for the hypothetical unprotected accident scenarios of Unprotected Loss of Heat Sink (ULOHS), Transient Over-Power (UTOP), Loss of Flow (ULOF), etc.



Kernkraftwerk Isar Nuclear Power Plant at night  
Photo courtesy of Creative Commons

# Appendix I.

## Acronyms

### Misc

---

~	Approximately
$\Delta \rho$	Delta Rho (denotes change in reactivity)
$\mu\text{m}$	Micrometer(s)
$\mu\text{g}$	Microgram(s)
2D	Two-Dimensional
3D	Three-Dimensional

### A

---

AECL	Atomic Energy of Canada Limited
Ag	Silver
Al	Aluminum
ANL	Argonne National Laboratory
ANRE	Agency of Natural Resources and Energy
APS	Advanced Photon Source
APT	Atom Probe Tomography
Ar	Argon
ARC	Advanced Reactor Concepts
ATLAS	Advanced Thermal-Hydraulic Test Loop for Accident Simulation

### B

---

bcc	Body-Centred Cubic
BDBA	Beyond Design-Basis Accident
BFS	Big Physical Stand (facility)
BWR	Boiling Water Reactor

### C

---

C	Carbon
C	Celsius
Ca	Calcium
CASL	Consortium for Advanced Simulation of Light Water Reactors
CBM	Condition-Based Monitoring
Ce	Cerium
CEA	Commissariat à l'énergie atomique et aux énergies alternatives
CEN	Comité Européen de Normalisation
Cf	Californium
CFD	Computational Fluid Dynamics
CG	Coarse-Grained
CGR	Crack Growth Rate
Cl	Chlorine
CLC	Current Life Consumption
cm	Centimeter(s)
CNY	Chungnam National University
Cr	Chromium
CRP	Coordinated Research Project
CSM	Colorado School of Mines
CTR	Crystal Truncation Rod
Cu	Copper
CW	Cold Worked
CY	Calendar Year

## D

---

D	Deuterium
DBA	Design-Basis Accident
DNBR	Departure from Nuclear Boiling Ratio
DNS	Direct Numerical Simulation
DOE	Department of Energy
dpa	Displacements Per Atom
DSA	Dynamic Strain Aging
DSC	Differential Scanning Calorimetry

## G

---

Gd	Gadolinium
GELINA	Geel Linear Accelerator
Gen IV	Generation IV
GETMAT	Generation IV and Transmutation Materials (Euratom program)
GIF	Generation IV International Forum
GPa	Gigapascal(s)
GT	Guide Thimble
GWD/MTU	Gigawatt – Days per Metric Ton of Uranium

## E

---

EBSD	Electron Backscatter Diffraction
ECAE	Equal Channel Angular Extrusion
ECAP	Equal Channel Angular Processing
EDM	Electrical Discharge Machining
EDS	Energy Dispersive X-Ray Spectroscopy
ENDF	Evaluated Nuclear Data File
EPMA	Electron Probe Microanalyzer (EPMA)
EPRI	Electric Power Research Institute
EU	European Union
Eu	Europium

## H

---

h	Hour(s)
H	Hydrogen
Hf	Hafnium
HIP	Hot Isostatic Press
HLM	Heavy Liquid Metal
HTGR	High-Temperature Gas-Cooled Reactor
HT-UPS	High-Temperature Ultrafine Precipitate-Strengthened (steel alloy)

## F

---

F	Flourine
F/M	Ferretic/Martensitic
FA	Fuel Assembly
fcc	Face-Centred Cubic
FCM	Fully Ceramic Microencapsulated (fuel)
FCR&D	Fuel Cycle Research and Development
Fe	Iron
FFTF	Fast Flux Test Facility
FIB	Focused Ion Beam
FIGARO	Fissile Interrogation Using Gamma Rays from Oxygen
FWHM	Full Width at Half Maximum
FY	Fiscal Year

## I

---

I&C	Instrumentation and Control
IAEA	International Atomic Energy Agency
IEEE	Institute of Electrical and Electronics Engineers
IFBA	Integral Fuel Burnable Absorber
IFNEC	International Framework for Nuclear Energy Cooperation
IMF	Inert Matrix Fuel
INC	International Nuclear Cooperation (framework)
I-NERI	International Nuclear Energy Research Initiative
INL	Idaho National Laboratory
INM	Internal Network Manager
INU	Internal Network Unit
IPPE	Institute of Physics and Power Engineering

---

IRIS	International Reactor Innovative and Secure
IRMM	Institute for Reference Materials and Measurements
ISO	International Organization for Standardization
IT	Instrument Thimble
ITU	Institute for Transuranium Elements

## J

---

J	Joule
JEFF	Joint Evaluated Fission and Fusion
JRC	Joint Research Centre

## K

---

K	Kelvin
K	Potassium
KAERI	Korea Atomic Energy Research Institute
$k_{\text{eff}}$	k-effective (neutron multiplication factor)
keV	Kiloelectron Volt(s)
keV <sub>ee</sub>	Electron Equivalent Recoil Energy (measured by scintillation light)
kPa	Kilopascal(s)
kW	Kilowatt

## L

---

LANL	Los Alamos National Laboratory
LANSCE	Los Alamos Neutron Science Center
LAS	Low-Alloy Steel
LCF	Low-Cycle Fatigue
LES	Large Eddy Simulation
Li	Lithium
LOCA	Loss-of-Coolant Accident
LOFA	Loss-of-Flow Accident
LRUS	Laser Resonant Ultrasonic Spectroscopy
LWR	Light Water Reactor

## M

---

M	Molar
MA	Mechanically Alloyed
MA	Minor Actinide
MatDB	MIPS Arabidopsis Thaliana Database
MATLAB	Matrix Laboratory
MCNP	Monte Carlo N-Particle
MEST	Ministry of Education, Science and Technology
MeV	Mega-Electron Volt
MEXT	Ministry of Education, Culture, Sports, Science, and Technology
mg	Milligram(s)
mm	Millimeter(s)
Mn	Manganese
Mo	Molybdenum
MONNET	Mono Energetic Neutron Tower
MOST	Ministry of Science and Technology (superseded by MEST)
MOX	Mixed Oxide
MPa	Megapascal(s)
MPa $\sqrt{m}$	Megapascal Square Root Meter (measure of fracture toughness)
MPM	Mechanical Properties Microscope
MST	Ministério da Ciência e Tecnologia
MV	Megavolt(s)
MWe	MegaWatt electric

## N

---

N	Newton(s)
Na	Sodium
NE	Office of Nuclear Energy
NE-6	Office of International Nuclear Energy Policy and Cooperation
NEA	Nuclear Energy Agency (of OECD)
NEAMS	Nuclear Energy Advanced Modeling and Simulation (program)
NFA	Nanostructured Ferritic Alloy
NGNP	Next Generation Nuclear Plant

---

Ni	Nickel
nm	Nanometer(s)
NRC	Nuclear Regulatory Commission
NRCan	Department of Natural Resources Canada

---

O	
O	Oxygen
ODS	Oxide Dispersion-Strengthened
OECD	Organisation for Economic Co-operation and Development
OPR	Optimized Power Reactor
ORNL	Oak Ridge National Laboratory

---

P	
Pb	Lead
pcm	Per Cent Mille
PEM	Process and Equipment Monitoring
PEP	Process and Equipment Prognostics
PFNS	Prompt Fission Neutron Spectrum
PI	Principal Investigator
ppm	Parts Per Million
ps	Picosecond(s)
Pu	Plutonium
PWR	Pressurized Water Reactor

---

R	
R&D	Research and Development
RCH	Rotating Cylinder Hull
RD&D	Research, Development and Demonstration
REA	Rod Ejection Accident
RG	Regulatory Guide
RHEED	Reflection High-Energy Electron Diffraction
RMS	Root Mean Square
ROK	Republic of Korea
RUL	Remaining Useful Life

---

S	
s	Second(s)
S	Sulfur
SA	Solution Annealed
SCC	Stress Corrosion Cracking
SEM	Scanning Electron Microscope/Microscopy
SF	Spontaneous Fission
SFR	Sodium-Cooled Fast Reactor
SG	Steam Generator
SHARP	Simulation-Based High Accuracy Advanced Reactor Prototyping
SiC	Silicon Carbide
SIMS	Secondary Ion Mass Spectrometry
SIMSA	Safety Index Monitoring during Severe Accidents
SMART	System-Integrated Modular Advanced Reactor
SMR	Small Modular Reactor
SND	Standard Neutron Detector
SRO	Short-Range Ordering
SSMT	Small-Scale Materials Testing
STIP	Swiss Spallation Neutron Source Target Irradiation Program

---

T	
T/H	Thermal-Hydraulic
TCM	Thermal Conductivity Microscope
TEM	Transmission Electron Microscope/Microscopy
Th	Thorium
Ti	Titanium
TKE	Total Kinetic Energy
TMT	Thermomechanical Treatment
TOF	Time of Flight
TRISO	Tristructural-Isotropic
TRU	Transuranic
TT	Thermally Treated

**U**

---

U	Uranium
UC	University of California
UFFC	Ultrasonics, Ferroelectrics and Frequency Control
UFG	Ultrafine-Grained
UNIST	Ulsan National Institute of Science and Technology
URL	Underground Research Laboratory
UT	University of Tennessee

**V**

---

V	Volt(s)
VERDI	Velocity for Direct Particle Identification
VHTR	Very High-Temperature (Gas-Cooled) Reactor

**W**

---

W	Tungsten
W	Watt
WNR	Weapons Neutron Research (facility)
WQ	Water Quenched
wt%	Weight Percent

**X**

---

XML	Extensible Markup Language
XRD	X-Ray Diffraction

**Y**

---

Y	Yttrium
---	---------

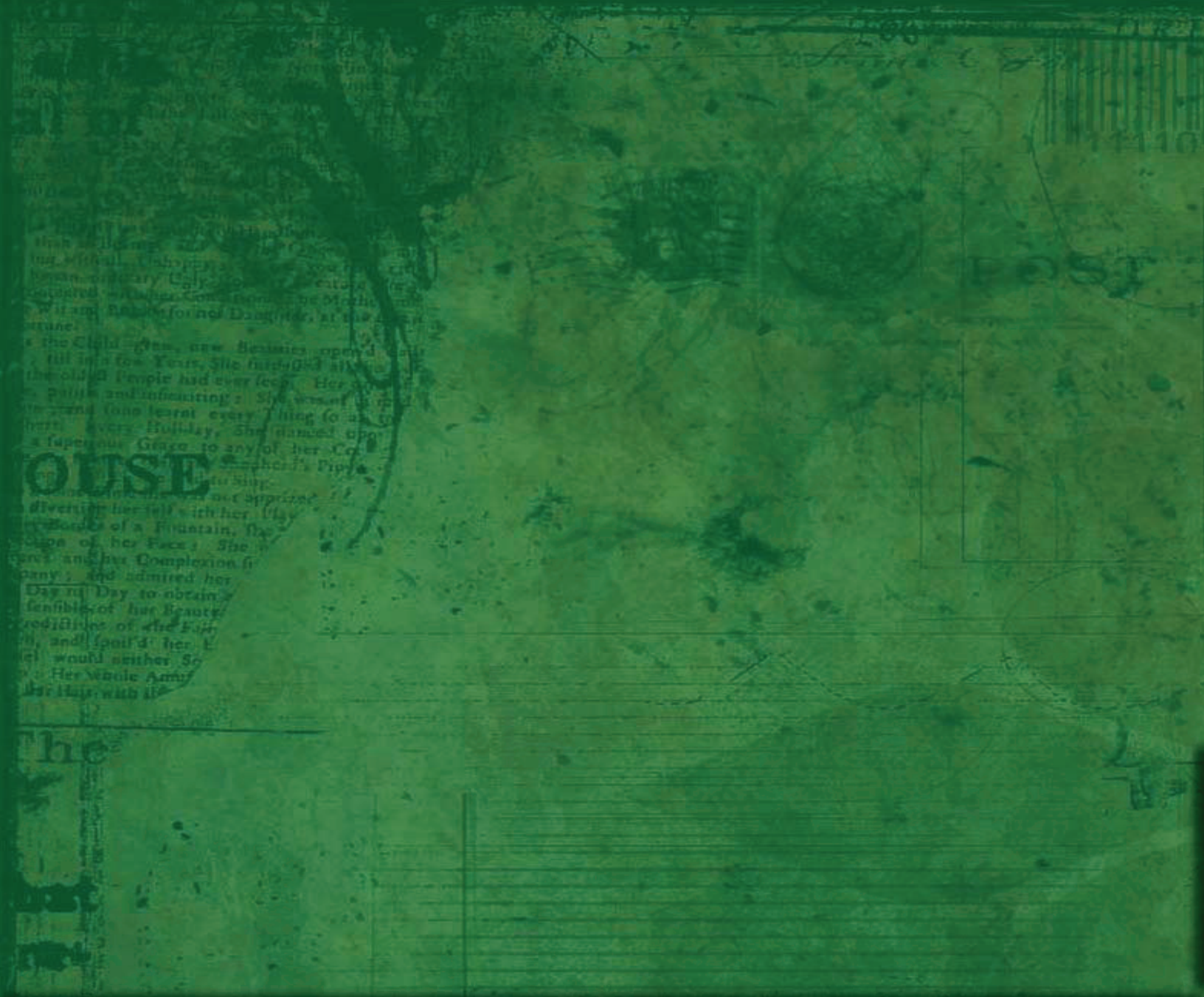
**Z**

---

ZPPR	Zero Power Plutonium Reactor
Zr	Zirconium



Nuclear Magnetic Resonance facility;  
Karlsruhe, Germany.  
Courtesy of Joint Research Center



... 44 ... *Adventus eius in tempore regni vestrum nullum finis dicitur ergo minus nisi extremitas eius Deus corporum velit, quia post hoc cessabit occasio. Quicquid enim auctoritate eius mortuorum numerus exstet. Quicquid autem propheta de vita resurrectionis vestrae dicit, et certe omnis omnibus miraculis, excusat amorem eius. Deinde in predicto tempore nostrum non est fieri audi ex illo, qui cum sensu eius invenimus nos ipsos in illis, rursum videntem nos, quoniam morte occidit.*